

OPTIMIZATION OF THE CONFIGURATION AND WORKING FLUID FOR A  
MICRO HEAT PIPE THERMAL CONTROL DEVICE

A Thesis

by

SCOTT JOSEPH COUGHLIN

Submitted to the Office of Graduate Studies of  
Texas A&M University  
in partial fulfillment of the requirements for the degree of

MASTER OF SCIENCE

December 2005

Major Subject: Mechanical Engineering

OPTIMIZATION OF THE CONFIGURATION AND WORKING FLUID FOR A  
MICRO HEAT PIPE THERMAL CONTROL DEVICE

A Thesis

by

SCOTT JOSEPH COUGHLIN

Submitted to the Office of Graduate Studies of  
Texas A&M University  
in partial fulfillment of the requirements for the degree of

MASTER OF SCIENCE

Approved by:

Co-Chairs of Committee,	Thomas R. Lalk
	Michael Schuller
Committee Member,	Kalyan Annamalai
Head of Department,	Dennis O'Neal

December 2005

Major Subject: Mechanical Engineering

## ABSTRACT

Optimization of the Configuration and Working Fluid for a Micro Heat Pipe

Thermal Control Device. (December 2005)

Scott Joseph Coughlin, B.S., University of Arizona

Co-Chairs of Advisory Committee: Dr. Thomas R. Lalk  
Dr. Michael Schuller

Continued development of highly compact and powerful electronic components has led to the need for a simple and effective method for controlling the thermal characteristics of these devices. One proposed method for thermal control involves the use of a micro heat pipe system containing a working fluid with physical properties having been specifically selected such that the heat pipes, as a whole, vary in effective thermal conductance, thereby providing a level of temperature regulation. To further explore this possibility, a design scenario with appropriate constraints was established and a model developed to solve for the effective thermal conductance of individual heat pipes as a function of evaporator-end temperature. From the results of this analysis, several working fluids were identified and selected from a list over thirteen hundred that were initially analyzed. Next, a thermal circuit model was developed that translated the individual heat pipe operating characteristics into the system as a whole to determine the system level effects. It was found that none of the prospective fluids could completely satisfy the established design requirements to regulate the device temperature over the entire range of operating conditions. This failure to fully satisfy design requirements was due, in large part, to the highly constrained nature of problem definition. Several fluids, however, did provide for an improved level of thermal control when compared to the unmodified design. Suggestions for

improvements that may lead to enhanced levels of thermal control are offered as well as areas that are in need of further research.

## ACKNOWLEDGMENTS

I would like to thank Dr. Schuller. The opportunity to work under his guidance at the Center for Space Power has greatly enhanced what I have taken from the classroom.

I would also like to thank Dr. Lalk for his patience as well as his continuing dedication to the intellectual development of his students.

I would like to acknowledge my colleagues at the Center for Space Power. Without the regular encouragement of Yuyan Guo, Olivier Godard, Tejas Shah, and Jayaram Sundararajan, the writing of this thesis would have been a much more daunting task.

Finally, I would like to thank my parents, John and Carol, for their unwavering support and encouragement throughout my life. It is to them that I owe many of my accomplishments.

## TABLE OF CONTENTS

CHAPTER		Page
I	INTRODUCTION . . . . .	1
	A. Overview of Thermal Management Systems . . . . .	1
	1. Thermoelectric Systems . . . . .	2
	2. Single Phase Liquid Cooling Systems . . . . .	2
	3. Dual Phase Cooling Systems . . . . .	3
	4. Holistic Thermal Management . . . . .	4
	B. Objective . . . . .	5
	1. Problem Definition . . . . .	5
	C. Thesis Format . . . . .	7
II	LITERATURE REVIEW . . . . .	9
	A. The Generalized Heat Pipe . . . . .	9
	B. Micro Heat Pipes . . . . .	12
	C. Variable Conductance in Heat Pipes . . . . .	15
III	THERMAL CONTROL SYSTEM DESIGN DESCRIPTION . .	20
IV	SYSTEM LEVEL MODELING METHODOLOGY . . . . .	27
	A. General Approach to Modeling . . . . .	27
	B. Possible System Level Modeling Approaches . . . . .	27
	1. Full Two-Phase Thermohydraulic Modeling . . . . .	28
	2. High Conductivity Solid Material Analogy . . . . .	28
	3. Thermal Circuit Model with Appropriate Resistances .	29
	C. Chosen System Level Model Description . . . . .	29
	D. System Model Thermal Circuit Analysis . . . . .	33
	E. Thermal Circuit Solution Process . . . . .	37
V	INDIVIDUAL HEAT PIPE MODELING METHODOLOGY . .	40
	A. The Capillary Limitation . . . . .	41
	1. Maximum Capillary Pumping Pressure . . . . .	42
	2. Liquid Pressure Drop . . . . .	45
	3. Vapor Pressure Drop . . . . .	46
	B. Other Important Heat Pipe Operating Limitations . . . . .	49

CHAPTER	Page
1. The Viscous Limitation . . . . .	49
2. The Sonic Limitation . . . . .	50
3. The Entrainment Limitation . . . . .	50
4. The Boiling Limitation . . . . .	51
C. Micro Heat Pipe Modeling Procedure . . . . .	54
1. Heat Transport Solution Methodology . . . . .	54
2. Working Fluid Property Data and Interpolation . . . . .	57
VI RESULTS AND DISCUSSION . . . . .	58
A. Results . . . . .	58
1. Individual Heat Pipe Modeling Results . . . . .	59
2. System Level Modeling Results . . . . .	65
B. Discussion . . . . .	79
1. Further Considerations . . . . .	83
C. Summary of Findings . . . . .	86
VII CONCLUSIONS . . . . .	89
VIII RECOMMENDATIONS FOR FUTURE WORK . . . . .	90
REFERENCES . . . . .	92
APPENDIX A . . . . .	95
APPENDIX B . . . . .	99
VITA . . . . .	128

## LIST OF TABLES

TABLE		Page
I	Established Design Requirements . . . . .	7
II	Design Needs due to Different Combinations of Operating Conditions	21
III	Individual Thermal Circuit Resistances . . . . .	37
IV	Resulting Working Fluids for Final Consideration . . . . .	65
V	Resulting Operational Regions for Various Fluids . . . . .	79
VI	Adjusted Performance of Various Fluids . . . . .	83



## LIST OF FIGURES

FIGURE		Page
1	Dimensioned Diagram of Aluminum Plate . . . . .	6
2	Conventional Heat Pipe Schematic . . . . .	11
3	Generalized Triangular-Shaped Micro Heat Pipe Schematic . . . . .	12
4	A Gas-Buffered Variable Conductance Heat Pipe with Reservoir . . . . .	16
5	Dimensioned Diagram of Aluminum Plate . . . . .	20
6	Aluminum Plate with Rubber Thermal Insulator Partition . . . . .	22
7	Detailed Cross Sectional Illustration of Embedded Micro Heat Pipe System . . . . .	24
8	Illustration of Embedded Micro Heat Pipe Placement and Orientation	24
9	Thermal Circuit Model Taken from Original Design Illustration . . . . .	31
10	Thermal Circuit Model Representation with Included Thermal Resistances . . . . .	32
11	Thermal Circuit Solution Routine . . . . .	39
12	Detailed Sketch of Micro Heat Pipe . . . . .	44
13	Three Dimensional Representation of an Individual Micro Heat Pipe Section . . . . .	48
14	Various Heat Transport Limitations over a Wide Range of Op- erating Temperatures for Micro Heat Pipe of Given Dimensions Using Water as a Working Fluid . . . . .	53
15	Individual Micro Heat Pipe Heat Transport Capacity Solution Process	56
16	Resulting Maximum Heat Transport Capacities of All Considered Working Fluids . . . . .	60

FIGURE	Page
17	The Eight Remaining Fluids for Further Consideration . . . . . 62
18	The Remaining Working Fluids with Highlighted Design Temperature Control Region . . . . . 64
19	Temperature Surface for Water as a Working Fluid Contained within Seven Embedded Micro Heat Pipes . . . . . 66
20	Resulting Temperature Surface for a Device Using Water as a Working Fluid with (a)Two, (b)Four, (c)Six, (d)Eight, (e)Ten, and (f)Twelve Embedded Micro Heat Pipes . . . . . 68
21	Multiple Temperature Surfaces Representing Varying Numbers of Micro Heat Pipes with Water as the Working Fluid . . . . . 69
22	Effective Operational Regions for Device Using Varying Numbers of Micro Heat Pipes with Water as the Working Fluid . . . . . 71
23	Effective Operational Regions for Device Using Varying Numbers of Micro Heat Pipes with Hydrogen Peroxide as the Working Fluid . . . . . 72
24	Operational Region for Twenty One Embedded Micro Heat Pipes Containing Thiacyclohexane as the Working Fluid . . . . . 73
25	Operational Region for Nine Embedded Micro Heat Pipes Containing Water as the Working Fluid . . . . . 74
26	Operational Region for Twelve Embedded Micro Heat Pipes Containing Deuterium Oxide as the Working Fluid . . . . . 75
27	Operational Region for Twenty Four Embedded Micro Heat Pipes Containing Hydrogen Peroxide as the Working Fluid . . . . . 76
28	Operational Region for Twenty Embedded Micro Heat Pipes Containing Hydrazine as the Working Fluid . . . . . 77
29	Operational Region for Twenty Embedded Micro Heat Pipes Containing Hydrazine as the Working Fluid . . . . . 78
30	Operational Region Resulting from the Use of a Continuous Aluminum Plate . . . . . 80

FIGURE		Page
31	Operational Region Resulting from the Use of “Perfect” Insulating Thermal Barrier Between the Two Sections of the Device . . . . .	81
32	Maximum Operational Region Using 24 Nonanal Heat Pipes Compared to Physically Possible Region . . . . .	82
33	Changes in Operating Region Given Changes in the Level of Thermal Insulation . . . . .	85

## NOMENCLATURE

**Standard Nomenclature**

A	cross-sectional area ( $m^2$ )
$Bo$	Bond number
$c_p$	specific heat ( $kJ/kg \cdot K$ )
D	pipe diameter ( $m$ )
$f$	friction factor
g	acceleration due to gravity ( $m/s^2$ )
H	height ( $m$ )
h	convection coefficient ( $W/m^2 \cdot K$ )
Kn	Knudsen number
k	thermal conductivity ( $W/m \cdot K$ )
L	length ( $m$ )
M	molecular weight ( $kg/kmol$ )
$\dot{m}$	mass flowrate ( $kg/s$ )
Nu	Nusselt number
P	pressure, perimeter ( $Pa, m$ )
$\Delta P$	pressure difference/drop ( $Pa$ )
q	power ( $W$ )
r	radius ( $m$ )
R	universal gas constant, thermal resistance ( $kJ/kmol \cdot K, K/W$ )
Ra	Rayleigh number

Re	Reynolds number
T	temperature ( $K$ )
t	time ( $s$ )
V	velocity ( $m/s$ )
We	Weber number

### Greek Characters

$\beta$	thermal expansion coefficient
$\lambda_{fg}$	latent heat ( $kJ/kg$ )
$\delta$	length ( $m$ )
$\mu$	viscosity ( $Ns/m^2$ )
$\gamma$	ratio of specific heat
$\kappa$	Boltzmann constant ( $1.38 \cdot 10^{-23} m^2kg/s^2 \cdot K$ )
$\rho$	density ( $kg/m^3$ )
$\lambda$	latent heat ( $kJ/kg$ )
$\nu$	kinematic viscosity ( $m^2/s$ )
$\sigma$	surface tension ( $N/m$ )

### Subscripts

$a$	adiabatic
$b$	boiling
$c$	capillary, condenser
$e$	evaporator, entrainment
$eff$	effective

<i>f</i>	film
<i>h</i>	hydraulic
<i>if</i>	interfacial
<i>l</i>	liquid
<i>m</i>	maximum
<i>n</i>	nucleation
<i>s</i>	sonic, surface
<i>sat</i>	saturation
<i>v</i>	vapor, viscous
$\omega$	wetted

## CHAPTER I

### INTRODUCTION

As the natural progression of technology has pointed increasingly in the direction of designs being more compact, more powerful and more efficient, those involved in the field of thermal management have, understandably, been presented with increasingly complex issues of their own. High levels of heat generation and physical material limits, coupled with the ever-present consumer demand for lightweight, compact, and aesthetically pleasing appearance, have often times lead to situations in which design constraints simply cannot be met using a traditional approach. Conventional methods for heat-producing component cooling are often best suited for larger-scale, stationary applications in which package size and power consumption are not of critical importance. These cooling techniques typically rely on conduction through a finned heat sink, in conjunction with the forced convection obtained with the use of a fan or blower. These standard methods of thermal management have presented clear limits, involving both cooling effectiveness as well as size and weight constraints. As a result of these inherent limitations, significant effort has recently been made to develop alternative methods for the effective dissipation of excess thermal energy.

#### A. Overview of Thermal Management Systems

As indicated, the field of thermal management has been in a state of constant change, as it is so closely tied in recent years to the ever-evolving computer and consumer electronics industries. With the shortcomings of conventional cooling becoming in-

---

The journal model is *IEEE Transactions on Automatic Control*.

creasingly apparent, alternative cooling techniques have been relied on to a much greater extent. Several of the techniques that have been developed in an effort to overcome these obstacles are presented briefly and discussed in the following sections.

### 1. Thermoelectric Systems

Thermoelectric coolers, sometimes referred to as “Peltier” coolers, are small, solid-state devices that function essentially as heat pumps. Typical units are only a few millimeters thick by as few as several millimeters square. These devices are constructed as two ceramic plates between which an array of small bismuth telluride cubes are sandwiched. When a current is applied to the device, heat is transferred from one side of the cubes to the other. The colder side of the device is commonly used to cool electronic devices. If one were to reverse the current applied to the system, the device would function in reverse fashion as a heater [1]. Due to their compact size, such devices are very well suited for small scale cooling applications. Drawbacks, however, include the fact that they remain quite inefficient in terms of power required for proper operation. Since the available power used by many portable electronic devices is a very limited resource, thermoelectric systems often remove themselves from consideration for thermal management in such applications.

### 2. Single Phase Liquid Cooling Systems

Liquid cooling systems offer significantly higher levels of heat removal through convection than their air cooled counterparts due to the convection coefficient of liquids being markedly higher than that of air. The simplest of liquid cooling systems is the traditional, single phase, pumped loop. Such systems have been used for quite some time in applications ranging from automotive to residential heating and cooling, and in recent times for electronics cooling [1]. There are several clear drawbacks,



however, to making use of such a system in the context of small-scale portable electronics. First, a method for circulating the working fluid around such a system must be introduced. Most often, this involves the introduction of a traditional liquid pump which, in addition to being noisy, in many cases requires significant space and levels of continuous power to operate. Further, although more efficient than air cooled systems, single phase liquid cooling systems still require significant surface area for heat absorption and release. In relatively compact applications, adding additional area to meet the cooling requirements may simply not be an option.

### 3. Dual Phase Cooling Systems

One of the most effective methods that has been developed for the dissipation of thermal energy involves the utilization of the phase change of a working fluid to transport heat over a considerable distance with a minimal change in temperature. This category of heat transfer devices, known in broad terms as heat pipes, has undergone a variety of permutations to include devices such as thermosyphons, loop heat pipes (LHPs), capillary pumped loops (CPLs), and micro heat pipes [2]. Although there are distinct differences between these devices including gravity dependence, wicking structure variation and separated flow phase channels, they all possess the ability to transport heat over a considerable distance using the same basic phase change principle. Additionally, all of these devices are passive in that they require no external source of power to achieve a circulation of working fluid. Overall, the dual phase family of heat transfer devices have been put to use and proven extremely successful in applications ranging from the cooling of spacecraft to electronics cooling to cryogenic biomedical applications [3]. It is for these reasons that it was decided that the dual phase type cooling system will be the system of interest for this research. Additional background information dealing with this family of cooling systems is provided in the

the following chapter.

#### 4. Holistic Thermal Management

Although the past several years has indeed seen a surfeit of research performed within the field of thermal management, the vast majority of this work has focused primarily on the goal of transferring a maximum possible amount of thermal energy from source to sink. In the process of designing such devices, engineers are typically focused solely on the extreme high temperature case as their governing design constraint. In the vast majority of instances, such as when dealing with typical electronic devices and components, this approach is perfectly acceptable. There does exist, however, the reverse case of extreme low temperatures that one must consider when expecting a device to function properly under the full range of possible operating conditions. Devices having been designed based solely with the high temperature/high heat flux case in mind may, in some cases, be responsible for the removal of too much heat, that is, working “too well,” and not providing an appropriate level of thermal insulation in the event of low temperatures. In order for a thermal control device to maintain the operating temperature of a device expected to function under a variety of conditions, it can be seen that the effective thermal conductance of such a device would be required to vary significantly over that range of expected operating temperatures.

It can be foreseen, that as small-scale, heat producing devices become increasingly compact and powerful, also increasing will be the extent to which their proper performance will be reliant on effective operating temperature regulation. Furthermore, the envisioned methods of supplying power to devices of the future, particularly more advanced and compact battery designs and miniature fuel cells, are themselves, often highly dependant on the temperature at which they are operating. It is for these reasons that it is currently a significant source of interest to develop a method

for, not simply heat dissipation, but a more holistic thermal control system using a small-scale, passively controlled device.

## B. Objective

It is quite clear that there is presently, and will continue to be, the need for simple and reliable methods for dissipating precise amounts of thermal energy while maintaining the operating temperature of small-scale, heat-producing, portable devices under a variety of operating conditions. With that said, it is the objective of this work to determine if there is a micro heat pipe thermal control system, composed of various combinations of heat pipes and working fluids, that can maintain the temperature of a device to within a specified range over a span of operating conditions, and if so what is that configuration?

The majority of the research within this effort involved the creation of several computer models to simulate and better understand the overall heat transfer characteristics of the system as a whole, as well as the creation of a model to determine the effective thermal conductance and heat transport capacity of individual micro heat pipes based on the operating conditions and given working fluid contained within them.

### 1. Problem Definition

As a means of addressing this seemingly broad issue and to address aspects of the problem that are truly of interest, the present research will focus on what could be considered a very generic situation. A thin, 1.25 mm thick plate of aluminum, consistent with what may be used in any number of electronics packaging applications will be exposed to an input of thermal energy on one end. The total dimensions of

the aluminum plate are to be 50 cm by 125 cm with the input heat area being 15 cm<sup>2</sup> located on one of the extreme ends of the plate. A diagram of this setup, which includes appropriate dimensions, can be seen in Fig. 1.

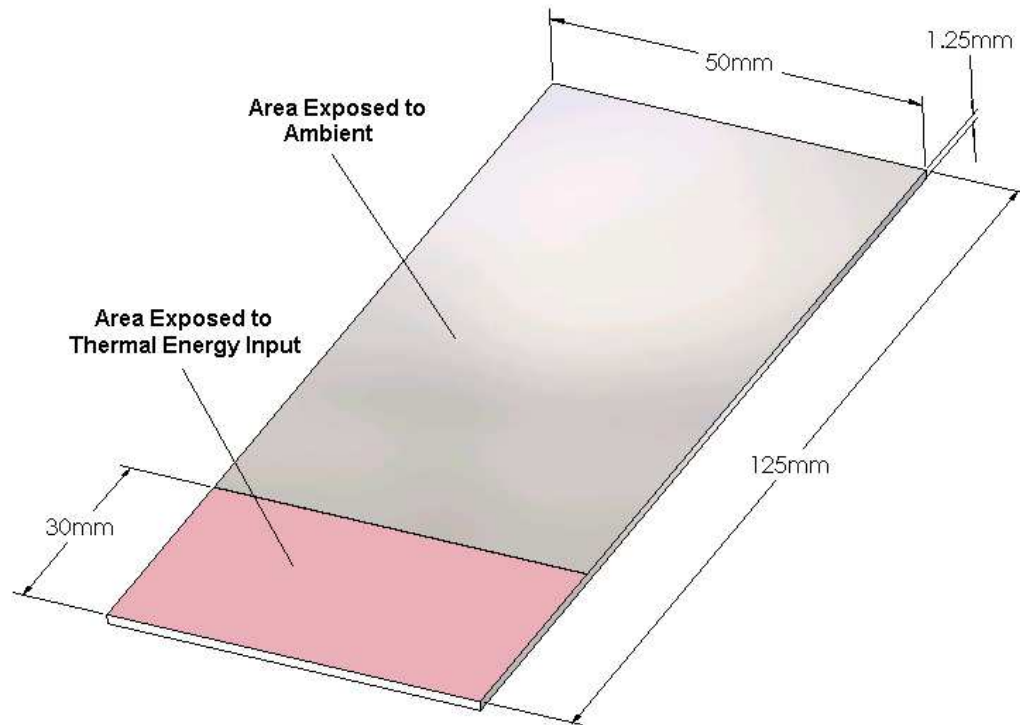


Fig. 1. Dimensioned Diagram of Aluminum Plate

The remaining section of the device, the portion not experiencing an input of thermal energy, is to be exposed to ambient air and thus experience heat loss through natural convection to the surrounding environment. This assumption of natural convection will allow for a conservative level of heat removal. The expected power input to the heated section of the aluminum plate will range from zero to two watts while the ambient temperature will range from zero to forty degrees Celsius. As another

design constraint, there is to be no power required to operate any conceived thermal control system. These design constraints, along with several others, have been summarized and are presented in the Table I.

Table I. Established Design Requirements

Parameter	Requirement
Maximum Heat Input	2.0 W
Minimum Heat Input	0 W
Heat Input Area	15 cm <sup>2</sup>
Heat Rejection Area	47.5 cm <sup>2</sup>
Desired Temperature Control Range	35 to 50 °C
Maximum Ambient Temperature	40 °C
Minimum Ambient Temperature	0 °C
Resistance to Ambient through Leakage	30 K/W
Power Consumption	0 W

### C. Thesis Format

In order to satisfy the described objective, a thermal circuit model of the proposed device as a whole was first developed. The heat transfer characteristics of individual heat pipes were then introduced into this system with an analytical model of an individual micro heat pipe making use of well established micro heat pipe performance and limitation equations. Performance characteristics of micro heat pipe arrays containing differing working fluids were determined and finally optimal working fluids

were identified based on their resulting level of thermal control.

This thesis is organized into chapters based on this basic process. The Background Information chapter contains a description of micro heat pipes and their general operating characteristics as well as a brief history of some of the work that has been done previously involving micro heat pipes and, in particular, variable conductance. The Thermal Control System Design Description chapter walks through the process by which the generalized design of the system currently under investigation was developed. The System Level Modeling Methodology chapter describes in detail the procedure by which the entire system was modeled as a thermal circuit. The Individual Heat Pipe Modeling Methodology chapter then goes on to describe how the individual micro heat pipes were analytically modeled and heat transfer characteristics calculated based on the physical properties of the given working fluids. The resulting data were then incorporated into a thermal circuit from the previous chapter to obtain a full representation of the system as a whole. The results and interpretation from these investigations is presented in the Results and Discussion chapter. Finally, the Conclusions and Recommendations for Future Work chapter presents a discussion regarding the accuracy of results, general closing remarks as well as some recommendations for areas of further investigation.

## CHAPTER II

### LITERATURE REVIEW

Before describing the development of the thermal device design and the model that was used in this study, it is important to first review some of the fundamental principals of micro heat pipe operation and variable conductivity and to have an understanding of experimental and analytical work that has been performed previously by others in this field. This chapter is divided into three sections related to these issues. The “Generalized Heat Pipe” section provides some additional background information to further what was discussed in the previous chapter while the “Micro Heat Pipes” and “Variable Conductance in Heat Pipes” discuss some of the detailed research dealing specifically with these areas.

#### A. The Generalized Heat Pipe

The concept of a heat pipe was first proposed by Gauler in 1944 and first developed and tested by Los Alamos National Lab in 1964. Since that time, these devices have been successfully utilized for a vast array of applications [2]. These uses range from extremely large thermal capacity heat pipes, containing liquid metals such as sodium as a working fluid, to pipes that are only a matter of microns in diameter that can be incorporated into the silicon boards upon which circuits are made. The majority of these heat pipes are designed, based on several important parameters such as expected temperature drop as well as condenser and evaporator area, in order to transfer a maximum possible amount of heat from heat source to heat sink.

The most basic heat pipe consists of an evacuated and sealed container, or “case,” containing a working fluid along with a wicking structure that runs the length of the device. When one end of the heat pipe is exposed to a heat source, the working

fluid present at that end is caused to evaporate. As the working fluid continues to evaporate, the vapor pressure rises in such a way as to force the vapor to travel to the condenser end of the heat pipe. When the vapor reaches the relatively cooler condenser end, it condenses back into its liquid form, releasing its latent heat of vaporization.

In order for the working fluid to return to the evaporator end of the heat pipe and complete the cycle, there must be some mechanism present by which to return the working fluid while in its liquid state. In the case of typical heat pipes, this task is accomplished with the use of a wicking structure. This structure, typically containing small parallel grooves, porous material or a mesh, allows the condensed fluid to travel back towards the evaporator end of the device via the capillary pumping phenomenon. It is the difference in the radius of curvature of the liquid-vapor interface meniscus that causes the pressure difference which is responsible for maintaining the return flow of liquid. This concept will be discussed in greater detail in the later chapters. Illustrated in Fig. 2 is the basic schematic for a generalized heat pipe which illustrates the most important heat pipe components.



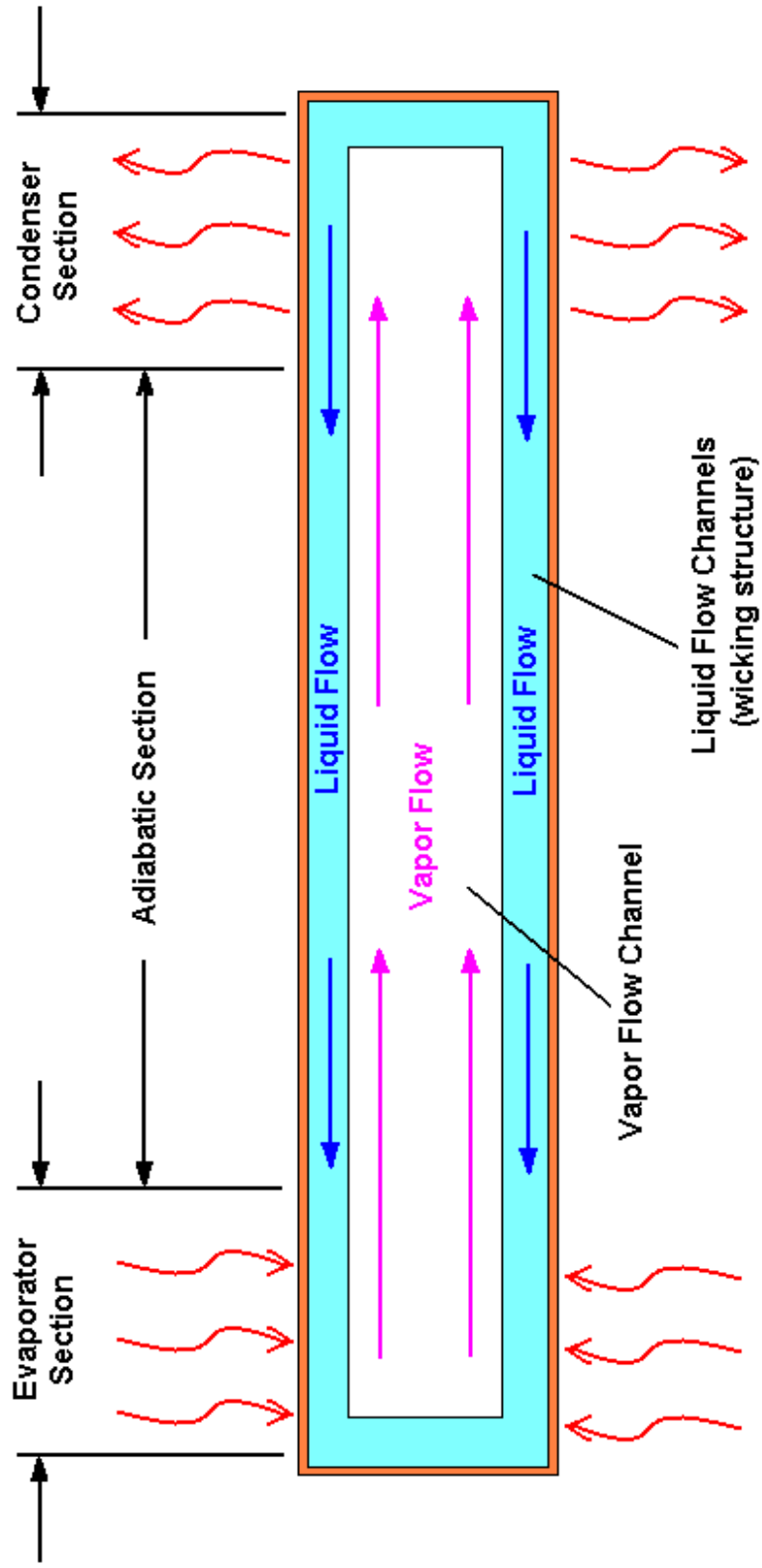


Fig. 2. Conventional Heat Pipe Schematic

## B. Micro Heat Pipes

The micro heat pipe is one of the aforementioned derivations of the generalized heat pipe. The distinct difference between the two, however, is that instead of a porous material, mesh or small parallel grooves, the liquid return arteries of the micro heat pipe are incorporated into the geometry of the device case. In order for a micro heat pipe to operate effectively, there must exist an internal crevice with an angle acute enough such that working fluid is able to, due to its surface tension, form a flow channel for the return flow of liquid. A generalized schematic of a typical micro heat pipe with a triangular cross sectional area can be seen in Fig. 3.

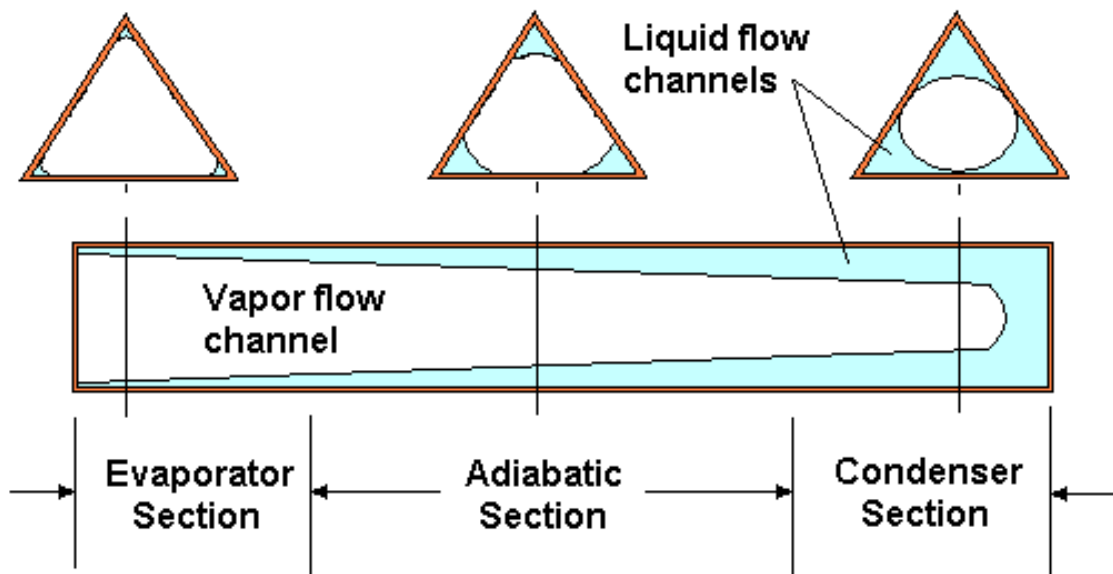


Fig. 3. Generalized Triangular-Shaped Micro Heat Pipe Schematic

The concept of a micro heat pipe was first introduced by Cotter [4] in 1984 as a means to promote uniform temperature distributions and promote thermal control within semiconductor devices. During that time, a micro heat pipe was defined

by Cotter as one “so small that the mean curvature of the liquid vapor interface is necessarily comparable in magnitude to the reciprocal of the hydraulic radius of the total flow channel” [4]. Peterson [5] later expressed Cotter’s statement in more succinct mathematical terms as:

$$\frac{r_c}{r_h} \geq 1 \quad (2.1)$$

where  $r_c$  is the mean radius of curvature of the liquid vapor interface and  $r_h$  is the hydraulic radius of the entire fluid flow channel. This expression serves to distinguish between true micro heat pipes and miniature heat pipes which are simply smaller versions of traditional heat pipes [2]. Again, it is the acute angles of the inner corners in the flow passages that serve as liquid return arteries rather than a mesh or porous wicking structure.

Over the past twenty years, there has been a great deal of research, both analytical and experimental, with the goal in mind of better understanding and improving micro heat pipe operation and performance. The earliest analytical model to describe the steady state heat transport capacity of a generalized micro heat pipe was developed by Cotter [4]. His model served as the basis for many of the subsequent models that have been developed since that time. Cotter’s model, like previously developed models for large heat pipes, was derived using the momentum equation and does provide for a fairly accurate prediction of micro heat pipe performance. Cotter’s model does, however, have several shortfalls and limitations which have since been addressed [2], [3].

The traditional modeling techniques as applied to standard heat pipes can be found explained in great detail in both Chi [6] and Dunn and Reay [7]. The approach

to heat pipe modeling presented in those resources involves the determination of what is known as the “capillary limit.” As mentioned previously, it is this capillary pumping phenomenon that allows the return of the liquid phase of the working fluid from the condenser to the evaporator. Should the capillary limit of such a device be exceeded, it would indicate that the combined liquid and vapor pressure drops that have developed along the length of the device have become greater than the maximum pumping ability of the wicking structure. This shortcoming in pressure would cause for the return flow of fluid to the evaporator to cease, effectively “stopping” the functioning of the device as a whole. The modeling approach presented by both Chi [6] and Dunn and Reay [7] involves the calculation of the maximum capillary pumping pressure with the use of the Young Laplace capillarity equation. The various pressure drops resulting from the liquid and vapor flows are calculated by integrating the pressure gradients along the length of the device.

Somewhat later, Babin et al. [8] developed a model for micro heat pipes that took into account other influential factors that govern micro heat pipe operation. Their model was shown to much more accurately predict micro heat pipe performance than the model developed by Cotter. Their new work included pressure drops due to body forces as a result of gravity, as well as new terms for both the vapor and liquid pressure drops. One primary assumption which has since been questioned is whether the flow of the working fluid in the liquid phase should be modeled after Hagen-Poiseuille flow. An additional important assumption was that at the condenser-end of a micro heat pipe, the radius of curvature of the liquid-vapor meniscus would be simply the largest possible given the cross section of the case.

In 1994, Duncan and Peterson [9] developed an analytical model to more accurately predict the radius of the liquid/vapor interface in the evaporator as a function of input power. Since, by calculating this radius and then assuming a linear change

in radius from evaporator to condenser, one can calculate the optimum liquid charge for a given power input.

Faghri [3] was later able to more accurately, under some conditions, predict the heat transport capability of a micro heat pipe using a two-dimensional analysis approach. It was found by his work that vapor-liquid interfacial interactions play significant roles on the total heat transport capacity.

Further studies in this area focused on the more complex heat transfer occurring at the liquid/vapor interfaces such as the thin liquid film existing at the evaporator end of the device. The evaporation of thin films in V-shaped channels, for example, was examined by Ha [10] in which a model was developed for the heat transfer characteristics of the evaporating thin film on the groove wall.

### C. Variable Conductance in Heat Pipes

Although maximizing the level of heat transferred is clearly an understandable goal in most cases for those working with devices such as a heat pipes, there are many other instances in which a variable conductance device would be more desirable [3]. A variable conductance heat pipe (VCHP) has the ability to not only transfer a significant amount of thermal energy when required, but also the resulting inverse ability to manage, to some extent, the thermal characteristics of a system and thereby maintain overall operating temperatures. This second characteristic is of considerable value when dealing with situations where low temperatures are just as detrimental to overall device operation as are excessively high temperatures.

As with heat pipes in general, over time there has spawned a great many VCHP design derivatives. Among these derivations are designs such as excess-liquid heat pipes, vapor-flow modulated heat pipes, liquid-flow modulated heat pipes or thermal

diodes, and electrical or mechanical feedback control VCHP's [7]. While all somewhat different in operational specifics, a generalized version of a non-condensable gas buffered VCHP is represented by the illustration in Fig. 4. It can be seen that the non-condensable gas and the working fluid of the device are separated by a distinct boundary. As this boundary moves along the length of the device due to changing operating temperatures, the effective condenser length of the device is also caused to change. The predictable nature of this physical change in condenser area over which heat transfer occurs is what may be utilized to effectively control the operating temperature of the device.

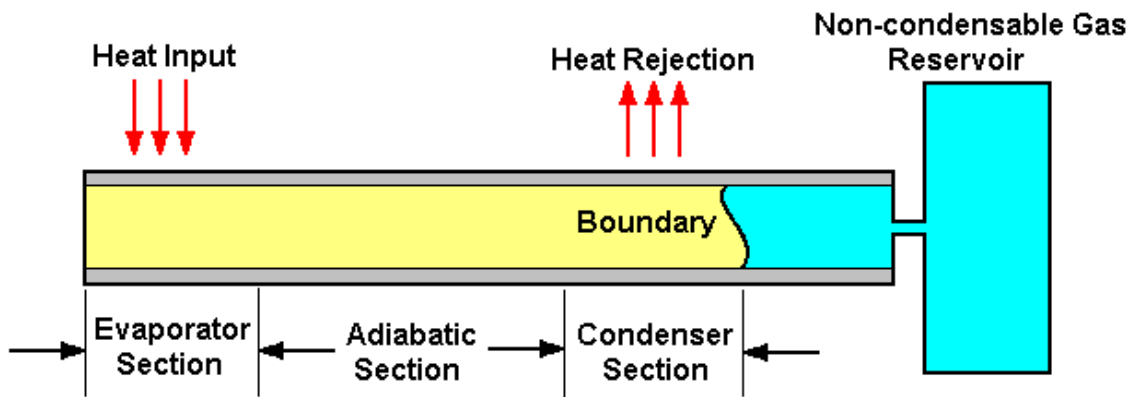


Fig. 4. A Gas-Buffered Variable Conductance Heat Pipe with Reservoir

There exist a great number of instances in which a variable conductance thermal management device has been employed, the majority of these devices having been met with great success. For example, in 2001, Wantanabe et al., [11] developed a high-temperature VCHP for the purpose of controlling the temperature of Sodium-sulfur batteries. In order to charge and discharge efficiently, these batteries must be kept above  $300^{\circ}\text{C}$ . Excess heat, however, often results in reduced lifetime. It was their

desire to construct the device in such way as to maintain the evaporator temperature at a constant value using a method that has no need for external power, sensors or moving parts. The high temperature, variable conductance heat pipe that they designed provided ample temperature control capability and, as a result, improved the charge/discharge efficiency of their batteries. Their method, much like the design illustrated in Fig. 4, was one of introducing a non-condensable gas into the condenser section of the heat pipe. By incorporating the use of a “gas-loaded” heat pipe into their design, they were able to effectively regulate the evaporator end temperature of the device and thereby improve the performance and longevity of their batteries.

Unfortunately, in order to be effective this VCHP method requires the use of a sizeable gas reservoir such that, in instances of high heat flux, the non-condensable gas has sufficient volume to collapse into so that the full length of available condenser area can be utilized for heat transfer. Additionally, the variable conductance heat pipes that are currently being manufactured on a commercial basis are nowhere near the size scale that would be acceptable for use in a smaller, more compact, and portable application.

There has, in an effort to address some these size constraint issues, been the development of altogether different designs that could possibly lend themselves to variable conductance. The size scale of interest for this investigation will be dealing with a device having a fluid flow hydraulic diameter on the order of one millimeter. It been shown, for example, that micro-CPL’s can be applied for chip level cooling applications [12] and could, along with LHP’s, certainly be applied to a study dealing with the size scale of current interest. Due to the fact, however, that micro heat pipes and micro heat pipe arrays have proven to be both reliable and effective in dissipating heat produced by small, compact devices [13], [14], [15], it would seem that a micro heat pipe would be of greatest interest in this particular study.

Another solution to this size constraint issue is the possibility of using a working fluid which itself, independently of case design, exhibits a variability in its own effective thermal conductivity. As would be expected, the majority of the attention that has been focused on heat pipes with regards to determining optimal working fluids (or combinations of fluids) has been addressed fluid candidates that would yield the maximum possible level of heat flux before dryout occurs [16]. There has, however, been several studies that point to the making use of inherent fluid properties as a means of temperature control.

One such study by Nagasaki and Hijikata [17], points to the use of a binary mixture of fluids as a means of varying the overall thermal conductance of the heat pipe as a whole. In their research, they use a binary vapor, a combination of R113 and R11 to achieve a level of conductance variability with respect to temperature. Through their numerical analysis and agreeing experimental data, it was shown that in the case of small heat loads, a non-condensing region was formed in the upper part of the condensing section due to the accumulation of the more volatile component of vapor. The length of the non-condensing region was shown to increase with decreasing heat load, thus limiting the amount of heat that could be radiated to ambient.

A similar study by Kiatsiroat [18], sought to enhance the heat transport characteristics of a thermosyphon with the use of an appropriate binary working fluid. Although only three working fluids (water, methanol and triethylene glycol) were considered and studied, other variables considered in this study were pipe diameter and working temperature. Most importantly, their work illustrated that, for mixtures, the weighted average of the heat transfer coefficient of each component can be used to predict the total heat transfer coefficient.

Overall however, these binary fluid combinations have been met with limited success, showing only marginal effectiveness in providing a sufficient level of thermal



control. It is the effort of this study, however, through an evaluation of a myriad of single component fluids, to identify fluids that exhibits this independent variable conductance property to the extent that it is able to maintain the operating temperature of the evaporator of the system regardless of heat input or ambient operating temperature.

## CHAPTER III

## THERMAL CONTROL SYSTEM DESIGN DESCRIPTION

Prior to analyzing the extent to which differing fluids allow for various levels of effective thermal control, it is necessary to first discuss the system level design; that is, how micro heat pipes are to be incorporated into the original aluminum plate as described in Chapter II. The diagram, as presented earlier to describe the aluminum plate, is shown again in Fig. 5.

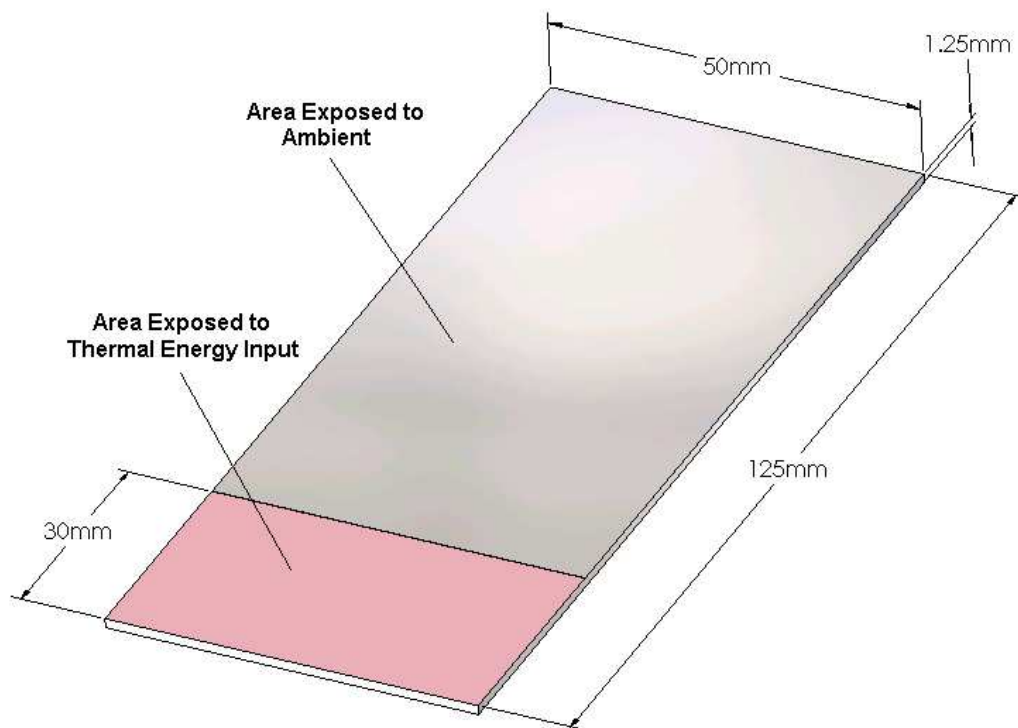


Fig. 5. Dimensioned Diagram of Aluminum Plate

As was discussed to some extent in Chapter II, the vast majority of micro heat pipes manufactured to date are machined or etched into one homogeneous substrate

material. A manufacturing process such as this is very much in line with Cotter's [4] originally envisioned micro heat pipe concept with heat pipes being contained within the boards upon which electrical circuits are printed and acting as a simple heat spreaders, removing thermal energy from hot electrical circuitry.

This straightforward manufacturing process, however, presents a clear dilemma in the case that is presently being considered. The process by which these heat pipes are created within a single substrate calls for one continuous material from which to begin the etching or machining process. It can be seen that the material remaining between the heat pipe channels, not removed in the manufacturing process serving as a container for the working fluid, represents a significant path for thermal leakage. Even if the substrate material containing the channels is of a relatively low thermal conductivity, this path for thermal leakage would allow energy to bypass the micro heat pipes, thereby limiting their effectiveness as a thermal control device.

Since it is the goal of this particular design to effectively regulate the evaporator-end temperature of the device, it follows that there must be a significant level of thermal separation between the heat source and sink such that the heat pipes alone are allowed to regulate the level of heat transfer between these two points. Shown in Table II are the different conditions that may arise as a result of the various combinations of operating conditions.

Table II. Design Needs due to Different Combinations of Operating Conditions

	Low Thermal Input	High Thermal Input
High Ambient Temp.	Variable	Maximize Heat Dissipation
Low Ambient Temp.	Minimize Heat Dissipation	Variable

It is obvious that in order to minimize the level of thermal energy that is dis-

sipated, which is a requirement at the low ambient temperature/low thermal input combination, there must be a significant thermal resistance between the heated section and ambient. In order for the heat pipes themselves to have more exclusive control over the amount of thermal energy being transferred, rather than the surrounding material, it was established that the evaporator section of the aluminum plate would be thermally separated from the condenser section with the use of a 5mm-wide section of thermally insulating rubber ( $k = 0.03 \text{ W/m} \cdot \text{K}$ ). This rigid section of rubber can be easily bonded to the two adjacent aluminum plates in such a way as to retain the overall structural integrity of the plate as well as to eliminate as much of the thermal contact resistance between the sections as possible. This rubber section is illustrated with appropriate dimensions in Fig. 6.

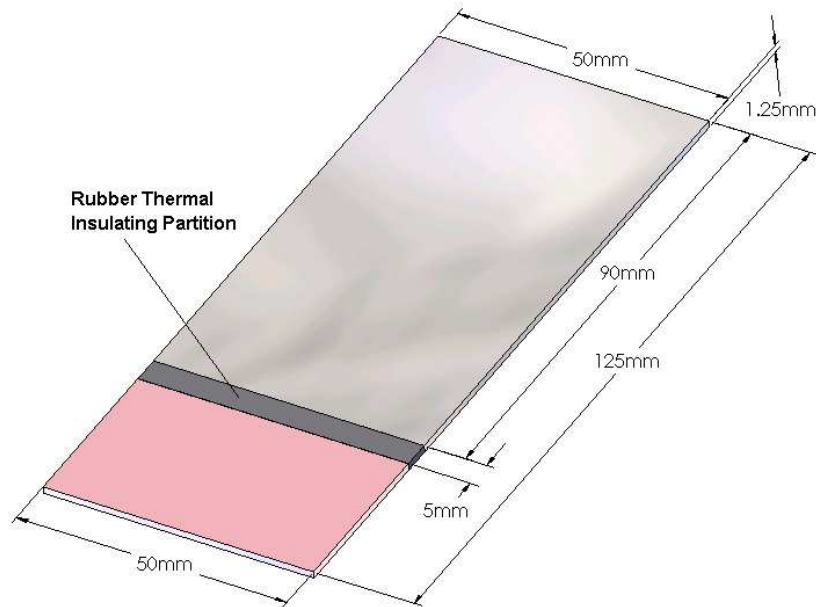


Fig. 6. Aluminum Plate with Rubber Thermal Insulator Partition

The next step is the determination of the method by which a micro heat pipe or series of pipes would be incorporated into this design. As previously mentioned, the traditional method for micro heat pipe fabrication involves the creation of small grooves into a substrate and then the sandwiching of another similar plate onto the machined or etched surface to form fully enclosed channels for fluid flow. Given that the “plate” in question is in fact three separate plates consisting of two different materials, this fabrication technique would not be feasible - especially when one considers the fact that sustaining a pressurized system would also be made significantly more difficult given the various adjoining materials.

It was for these reasons that the walls of the heat pipes are to be made of a continuous, thin-walled commercially available, triangular-shaped, stainless steel hypodermic tubing. To incorporate the tubes into this design, each of the plate sections could be machined at the horizontal midplane and then sandwiched around the tubing, creating an embedded micro heat pipe system. Fig. 7 provides a cross sectional view of this design while Fig. 8 provides a wider view with an arbitrary number of parallel embedded micro heat pipes for illustrative purposes.

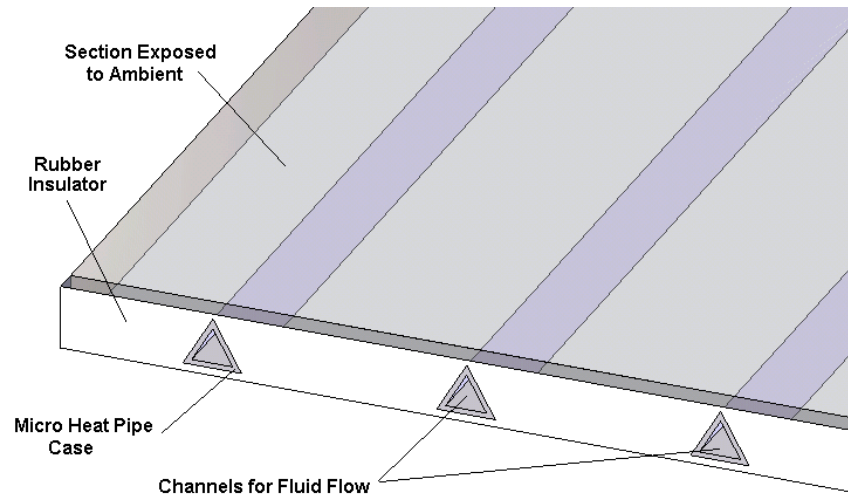


Fig. 7. Detailed Cross Sectional Illustration of Embedded Micro Heat Pipe System

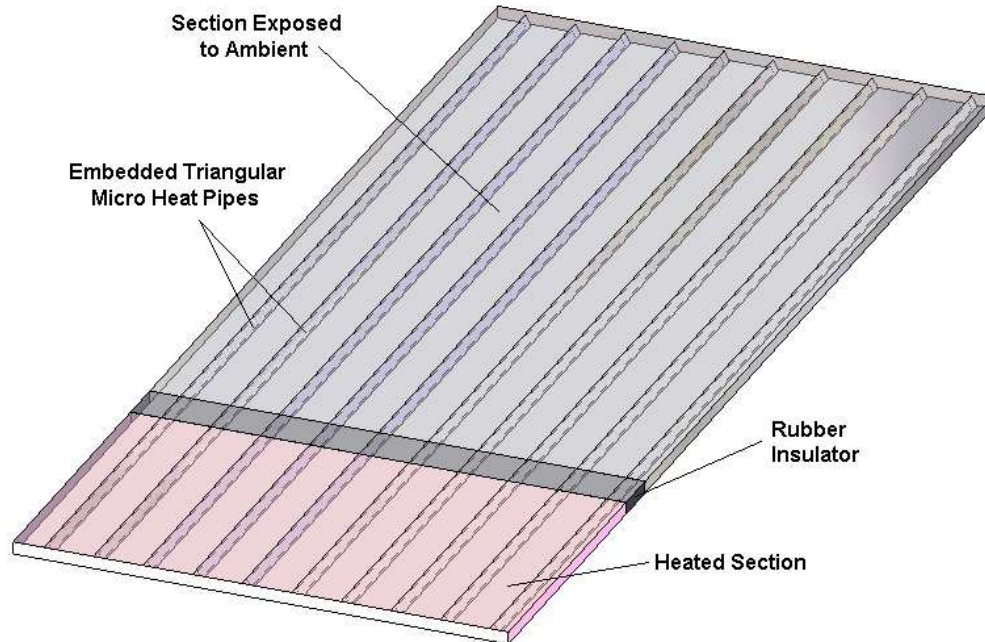


Fig. 8. Illustration of Embedded Micro Heat Pipe Placement and Orientation

Upon further examination of such a system, however, one may be quick to question whether the placement of a continuous length of conductive material through the length of the device would bring about the same thermal leakage issues that were present prior to the addition of the rubber insulator. This question is resolved upon examining the geometries and physical properties of the various components.

Although it is desired to limit the amount of heat being conducted through the axial length of the shell to the condenser at times of low heat input, this should not be at the expense of limiting the amount of thermal energy that is allowed to conduct through the shell radially within the evaporator and into the working fluid of the micro heat pipe.

The micro heat pipe shell walls are constructed of stainless steel, a material with a relatively low thermal conductivity ( $17 \text{ W/m}\cdot\text{K}$ ) when compared to the surrounding aluminum ( $215 \text{ W/m}\cdot\text{K}$ ). The resistance to conduction through a given material can be expressed by the following:

$$R = \frac{L}{kA} \quad (3.1)$$

Where  $L$  is the length,  $A$  represents the cross sectional area and  $k$  is the thermal conductivity of the material. The cross sectional area of a 0.1mm thick, 1mm tall triangular section of tubing is nearly 250 times less than the area through which heat would be conducted radially. Furthermore, length is nearly 650 times greater. Because of this geometry, it is seen that the resistance to thermal conduction axially through the shell of the heat pipe is several orders of magnitude greater than the resistance radially into the working fluid of the heat pipe.

Thus, having almost entirely separated the two sections of the device from one

another on a thermal basis, it can be seen that the only path of reasonable conductance through which thermal energy can travel to the cooler end is through the working fluid of the heat pipe. Therefore, by employing this design, the amount of heat transferred between these two sections is made to depend almost exclusively on the operating characteristics of the embedded heat pipe(s). With the size of the heat pipe having been selected to be an equilateral triangle with height 1mm and wall thickness 0.1mm, the only remaining factors that can influence the heat transfer of the system are the number and spacing of the individual heat pipes and the working fluid contained within them.

The overall design having been established, it is the remaining goal of this thesis is to identify the working fluid and corresponding optimal number of channels that will allow for the greatest level of thermal control, that is the ability to keep the evaporator-end temperature to within the specified limits.



## CHAPTER IV

### SYSTEM LEVEL MODELING METHODOLOGY

#### A. General Approach to Modeling

The first step in the overall analysis process is the modeling of the entire device at the system level. This chapter discusses the steps that were taken to achieve this goal while the following chapter explains how individual heat pipes were modeled such that they can be incorporated into this system level model.

The “Possible System Level Modeling Approaches” section of this chapter presents several of the approaches to modeling a system containing heat pipes that were initially considered and highlights some of the advantages and disadvantages to each of these choices. The “Chosen System Level Model Description” section further elaborates on the method that was chosen and the justification for doing so while the “System Model Thermal Circuit Analysis” walks through the details of establishing this model including the calculation of each of the individual resistances. Finally, the “Thermal Circuit Solution Process” section describes the actual solution routine that was implemented.

#### B. Possible System Level Modeling Approaches

There currently exist several approaches that may be applied to the task of modeling a thermal system containing heat pipes. A few of the most common of these approaches are presented and discussed briefly in the following subsections.

## 1. Full Two-Phase Thermohydraulic Modeling

One possible method that was considered was the development of a full, two-phase model that would require the use of both computational fluid dynamics and finite element analysis. This approach would have likely been very accurate in describing the thermal properties of the system and would provide a great level of detail as to the temperature distribution across the device. Drawbacks to this approach, however, would have involved the difficulty in accurately modeling the complexities of phase change at specific locations within the heat pipe as well as the process being both time consuming and excessive.

## 2. High Conductivity Solid Material Analogy

Another method, which is actually practiced by engineers with some degree of regularity involves using commercial thermal analysis software to simply model a heat pipe as a slender solid rod, possessing an extremely high level of thermal conductivity. Although this method does provide a good first order estimate of a temperature distribution that would result from the use of a heat pipe, there are many that would disagree with the appropriateness of such an approach. For example, Johnson et al, [19] noted that it “is a common misconception that heat pipes can be modeled as solid bars or rods with an artificially high thermal conductivity.” They go on to note that some of the inaccuracies in this modeling approach arise from the fact that the conductance of heat pipes are independent of transport length provided that the limitations are not exceeded which is not the case with a solid material. Additionally introducing nodes with artificially high thermal conductivities can be disruptive to numerical solution routines, giving way to situations where solutions cannot converge [19].

### 3. Thermal Circuit Model with Appropriate Resistances

The thermal circuit analogy is a method that serves to link a heat source to a heat sink through a network of thermal resistances. The thermal circuit model is a method that is accurate, simple to implement, widely accepted, and relied on throughout the literature. Much like an electrical circuit, such a model allows for a series of equations to be established which, when solved, yield both individual temperatures at locations between resistances within the circuit as well as heat flux through a given thermal circuit path. For these reasons, a thermal circuit setup was chosen as the means by which the final analysis step would be taken.

#### C. Chosen System Level Model Description

For the present case, the thermal circuit analogy serves to link the evaporator end of the device, where the input of thermal energy is seen, to the heat sink that is the ambient environment, through a series of thermal resistances, both in series and parallel. The majority of these resistances are, for the most part, constant, in that they depend solely on material properties and geometric factors of the device which do not change significantly with temperature. These simple resistances in the thermal circuit were calculated based on the thermal conductivity of the material, the cross sectional area and the distance through which the heat transfer is taking place.

The effective thermal conductivities of the heat pipes, on the other hand, will vary to a much greater extent as well as in a much more complicated manner, depending not simply on the total temperature drop, but instead on the evaporator-end temperature of the device and various thermophysical properties of the given fluids. By combining the characteristic equations describing the thermal resistance for heat pipes containing various fluids with the simple resistances presented by the other materials, a comprehensive thermal circuit system was developed that will provide an adequate understanding of how this device would behave thermally, on a system level.

A generalized schematic of the thermal circuit system that was used can be seen, first described in Fig. 9 and illustrated in more detail as a more abstract representation in Fig. 10. It should be noted that Fig. 10 illustrates only one embedded heat pipe whereas, in most cases, there would be multiple heat pipes operating in parallel. The thermal circuit model, in the cases of multiple heat pipes, can be simply extended with additional heat pipes appearing identical to the original one, to add the additional paths for the transfer of thermal energy.

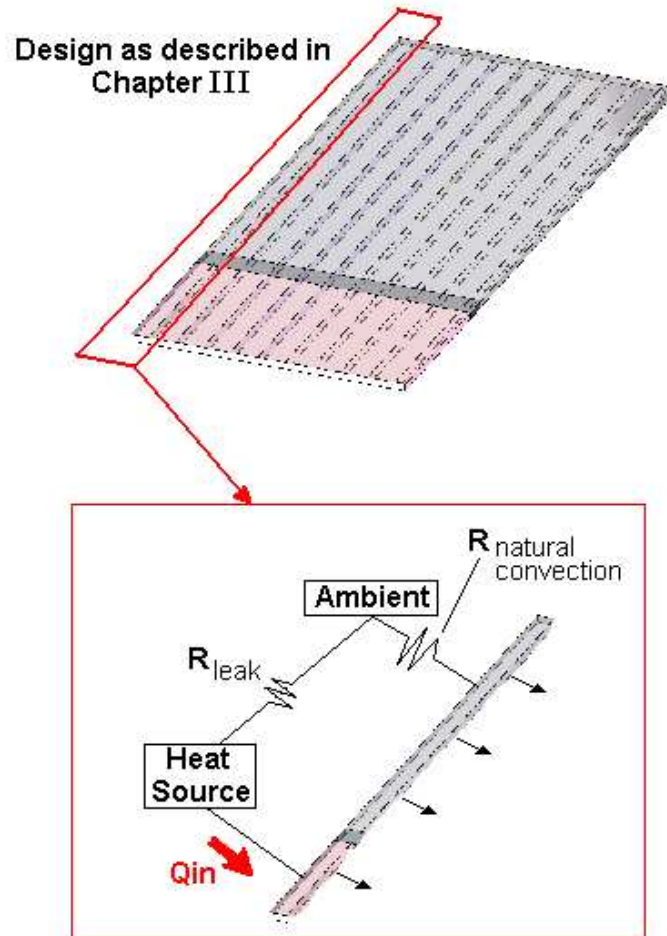


Fig. 9. Thermal Circuit Model Taken from Original Design Illustration

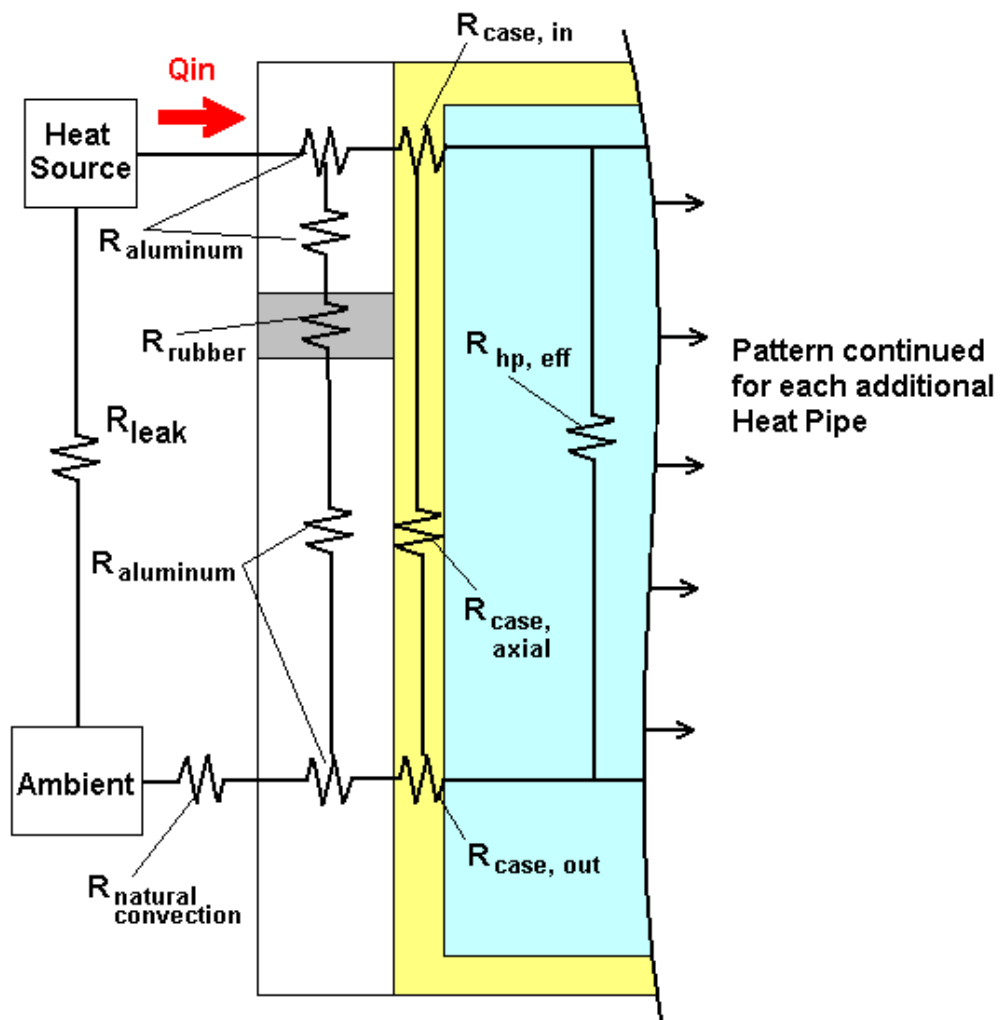


Fig. 10. Thermal Circuit Model Representation with Included Thermal Resistances

#### D. System Model Thermal Circuit Analysis

In order to create an analogous thermal circuit system, it was first necessary to accurately calculate each of the various thermal resistances. The method for determining the majority of these thermal resistances within the system is a fairly standard procedure and can be found explained in great detail by Incropera and DeWitt [20]. Since the aluminum, rubber and stainless steel are homogenous materials with constant geometry for a given number of heat pipes, the majority of the resistances involving these materials can be represented as standard one dimensional conduction through a homogenous material and thus are able to take the following form:

$$R = \frac{\delta}{kA} \quad (4.1)$$

where  $\delta$  is the length through which the conduction of taking place,  $A$  is the cross sectional area and  $k$  is the coefficient of thermal conductivity of the given material.

What was found to be one of the more influential of the thermal resistances existing in the circuit is that which represents the convection occurring between the condenser section of the plate and the ambient environment. This resistance can be expressed in the following form:

$$R_{nat} = \frac{1}{\bar{h}A_{surf}} \quad (4.2)$$

where  $A_{surf}$  is the surface area of the condenser section of the device that is exposed to ambient and  $\bar{h}$  is the convection coefficient between the surrounding air and the surface that can be described by the following correlation involving the Nusselt number:

$$\bar{N}u_L = \frac{\bar{h}L}{k_f} \quad (4.3)$$

where  $L$  is the characteristic length of the geometry and  $k_f$  is the thermal conductivity of the fluid. The Nusselt number  $Nu$ , meanwhile, is given as the following [20]:

$$\bar{N}u_L = 0.54 Ra_L^{1/4} \quad (10^4 \leq Ra_L \leq 10^7) \quad (4.4)$$

$$\bar{N}u_L = 0.15 Ra_L^{1/3} \quad (10^7 \leq Ra_L \leq 10^{11}) \quad (4.5)$$

Where the Rayleigh number,  $Ra_L$ , is defined as:

$$Ra_L = \frac{g\beta(T_s - T_\infty)L^3}{\alpha\nu^2} \quad (4.6)$$

In equation (4.6),  $\alpha$  represents the thermal diffusivity of the ambient air while  $\nu$  can be interpreted as the momentum diffusivity. For an ideal gas,  $\rho = p/RT$ , the volumetric thermal expansion coefficient  $\beta$ , can be reduced as follows:

$$\beta = -\frac{1}{\rho} \left( \frac{\partial \rho}{\partial T} \right)_p = \frac{1}{\rho} \frac{p}{RT^2} = \frac{1}{T} \quad (4.7)$$

It should also be noted that all thermodynamic properties for the fluid, being air in this case, are evaluated based on the film temperature,  $T_f$  which is a average of the ambient and surface temperatures given as:



$$T_f = \frac{(T_s + T_\infty)}{2} \quad (4.8)$$

By combining equations (4.2) through (4.8) for each of the operating conditions of each proposed fluid, the resistance due to natural convection can be calculated and incorporated into the model. In keeping with the assumption of natural convection being the only mode of heat removal from the cool end of the device a more conservative result will be obtained.

Another set of thermal resistances that must be considered which are later incorporated into the effective resistance of the heat pipe are the solid/liquid and liquid/vapor interfacial resistances existing between the flow phases within the heat pipes. It has been found that the resistance at the liquid/solid interface can be neglected in almost all cases [3]. However, the liquid/vapor interface resistance can at times be much more significant. Faghri [3] developed an expression to describe the liquid/vapor interfacial resistance within a heat pipe operating at steady state, which is given as the following:

$$R_{if} = \frac{1}{h_{if}A_{if}} \quad (4.9)$$

where  $A_{if}$  is the total interfacial area and  $h_{if}$  is given by the following:

$$h_{if} = \left( \frac{2\alpha}{2 - \alpha} \right) \left( \frac{\lambda^2}{T_v v_{fg}} \right) \sqrt{\frac{M_v}{2\pi R T_v}} \left( 1 - \frac{p_v v_{fg}}{2\lambda} \right) \quad (4.10)$$

where  $\lambda$  is the latent heat of vaporization,  $M$  is the molecular weight,  $P$ , and  $T$ , represent pressure and temperature, respectively, and  $\alpha$  is assumed to be close to

unity for single component fluids.

In addition to interfacial resistances, there is a small thermal resistance within the vapor column along the length of the heat pipes. This resistance, the axial resistance of the vapor as described by Peterson [2], is given by the following expression:

$$R_{v,a} = \frac{T_v(P_{v,e} - P_{v,c})}{\rho_v \lambda q} \quad (4.11)$$

where  $P_{v,e}$  and  $P_{v,c}$  represent the vapor pressure at the evaporator and condenser ends, respectively. Finally, the thermal resistance of the liquid channels along the length of the heat pipes is typically calculated, for standard heat pipes on the basis of a wick structure/fluid combination based on cross sectional area. Given the fact that there is no wicking structure in the case of micro heat pipes and the fact that this resistance is working in parallel with that of the vapor column which is seen to be several orders of magnitude smaller, it is a reasonable assumption to disregard this very large resistance.

For calculation purposes, the effective thermal resistance of the individual heat pipes were calculated and then inserted into the model of the system. The effective thermal resistance of the heat pipe is made up of the liquid/vapor interfacial resistance and axial vapor column resistance. The complete list of resistances found in the thermal circuit model can be seen summarized in Table III. Accompanying the resistances are order of magnitude approximations which better indicate which of the resistances are most influential to the circuit as a whole. The actual values for many of the resistances will vary depending on both operating conditions as well as number of heat pipes that are present.

Table III. Individual Thermal Circuit Resistances

Resistance	Expected Order of Magnitude
Aluminum Spreading Resistance ( $R_{Al,s}$ )	$10^{-3}$ K/W
Stainless Steel Case Resistance In ( $R_{ss,e}$ )	$10^{-2}$ K/W
Stainless Steel Case Resistance Out ( $R_{ss,c}$ )	$10^{-2}$ K/W
Axial Stainless Steel Case Resistance ( $R_{ss,a}$ )	$10^{+4}$ K/W
Axial Effective Heat Pipe Resistance ( $R_{hp}$ )	$10^{-2}$ to $10^0$ K/W
Axial Resistance Aluminum (evap.) ( $R_{Al,e}$ )	$10^{-1}$ K/W
Axial Resistance Aluminum (cond.) ( $R_{Al,c}$ )	$10^0$ K/W
Axial Resistance Rubber ( $R_{insul}$ )	$10^{+3}$ K/W
Resistance from Condenser to Ambient ( $R_{nat}$ )	$10^1$ K/W

### E. Thermal Circuit Solution Process

During the solution process, two factors were varied, the ambient temperature and the power input to one end of the aluminum plate. These two factors varied over a range of 0 to 40 degrees Celsius and from 0 to 2 watts, respectively. The resulting temperature was determined over this range of operating conditions for all combinations of fluid choice and configuration (number of heat pipes). Resulting from the thermal circuit model was a series of equations that were solved simultaneously, yielding all individual temperatures existing between the established resistances in the circuit including the evaporator temperature, which is the value of primary interest. Upon the completion of each solver routine, a check was made with respect to the heat transport limitation of the heat pipe. These determination of these limitations is discussed in great detail

in the following chapter. If the heat transport limit was in fact exceeded, the heat pipes were assumed to be in an “off” state, effective resistance reevaluated to reflect this change, and the solution process repeated. This solution process can be seen in Fig. 11.

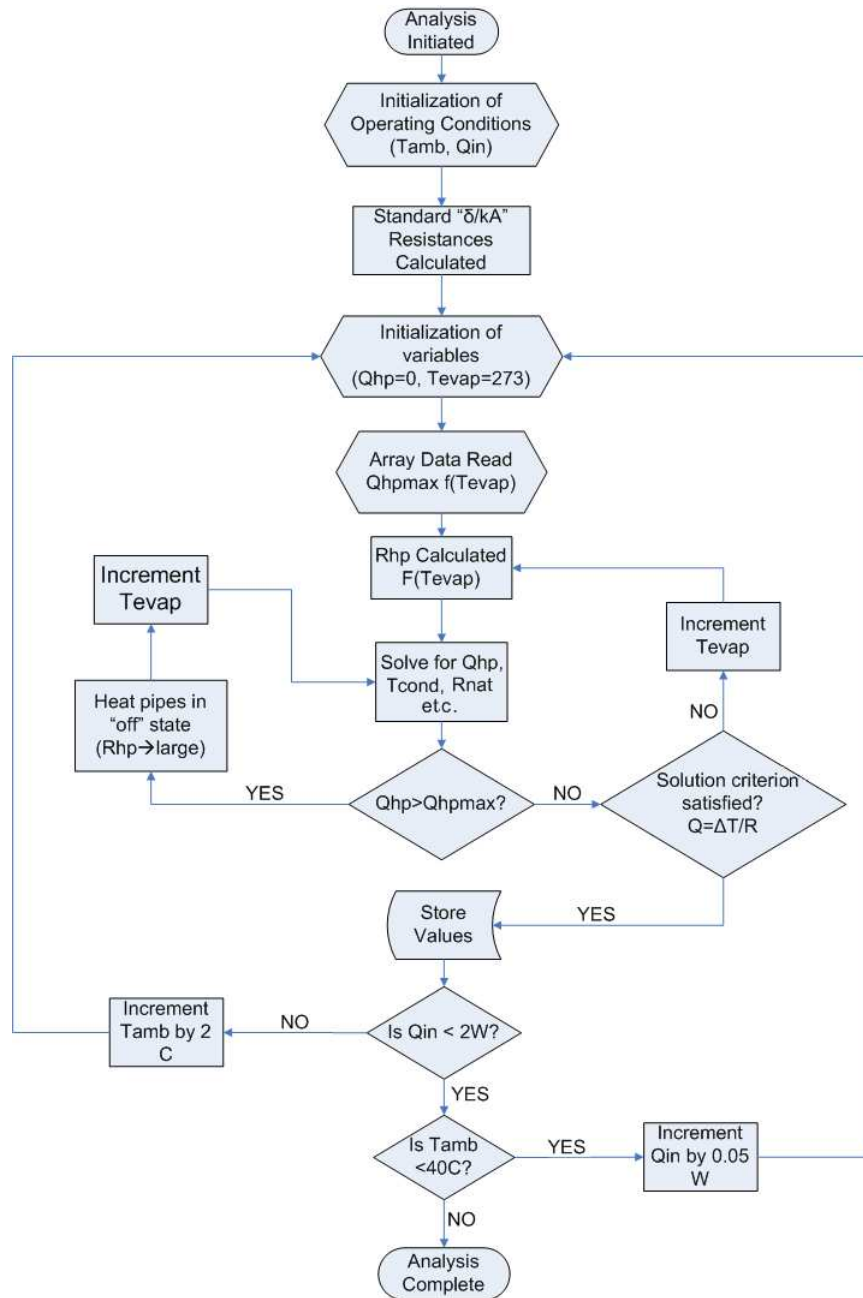


Fig. 11. Thermal Circuit Solution Routine

## CHAPTER V

### INDIVIDUAL HEAT PIPE MODELING METHODOLOGY

In order to verify the system level modeling work, it is necessary to determine the actual heat transport capacity of an individual micro heat pipe. In the previous chapter, a method for determining resistances was established which will yield the necessary thermal energy that should be transported by a heat pipe to satisfy the system. This chapter will discuss the process by which transport limitations were determined which can then be compared to the results from the system level calculations.

As discussed in the Literature Review Chapter, there have already been a number of studies done with the primary focus being that of numerically modeling and accurately predicting the performance of micro heat pipes. The issue that is currently being addressed is further obfuscated, however, by the fact that it is not desired to simply design for a single input power and operating temperature, which has typically been the case, but rather for an appropriate response over a range of operating conditions.

The basic analysis process in this case, however, can proceed along a path similar to that of the more standard scenario. The maximum heat transport capacity for a heat pipe at a given operating temperature may be limited by a number of factors which depend greatly on the thermophysical properties of the chosen working fluid.

These operational limits will be discussed in detail in the following sections. What is generally understood to be the most important operating limit is discussed in the “Capillary Limitation” section with its various components broken down in the subsections therein. The “Other Important Heat Pipe Operating Limits” sections introduces these lesser influential operating limits. Finally, the “Micro Heat Pipe Modeling Procedure” section describes the calculation procedure by which solutions

were generated as well as the process by which working fluid property data were gathered.

#### A. The Capillary Limitation

It can be seen from previous investigations [2], [3], that for the case of micro heat pipes, as opposed to standard heat pipes, the performance limitations are almost exclusively a function of the capillary limit of the device. Because of this, the capillary limitation is to be used in the calculation of the maximum heat transport limit, with the lesser performance limitations that have been developed being used simply for validation purposes.

It has been found that in order for any heat pipe to operate, The available capillary forces must be larger than that needed to circulate the fluid [7]. This relationship may be better thought of in terms of a pressure drop balance which can be expressed by the following inequality:

$$\Delta P_c \geq \Delta P_l + \Delta P_v + \Delta P_g \quad (5.1)$$

where  $\Delta P_c$  is the total change in capillary pressure between the evaporator and condenser ends of the device,  $\Delta P_l$  is the pressure drop resulting from the inertial and viscous forces in the return of liquid to the evaporator from the condenser, and  $\Delta P_v$  is the pressure drop resulting from similar forces in the vapor flow in the reverse direction.  $\Delta P_g$ , meanwhile, represents the pressure drop due to gravitational forces. Investigations by Peterson et al. [2] have determined that the pressure drop due to gravitational forces may be split into axial and normal hydrostatic pressure drops which are dependant on the angle the heat pipe makes with the horizontal. It was later

stated by Peterson [5] however, that “in cases where surface tension forces dominate, such as micro heat pipes, both of these terms can be neglected.” To determine whether this is in fact the case for the application at hand, one can simply evaluate the Bond number, which is a ratio of gravitational and surface tension forces. The Bond number is defined to be the following:

$$Bo = \frac{g(\rho_l - \rho_v)L^2}{\sigma} \quad (5.2)$$

where  $g$  is the acceleration due to gravity,  $L$  is the characteristic length,  $\sigma$  is the surface tension of the working fluid and  $\rho_l$  and  $\rho_v$  are its liquid and vapor densities, respectively. A quick evaluation of prospective fluids at expected operating temperatures clearly indicates, that for the size scale currently under investigation, the force due to the surface tension acting on the fluid is the dominant factor; for the majority of fluids, by several orders of magnitude. Thus, it can be seen that the pressure drop terms of interest when dealing with micro heat pipes are simply the liquid and vapor pressure drops and that equation (5.1) may be reduced to the following form:

$$\Delta P_c \geq \Delta P_l + \Delta P_v \quad (5.3)$$

### 1. Maximum Capillary Pumping Pressure

The term on the left side of equation (5.3),  $\Delta P_c$ , represents the maximum available capillary pumping pressure between the two ends of the micro heat pipe. This available pumping pressure will be the difference in capillary pressures at the evaporator and condenser, or



$$\Delta P_c = (P_v - P_l)_e - (P_v - P_l)_e \quad (5.4)$$

This capillary pressure differential is related to the difference between the radii of the liquid-vapor interface menisci present within the micro heat pipe. This value may be evaluated, for the pressures at each of these locations with the application of the Young-LaPlace equation of capillarity which is given to be the following:

$$P_v - P_l = \sigma \left( \frac{1}{r_1} + \frac{1}{r_2} \right) \quad (5.5)$$

where  $\sigma$  is the surface tension of the working fluid, and  $r_1$  and  $r_2$  are the principal radii of curvature of the liquid-vapor interface meniscus.

By applying equation (5.5), and operating under the assumption that the radius of curvature in the condenser region of the heat pipe is equal to the largest radius that can exist given the cross sectional dimension,  $\Delta P_c$  can be expressed as the following:

$$\Delta P_c = \frac{2\sigma}{r_{c,e}} - \frac{2\sigma}{r_{c,c}} \quad (5.6)$$

where  $r_{c,c}$ , the capillary radius at the condenser is equal to  $233.3\mu m$  for the 1mm tall stainless steel case with wall thickness of 0.1mm. This is the largest possible radius of curvature of the liquid-vapor interface given the cross sectional area which is an assumption consistent with that of the work done by Peterson [2]. Fig. 12 more clearly illustrates these different radii at the opposing ends of the micro heat pipe.

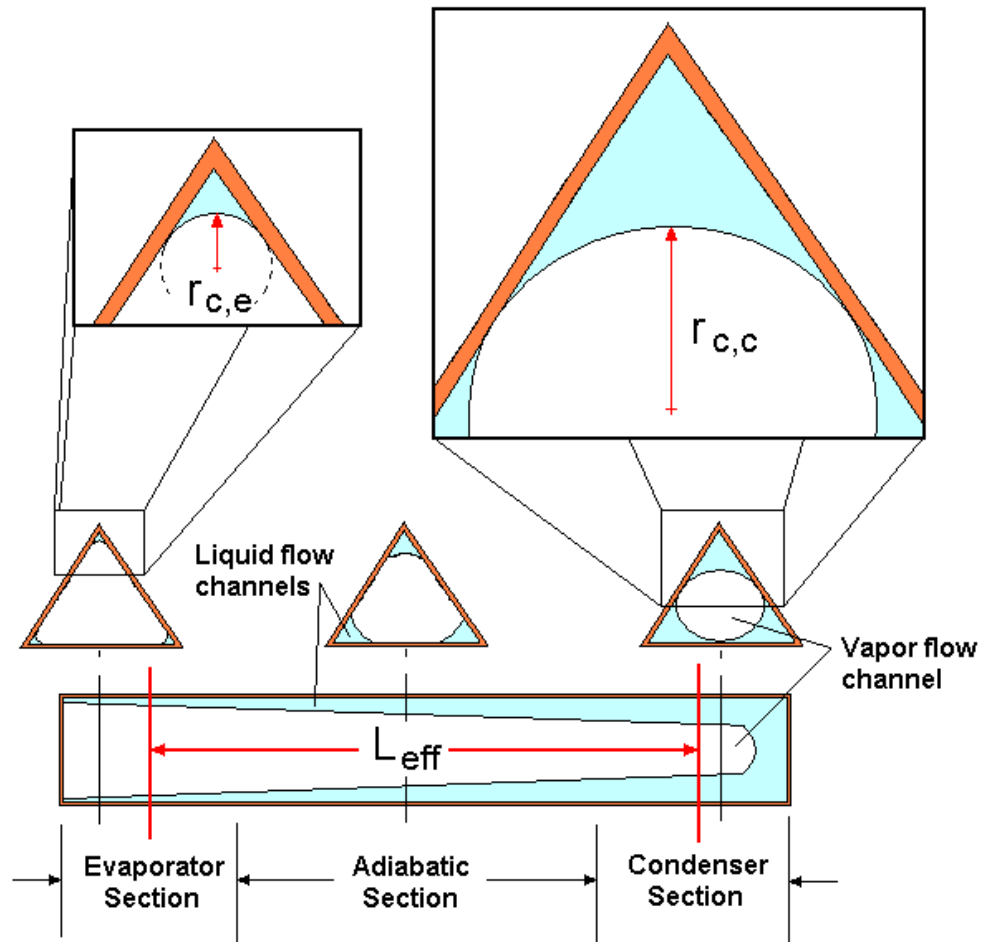


Fig. 12. Detailed Sketch of Micro Heat Pipe

While the condenser-end radius is assumed constant for calculation purposes, the radius of curvature on the evaporator-end is expected to vary, depending on the level of heat input, and must be determined using an analytical solving technique. This solving technique would be required to vary the value for the evaporator end meniscus radius until reaching a point the opposing pressures are balanced.

By substituting the constant value of  $233.3\mu m$  for the condenser-end meniscus radius terms into equation (5.6), an final equation is developed that gives the maximum available capillary pumping pressure as a function of the evaporator-end liquid-vapor capillary meniscus radius. This expression, for a triangular shaped micro heat pipe at steady state operating conditions, can be expressed as follows:

$$\Delta P_c = 2\sigma \left( \frac{1}{233.33\mu m} - \frac{1}{r_{c,e}} \right) \quad (5.7)$$

## 2. Liquid Pressure Drop

The first term on the right side of equation (5.3), the pressure drop due to the liquid fluid flow within the pipe,  $\Delta P_l$ , is given by the following expression:

$$\Delta P_l = \frac{(f_l Re_l) \mu_l L_{eff} q}{2A_l r_{h,l}^2 \lambda \rho_l} \quad (5.8)$$

where  $f_l Re_l$  is the friction factor-Reynolds number product,  $q$  is the heat transported by the device,  $A_l$  is the cross sectional area of liquid flow,  $r_{h,l}$  is the hydraulic radius of the liquid flow channel,  $\mu_l$ ,  $\lambda$ , and  $\rho_l$  are the liquid viscosity, enthalpy of vaporization and liquid densities of the working fluid, respectively.  $L_{eff}$  is the effective length the heat pipe which is given by the following expression:

$$L_{eff} = L_a + \frac{L_e + L_c}{2} \quad (5.9)$$

where  $L_a$ ,  $L_e$  and  $L_c$  represent the adiabatic, evaporator, and condenser section lengths of the heat pipe, respectively. The effective length of the micro heat pipe is also labeled in Fig. 12. A much more thorough derivation for equation (5.8) can be found in Appendix A as well as in Peterson [2], Chi [6], and Dunn & Reay [7].

### 3. Vapor Pressure Drop

The second of the terms on the right side of equation (5.3) is that which represents the vapor pressure drop,  $\Delta P_v$ . The vapor pressure loss term was originally derived by Chi [6], under the assumption of a steady-state, laminar, fully developed velocity profile. This term takes a similar form as the liquid pressure drop term and like the liquid pressure drop, a much more thorough explanation of that derivation may be found in Appendix A. The results of that derivation, however, are given by the following expression:

$$\Delta P_v = \frac{(f_v Re_v) \mu_v L_{eff} q}{2 A_v r_{h,v}^2 \lambda \rho_v} \quad (5.10)$$

where each of the above terms are representatively similar to those in equation (5.8), involving the liquid pressure drop. In the case of the present equation, however, each of the terms relate specifically to the vapor flow region of the micro heat pipe and the properties of the working fluid while in its vapor phase.

To determine the liquid and vapor cross sectional flow areas, ( $A_l$  and  $A_v$ ), as well as the the hydraulic radii of the liquid and vapor flow regions, ( $r_l$  and  $r_v$ ), for calculation purposes, an method will be employed whereby the dimensions corresponding to

the evaporator and condenser ends will be averaged. With this approach, the liquid and vapor flow cross sectional areas are expressed by the following:

$$A_l = \frac{A_{l,e} + A_{l,c}}{2} \quad (5.11)$$

$$A_v = \frac{A_{v,e} + A_{v,c}}{2} \quad (5.12)$$

The hydraulic radius of the vapor and liquid flow areas will be calculated using the standard convention of the cross sectional area divided by the “wetted perimeter,” or:

$$r_h = \frac{A}{P_w} \quad (5.13)$$

The value for the wetted perimeter to be used in subsequent calculations will be determined in a similar fashion as that of the cross sectional area, which is to average the values for the condenser and evaporator ends. Thus, the wetted perimeter of the liquid and vapor flow are given by the following:

$$P_l = \frac{P_{l,e} + P_{l,c}}{2} \quad (5.14)$$

$$P_v = \frac{P_{v,e} + P_{v,c}}{2} \quad (5.15)$$

Fig. 13 provides a clearer, three dimensional representation of a micro heat pipe with deliberately exaggerated proportions to clearly illustrate the difference between

the evaporator and condenser end capillary radii and to bring a greater understanding to the importance of the previous several equations for the average cross sectional areas and hydraulic radii.

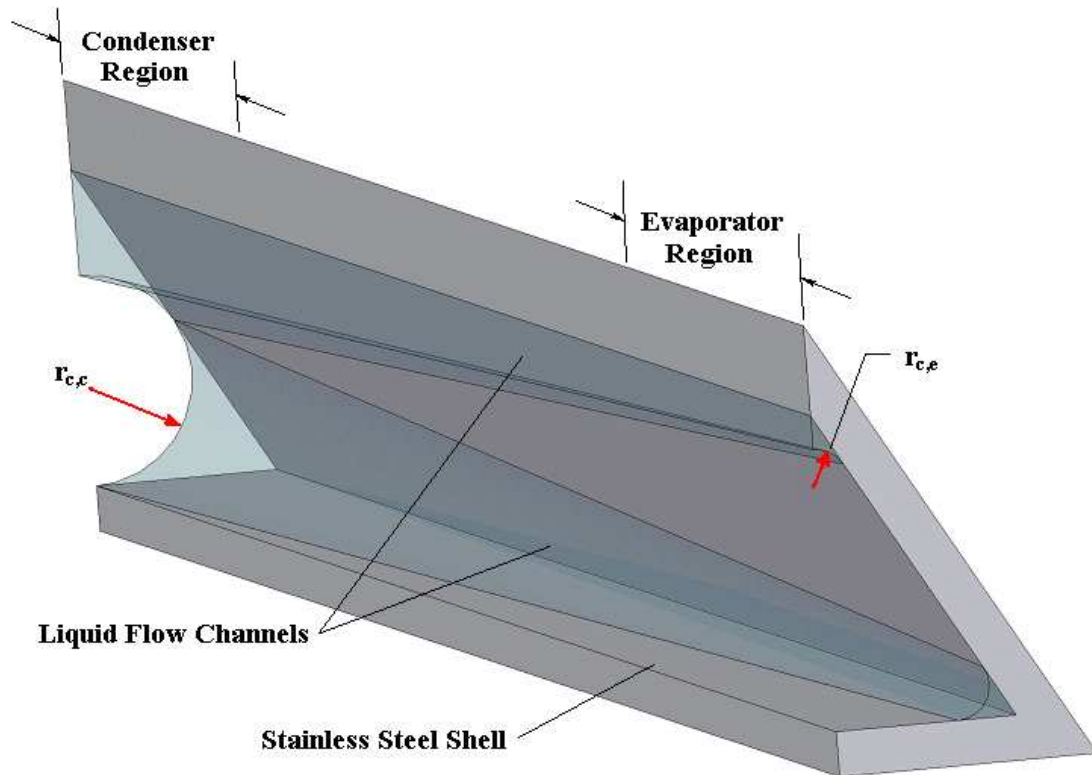


Fig. 13. Three Dimensional Representation of an Individual Micro Heat Pipe Section

## B. Other Important Heat Pipe Operating Limitations

The analytical approach of solving for the heat transport capacity by the balancing of pressure drop terms is one that is widely supported by previous literature. In order to successfully model the device to the extent that one can be sure of the meaningfulness of the results however, it is important to take into account some of the other known operating limits of a micro heat pipe, if only for verification purposes. These limits have been previously studied in great detail [2], [3], [6], [7], and are summarized briefly in the following subsections. It is important that each prospective working fluid be checked with respect to each of these limitations to assure that the pressure balance solution has real world significance. For this reason, each of the heat pipe designs were evaluated, prior to solving for performance using the chosen method, based on the following limitations.

### 1. The Viscous Limitation

The Viscous Limitation, as described by Dunn and Reay [7] and Peterson [2], suggests that a heat pipe operating at low temperatures may experience a smaller total pressure drop than would be acceptable to overcome the viscous forces within the vapor region. This limitation, however, is typically only of concern at extremely low levels of heat input. It can be estimated by the following equation:

$$q_v = d_v^2 \lambda A_v \frac{P_v \rho_v}{64 Re_v L_{eff} \mu_v} \quad (5.16)$$

where  $d_v$  is the average diameter of the vapor flow channel,  $A_v$  is the corresponding cross-sectional area,  $P_v$  is the pressure of the working fluid in the vapor phase, and  $L_{eff}$  is the effective length of the heat pipe defined by equation (5.9).  $\lambda$ ,  $\rho$ , and  $\mu$  are,

again, the latent heat of vaporization, density and viscosity of the fluid, respectively.

## 2. The Sonic Limitation

The Sonic Limitation occurs when the vapor velocity resulting from the pressure difference between the two ends of the device reaches that of sound. The mass flow rate of vapor is then limited by this choked flow situation. This scenario is typically of concern only in heat pipe design when there exists a variation in the amount of phase change undergone by the working fluid along the length of the heat pipe [3]. The maximum heat transfer capacity of a heat pipe experiencing a limitation as a result of this phenomenon is given by the following:

$$q_{s,m} = A_v \rho_v \lambda \left( \frac{\gamma_v R T_v}{2(\gamma_v + 1)} \right)^{1/2} \quad (5.17)$$

where  $A_v$  is the cross sectional area of the vapor flow channel,  $R$  is the universal gas constant, and  $\gamma$  is the ratio of the specific heats for the working fluid in its vapor phase.

## 3. The Entrainment Limitation

The Entrainment Limitation of a heat pipe indicates to what level the opposing vapor and liquid flows will affect one another due to their opposing shear forces at the interface. If a sufficient number of liquid droplets from the liquid flow channels happen to become entrained within the vapor flow, the result will be a dryout of the liquid working fluid at the evaporator end of the device [3]. In order to avoid this limit, the ratio of the viscous forces to the forces resulting from the liquid surface tension, must have a value of less than one. The relationship between these forces is



expressed by the Weber number, which is given as the following:

$$We = \frac{2(r_{h,l})\rho_v V_v^2}{\sigma} \quad (5.18)$$

where  $r_{h,l}$  is the hydraulic radius of the liquid flow channel and  $V_v$  is the bulk velocity within the vapor flow channel. The maximum heat transport capacity of the heat pipe, based on the Weber number, is given to be the following:

$$q_{e,m} = A_v \lambda \left( \frac{\sigma \rho_v}{2(r_{h,w})} \right)^{1/2} \quad (5.19)$$

where each of the terms similarly representative to those in equations (5.16) and (5.17).

#### 4. The Boiling Limitation

The Boiling Limitation of a heat pipe occurs when an excessive level of heat input to the evaporator causes vapor bubbles to block the return flow of condensed fluid from making its way back to the evaporator. An expression that describes the boiling limit of a heat pipe was originally developed by Chi [6] and later modified by Dunn and Reay [7]. This expression is given to be the following:

$$q_{b,m} = \left( \frac{2\pi L_{eff} k_{eff} T_v}{(\lambda \rho_v \ln(r_i/r_v))} \right) \left( \frac{2\sigma}{r_n} - \Delta P_{c,m} \right) \quad (5.20)$$

where  $L_{eff}$  is the effective length of the heat pipe defined in equation (5.9),  $T_v$  is the vapor temperature, and  $k_{eff}$  is the effective thermal conductivity of the liquid-wick combination, which, in the present case, will be simply that of the fluid due to the absence of wicking structure in a micro heat pipe. Finally,  $r_n$  is the nucleation site radius which, according to Dunn and Reay [7], is anywhere from  $2.5 \times 10^{-7}$  to  $2.5 \times 10^{-5}$  meters in nearly all cases.

It can be seen that all of the previously mentioned performance limitations provide a restriction on a heat pipe's ability to function properly above a particular level of input thermal energy. In order to compare the significance of these limitations with respect to one another, one may simply evaluate the expressions over a range of operating temperatures for a given fluid. Plotted in Fig. 14 are the performance limitations for a single microheat pipe, as described in Chapter III, which uses water as its working fluid.

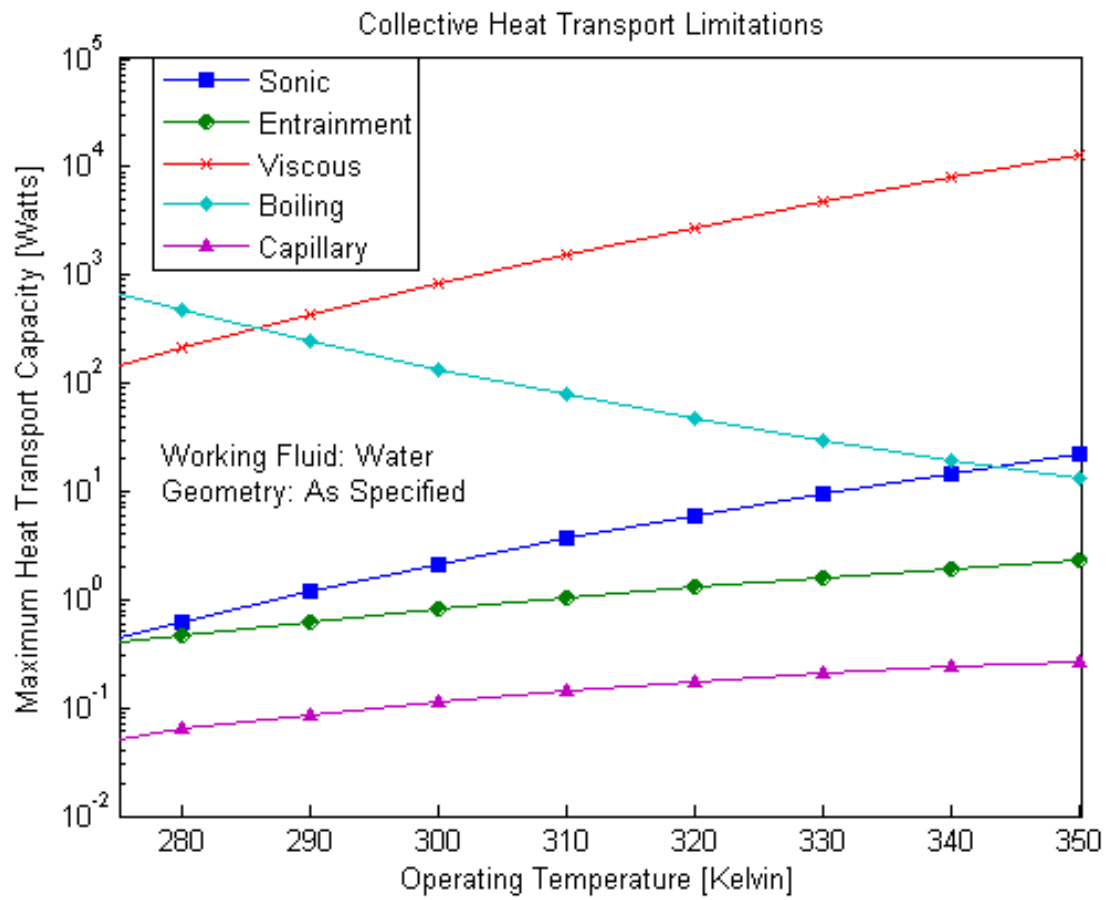


Fig. 14. Various Heat Transport Limitations over a Wide Range of Operating Temperatures for Micro Heat Pipe of Given Dimensions Using Water as a Working Fluid

From Fig. 14, it can clearly be seen that, for the size scale and much broader than the temperature range of interest, it is indeed the capillary limitations that will remain the governing constraint relating to the heat pipe functionality. For this reason, the capillary limitation will be used for the determination of appropriate working fluids and, as a final check, it will be verified that the none of the other limitations are encountered.

### C. Micro Heat Pipe Modeling Procedure

#### 1. Heat Transport Solution Methodology

With the use of the well-established equations that are able to accurately describe the capillary limitation of a heat pipe, the solution procedure is able to proceed in a relatively straightforward manner. One may simply substitute equations (5.7), (5.10), and (5.8) in to equation (5.3), to develop the following equation representing the capillary limitation.

$$2\sigma \left( \frac{1}{r_{c,e}} - \frac{1}{233.33\mu m} \right) = \frac{(f_l Re_l)\mu_l L_{eff} q}{2A_l r_{h,l}^2 \lambda \rho_l} + \frac{(f_v Re_v)\mu_v L_{eff} q}{2A_v r_{h,v}^2 \lambda \rho_v} \quad (5.21)$$

It can be seen that the majority of the terms in equation (5.21) are simply functions of either the geometry of the heat pipe (further clarified by equations (5.11) through (5.15)) or the temperature of the working fluid. In fact, the only term in the above expression that is able to vary independently of these two factors is the radius of the liquid vapor interface,  $r_{c,e}$ , which is located at the evaporator-end of the device.

Furthermore, from the same equation, it can be shown that as the evaporator-end capillary radius,  $r_{c,e}$ , is decreased, the capillary pumping pressure decreases as well, which in turn, increases the heat transport capacity of the device as a whole. A

decrease in this capillary radius has the additional effect, however, of limiting the cross sectional area through which the return flow of liquid working fluid makes its way back to the evaporator. This reduction in cross sectional area for liquid flow results in an increased liquid pressure drop. It is from a balance of these counteracting forces that there exists an optimal value for the liquid vapor interface radius,  $r_{c,e}$ , such that equation (5.21) is satisfied. The point at which this balance takes place is the capillary limitation of the heat pipe.

Since it is the interest of this work to observe how the maximum heat transport capacity varies over a range of operating temperatures, the solution process involves setting a given operating temperature, solving for  $q$  by iteratively varying  $r_{c,e}$  from equation (5.21), and then incrementally increasing the operating temperature and repeating the solving process until a series of solutions has been generated that spans the desired temperature range. At each temperature increment, it is required to recalculate the physical properties of the given working fluid to ensure accurate results. This set of solutions can then be plotted to reveal how the heat transport capacity varies with temperature for a given working fluid. This solution process can be seen represented in graphical form as the flowchart in Fig. 15 on the following page.

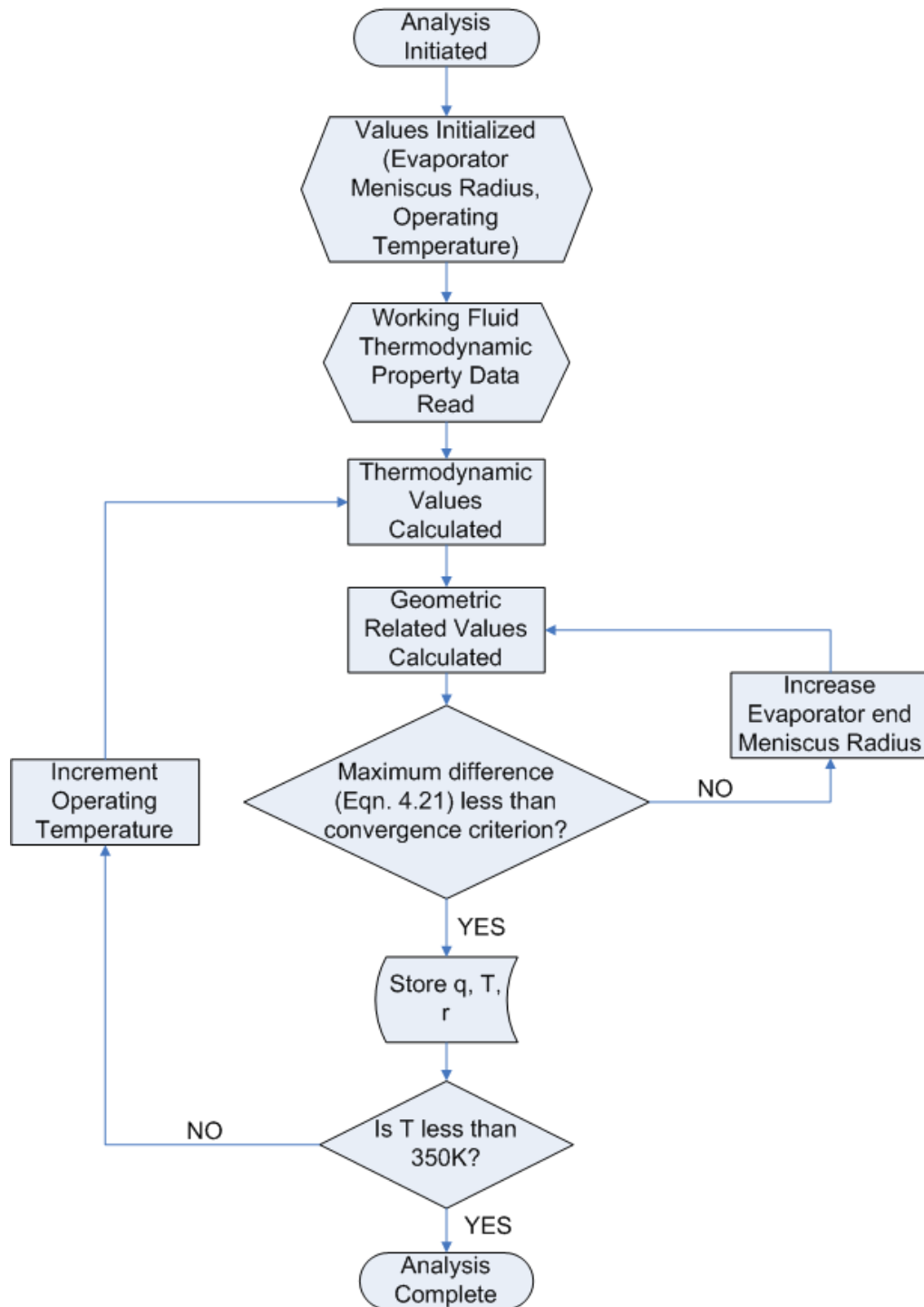


Fig. 15. Individual Micro Heat Pipe Heat Transport Capacity Solution Process

## 2. Working Fluid Property Data and Interpolation

It is likely that one may have already considered the fact, after reading the previous sections, that many of the physical properties of the working fluid, which have a significant effect on heat pipe performance, are themselves, very much dependant upon temperature. A great number of possible working fluids were considered in this study. Initially, working fluid property data were gathered from a variety of sources. This effort proved to be very time consuming and somewhat inaccurate considering the vast number of sources that were required and the fact that many of these sources may be considered dated. It was found that Yaws [21] provides thermophysical property data over the temperature range of interest for over 1500 different materials. It was these data that were used as the source of working fluid chemical properties. Property data were expressed as polynomial functions of temperature which could be easily inserted into any of the previously discussed equations. The data taken from this source included functions for surface tension, liquid density, vapor density, liquid viscosity, vapor viscosity, and latent heat of vaporization. The 1301 fluids chosen for analysis are listed alphabetically in organic and inorganic sections in Appendix B.

## CHAPTER VI

### RESULTS AND DISCUSSION

Once the thermophysical property data were obtained for the working fluids of interest, solution routines matching those pictured in Figs. 11 and 15 of the preceding chapters were performed with the use of the software package MATLAB. This chapter is separated into three sections with the first of these, “Results,” presenting and interpreting the product of these calculations. The “Discussion” section makes mention of what these resulting data mean in terms of thermal management and goes on to discuss some other aspects of this work that may not be initially apparent as well as how well the resulting data corresponds to the initial design requirements. The final section, “Summary of Findings” lists, in more succinct terms, the important aspects of what was learned from this work.

#### A. Results

This section is organized into two subsections; the first of which presents the results from Chapter V, the Individual Heat Pipe Modeling, while the second subsection presents the Chapter IV results which deals with the System Level Modeling.



## 1. Individual Heat Pipe Modeling Results

The process represented by the flowchart shown in Fig. 15 of Chapter V represents the series of calculations that were performed for each of the prospective working fluids. As described, these calculations were performed over a range of micro heat pipe operating temperatures stretching from 275 to 340 Kelvin. This range of operating temperatures, although much broader than ultimately needed, does lead to a fuller understanding of the behavior of the capillary limitation as a function of temperature.

Shown in Fig. 16 are the resulting heat transport limitations of the 1301 prospective working fluids over that wide range of possible operating temperatures. Again, this plot represents the points at which, for a given fluid at a given temperature and in the case of the specified dimensions, the capillary pumping pressure is less than the pressure drops that result from the liquid and vapor flows, rendering the heat pipe inoperative. In the region above these curves for a particular fluid, the heat pipe will not be able to circulate the working fluid back to the evaporator in its liquid phase. The full list of working fluids, both organic and inorganic, that were analyzed during this process may be found listed alphabetically in Appendix B.

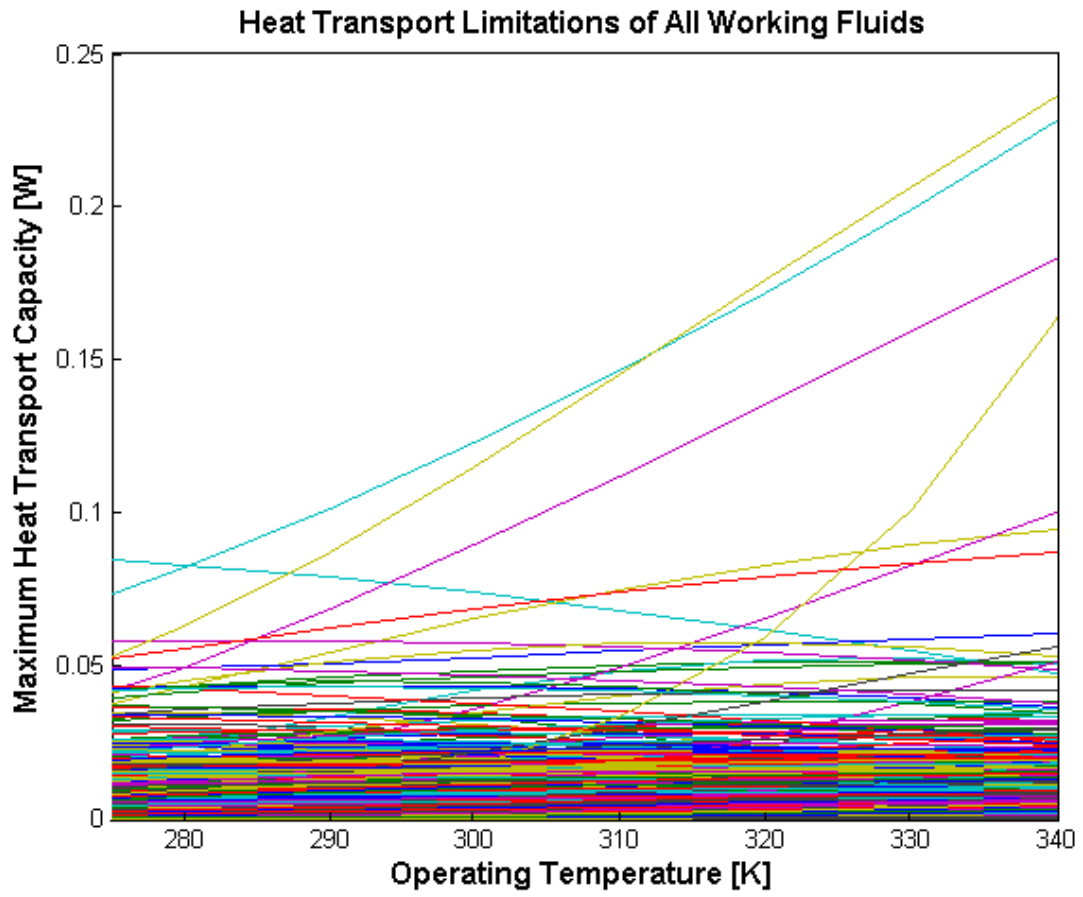


Fig. 16. Resulting Maximum Heat Transport Capacities of All Considered Working Fluids

From the calculation process described in Chapter IV, a significant amount of data were generated and it can be seen the previous figure is quite busy, having such a great number of fluids shown collectively on only one set of axis. Although this plot obviously does not provide sufficient information at a level of clarity such that it may lead to individual fluid identification and study (even if every fluid were individually labeled), what it does clearly illustrate, is the relative working fluid performance, in that several of the fluids are clearly better suited for transporting higher levels of thermal energy than others. Furthermore, this plot lends significant insight, from a simple visual inspection, into which of the prospective working fluids can be immediately excluded from consideration. The first step in the interpretation of these data lies in the of elimination of fluids that are not of interest in order to cut the number of fluids in need of further scrutiny. In terms of selecting a suitable working fluid, there are several important criteria that one must consider.

The first of these criteria relates to the magnitude of the heat transport capacity. Although there is no explicit minimum required level of thermal energy that each individual heat pipe must be capable of carrying, there actually exists a clear limit when taking into account geometric considerations of the device as a whole. With the cross sectional area of the aluminum plate being what it is, 1.25 millimeters thick and 50 millimeters in width, it was decided that no more than thirty parallel heat pipes should be embedded within this area. This number of micro heat pipes represents the maximum reasonable number which can be present given the available cross sectional area. As a result of this decision and the fact that, at some point in the operating region, the heat pipes would be called upon to carry a combined heat load of nearly two watts, the highest level of thermal input in the operating region, the fluids having an individual heat transport capacity that does not surpass 0.06 watts at any operating temperature are obviously not acceptable choices. This requirement

severely reduces the number of possible candidate fluids from a selection of over 1300 to a limited selection of just eight.

With the poorly performing fluids having been removed from the list of possible candidates based on this first selection criteria, the remaining working fluids from both the organic and inorganic lists were again plotted and are shown together in a much more clear fashion in Fig. 17.

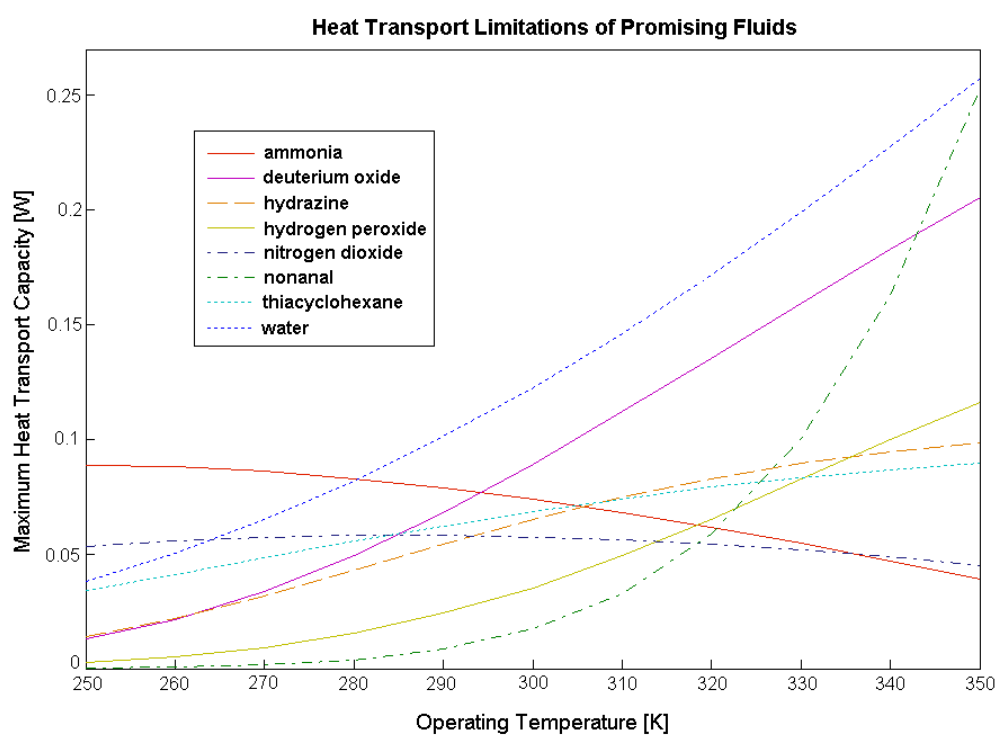


Fig. 17. The Eight Remaining Fluids for Further Consideration

The second of the criteria that was used in the initial selection of appropriate fluids for further examination was not the total level of heat transfer, but rather, the level of variation in heat transfer capacity over the operating temperature range of interest. It is fairly obvious from casual observation that in order to provide some level of thermal control, which is the goal of this research, the heat transport capacity should be higher at elevated temperatures and lower at operating temperatures towards the cooler end of the operating range. The inverse of this case would simply serve to “turn off” the heat pipes in the event of high temperatures, further raising temperatures and cause the heat pipes to remain operational during cases of low temperatures, further reducing temperatures. This is the opposite of providing a level of thermal control and, rather, further extends the evaporator temperature operating range. For this reason, working fluids that exhibit levels of thermal transport capacities higher at low temperatures than at high temperatures may be immediately excluded from consideration. As can be seen from Fig. 17, this restriction eliminates both nitrogen dioxide and ammonia from consideration. It is interesting to note that the latter of these fluids, ammonia, is a common fluid used in heat pipes, however due to the specific operating temperatures of interest in this case, it proves to be a poor choice for this application.

With unacceptable fluids having been removed from the list of potential candidates, a final list of prospective fluids was generated. These remaining fluids are again plotted in Fig. 18, this time over a much more narrow range of operating temperatures with the desired temperature control region highlighted. Additionally, these fluids are listed, with important performance values summarized, in Table IV.

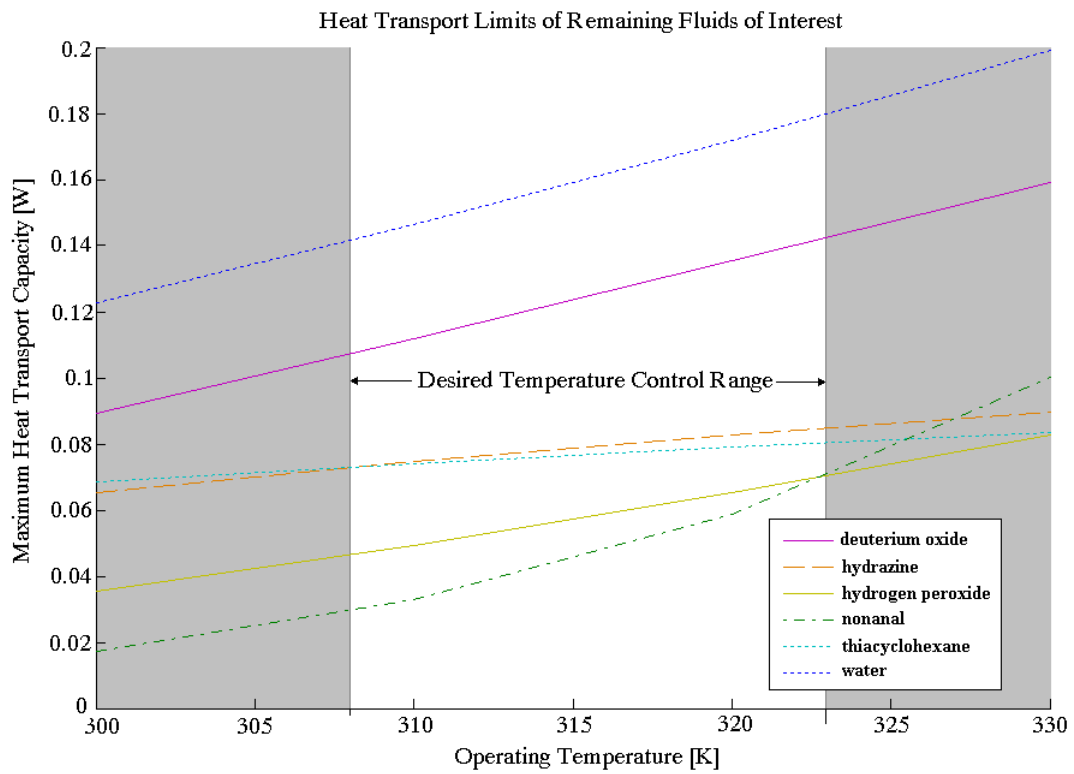


Fig. 18. The Remaining Working Fluids with Highlighted Design Temperature Control Region

Table IV. Resulting Working Fluids for Final Consideration

Working Fluid	Capacity at 40 °C (W)	Capacity at 50 °C (W)
Deuterium Oxide	0.112	0.135
Hydrazine	0.075	0.083
Hydrogen Peroxide	0.049	0.065
Nonanal	0.033	0.059
Thiacyclohexane	0.074	0.079
Water	0.145	0.176

## 2. System Level Modeling Results

These six remaining fluids from the preceding table were then analyzed as being part of the system as described in Chapter V and the process was followed as illustrated by Fig. 11. Resulting from this series of calculations that make use of the thermal circuit analogy of the system, is a surface representing the evaporator temperature of the device over a range of ambient temperatures and heat inputs. One such example of a resulting surface can be seen on the following page in Fig. 19. This particular surface that is illustrated represents the resulting evaporator temperatures for the device containing seven embedded heat pipes using water as a working fluid.

Device Temperature with Seven Heat Pipes Using Water as a Working Fluid

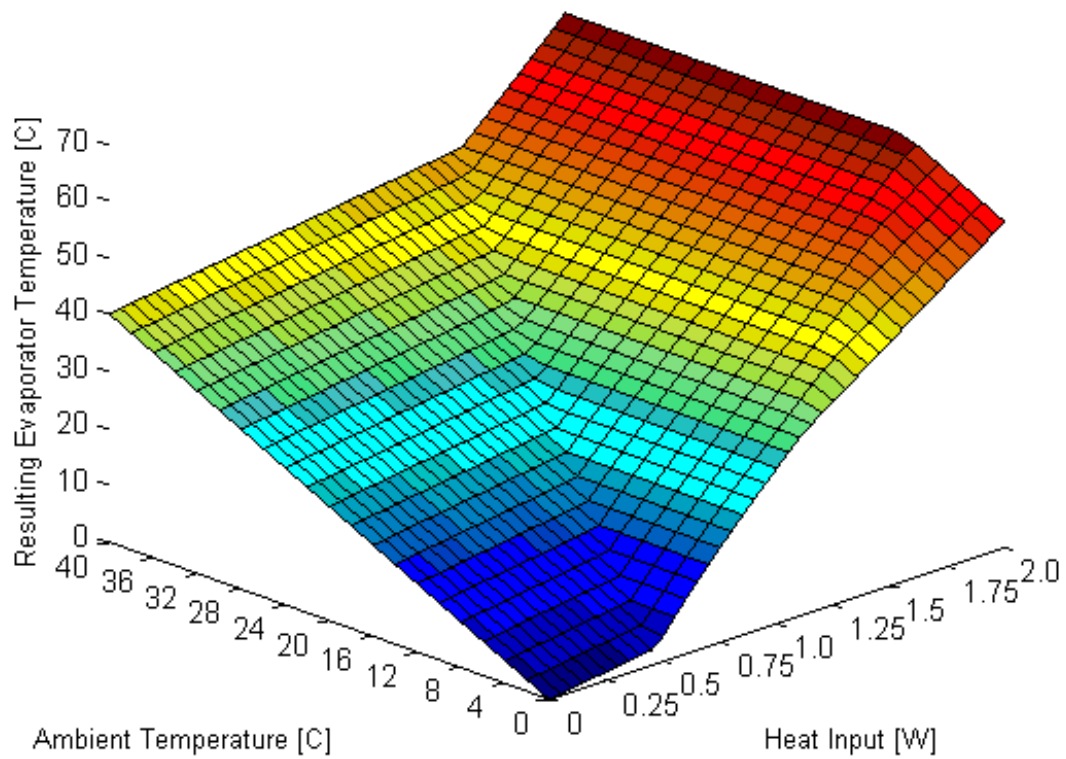


Fig. 19. Temperature Surface for Water as a Working Fluid Contained within Seven Embedded Micro Heat Pipes



It can be seen that the resulting surface varies from 0 °C at the combined conditions of low heat input and low ambient temperature up to temperatures well over 70 °C at two watts of heat input and an ambient temperature of 40°C. As would be expected, this surface will vary greatly depending on the working fluid as well as the number of embedded heat pipes. It is seen that as the number of heat pipes is increased, the resulting evaporator temperature is caused to lower as well as the micro heat pipes syphon away thermal energy from the area of heat input. This causes the resulting temperature of the system to drop. Conversely, as the number of micro heat pipes is reduced, individual pipes will be forced to assume a greater individual role in carrying the total thermal load, which may cause them to exceed their individual capillary limitations. This resulting dry-out will then cause the temperature of the device to rise, again changing the shape of the resulting temperature surface.

As a clear illustration of this changing of the temperature surface with corresponding changes in number of embedded micro heat pipes, Fig. 20 is provided on the following page which clearly shows to what extent this phenomena is taking place as the number of heat pipes is varied. In this series of plots, the resulting temperature surface for the device using water as a working fluid undergoes a change in the number of embedded micro heat pipes from two to twelve, in increments of two pipes.

The process of calculations to determine the resulting evaporator temperatures was repeated for varying numbers of heat pipes contained within the device which, in turn, was performed for each of the remaining prospective working fluids. Again, this method was outlined in Chapter IV.

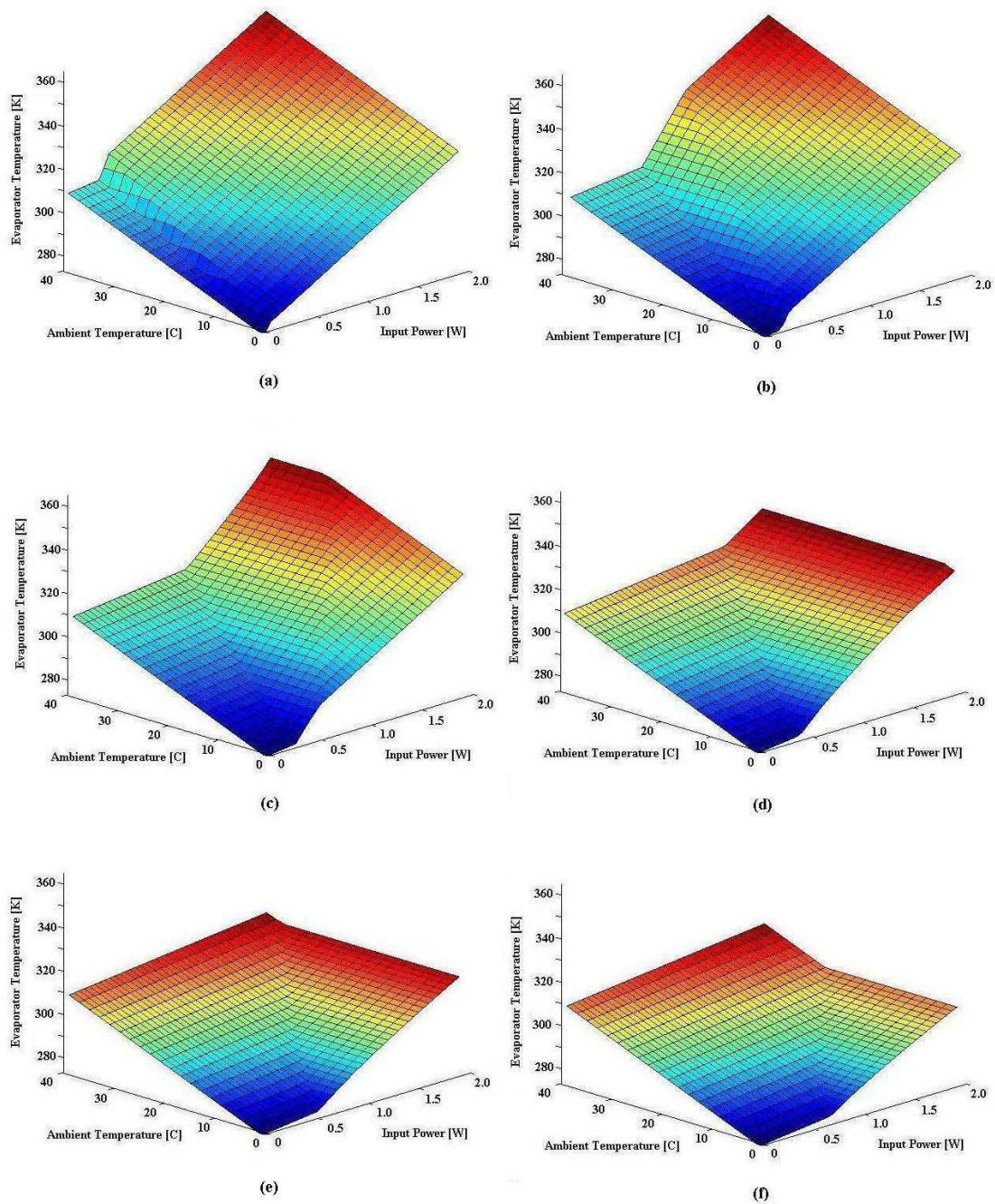


Fig. 20. Resulting Temperature Surface for a Device Using Water as a Working Fluid with (a)Two, (b)Four, (c)Six, (d)Eight, (e)Ten, and (f)Twelve Embedded Micro Heat Pipes

With the resulting data from the process existing in the form of a series of surfaces, the task of evaluating which of these surface represents a better level of thermal control is relatively straightforward. Making this, even qualitative, comparison of the surfaces on the basis of a visual inspection from a three-dimensional perspective, however, proves to be quite difficult as seen from Fig. 21, which shows surfaces representing the resulting temperature of the evaporator-end of the device with two and twelve embedded micro heat pipes. Again, in this plot, water used as the working fluid.

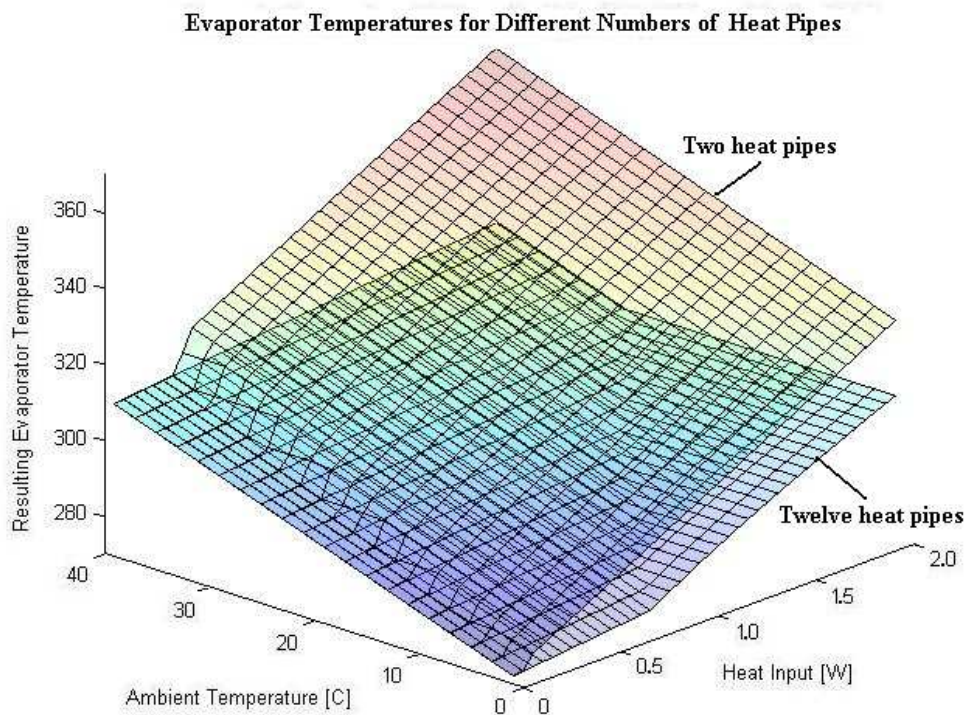


Fig. 21. Multiple Temperature Surfaces Representing Varying Numbers of Micro Heat Pipes with Water as the Working Fluid

Understandably, from a perspective such as the one shown in the preceding figure, it is somewhat difficult to quantitatively determine which number of pipes is most appropriate as defined by the original design requirements. In order to better compare these variations between surfaces representing different numbers of heat pipes, the plot will be viewed in a two dimensional form with only values lying between the prescribed 35°C to 50°C temperature band being illustrated. The surface lying outside of these two limits is essentially “cut away” and not represented on the plot. When visualized in this manner, the resulting plot will instead be a two-dimensional operational region, within which, the design satisfies the design requirements. Fig. 22 represents the same surfaces that were shown in Fig. 21, however only temperature values lying within this control temperature band and thereby satisfying design requirements are shown. This style of displaying the resulting surfaces makes very clear how well a given fluid with a given number of embedded heat pipes is able to satisfy the design requirements and it is with such a plot that a comparison may be made with respect to a system containing different numbers of embedded heat pipes.

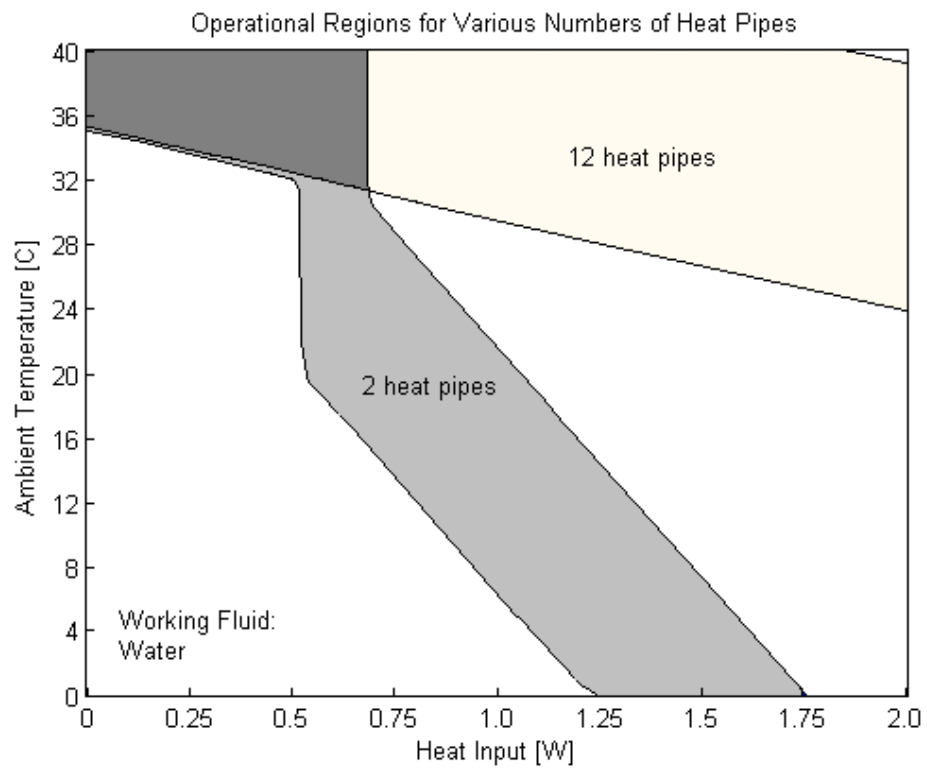


Fig. 22. Effective Operational Regions for Device Using Varying Numbers of Micro Heat Pipes with Water as the Working Fluid

As another example of this style of plot, Fig. 23, in this case with hydrogen peroxide as the chosen working fluid, illustrates how the change in the chosen number of heat pipes from 15 to 25 will affect the amount of acceptable operating region that is caused to fall within acceptable limits.

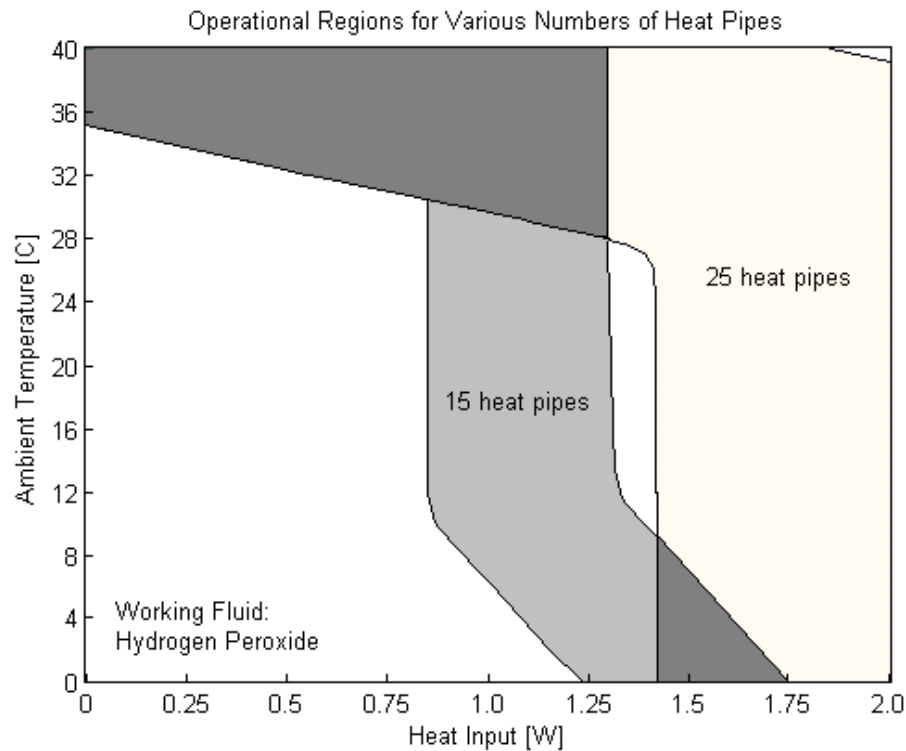


Fig. 23. Effective Operational Regions for Device Using Varying Numbers of Micro Heat Pipes with Hydrogen Peroxide as the Working Fluid

By taking each of the remaining fluids individually that had made the final list of acceptable fluid choices and calculating the area of operating region that falls within acceptable temperature limits, the optimal number of heat pipes was determined for each of the given fluids. Figs. 24 through 29 on the following several pages illustrate the operational regions for each of these fluids given that the device contains the

optimal number of embedded micro heat pipe corresponding to that fluid.

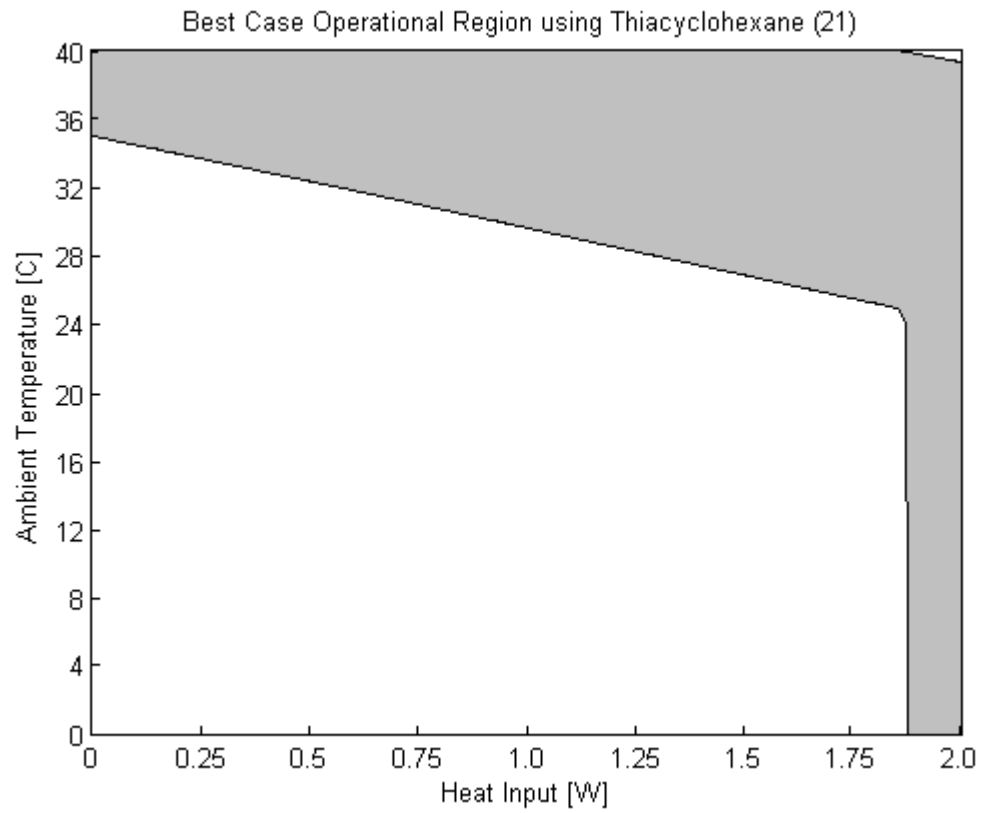


Fig. 24. Operational Region for Twenty One Embedded Micro Heat Pipes Containing Thiacyclohexane as the Working Fluid

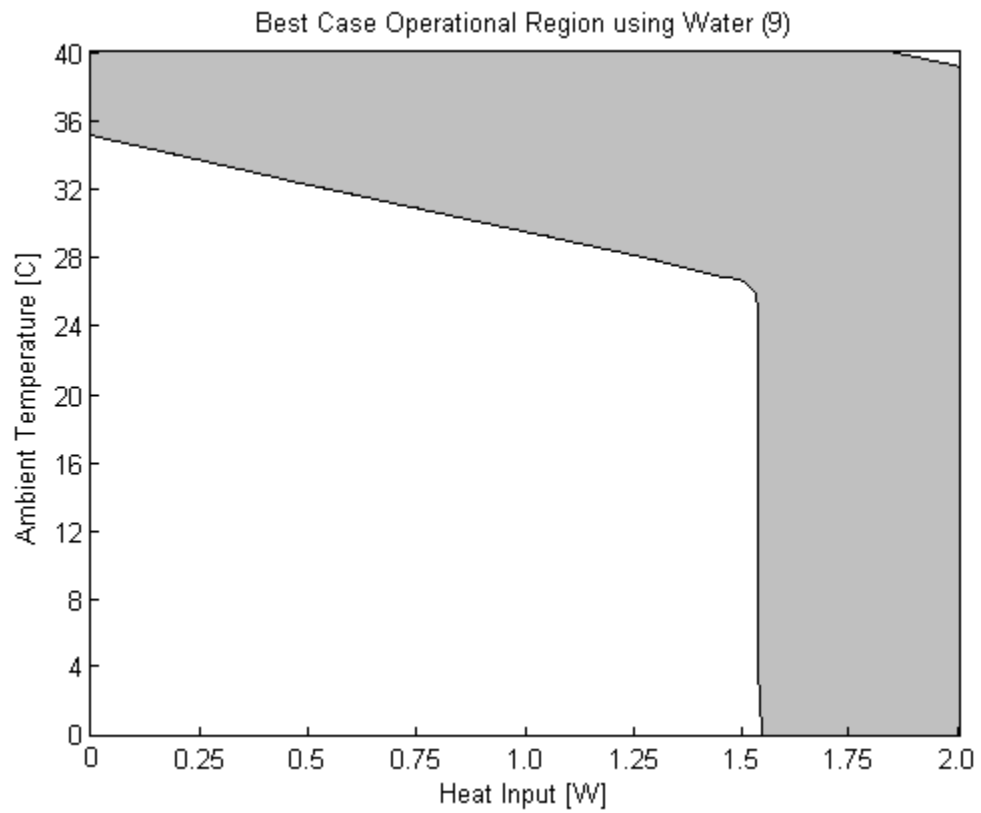


Fig. 25. Operational Region for Nine Embedded Micro Heat Pipes Containing Water as the Working Fluid



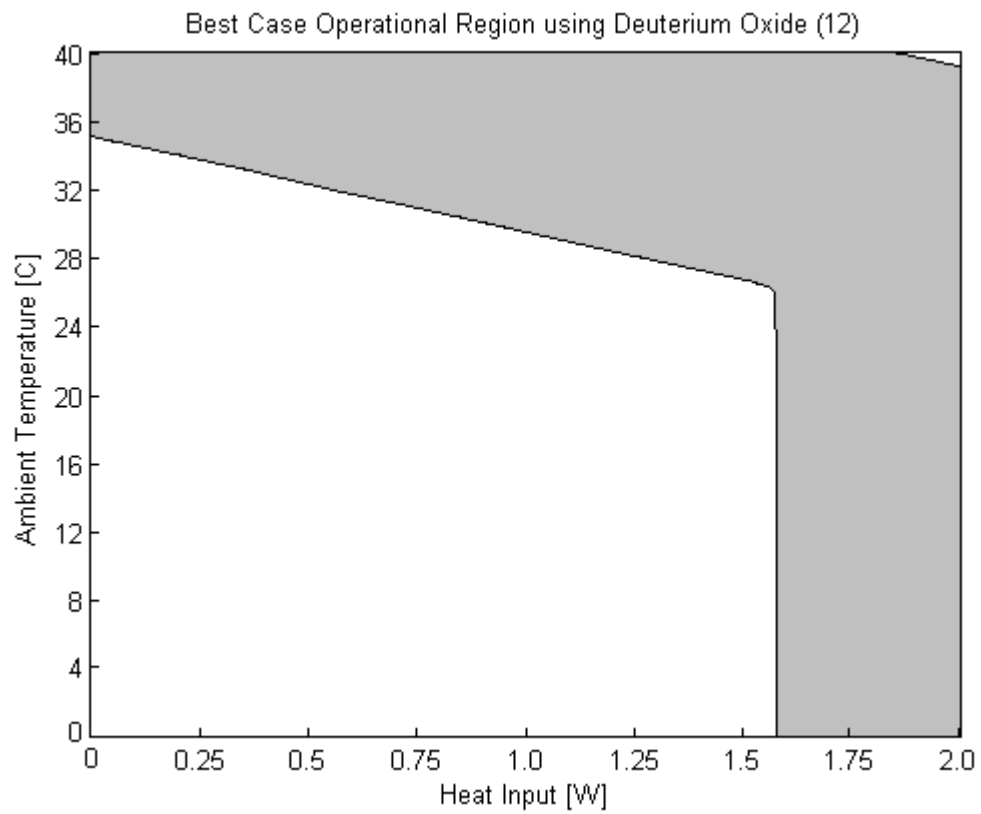


Fig. 26. Operational Region for Twelve Embedded Micro Heat Pipes Containing Deuterium Oxide as the Working Fluid

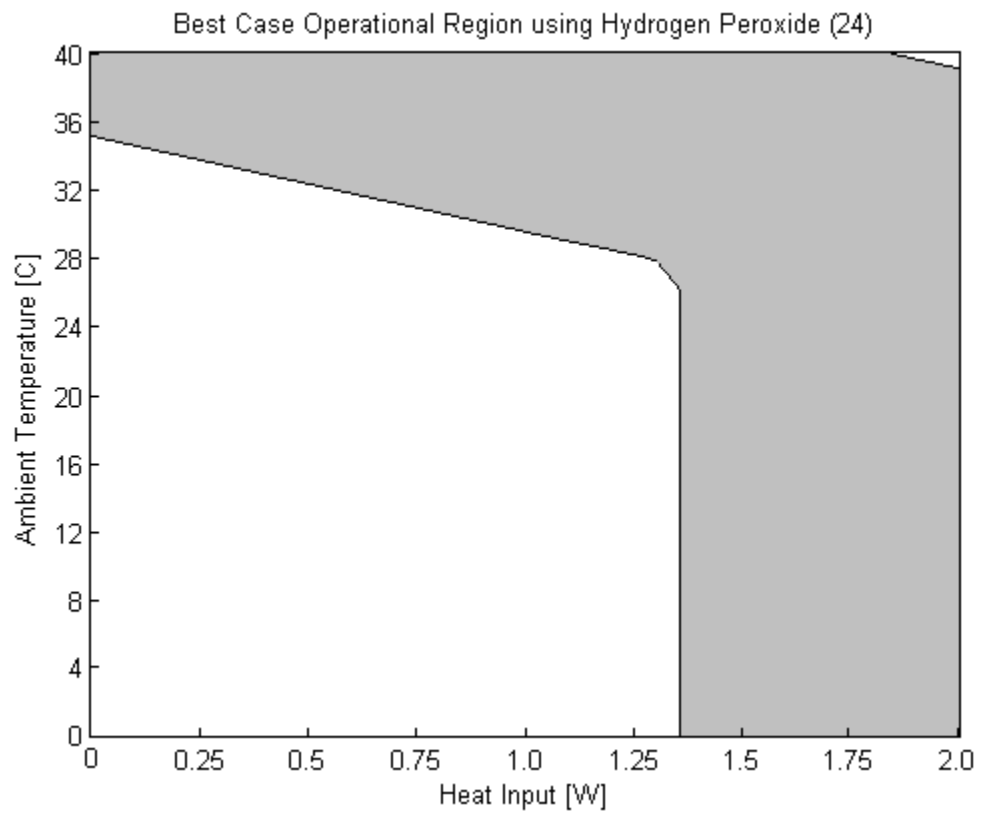


Fig. 27. Operational Region for Twenty Four Embedded Micro Heat Pipes Containing Hydrogen Peroxide as the Working Fluid

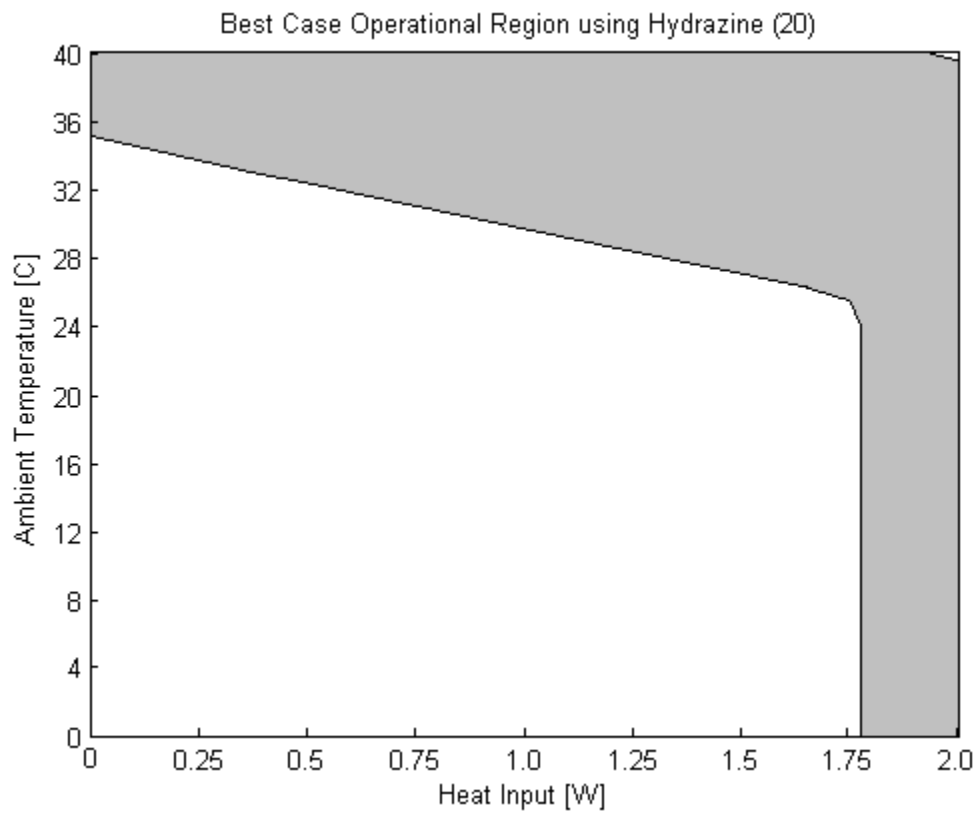


Fig. 28. Operational Region for Twenty Embedded Micro Heat Pipes Containing Hydrazine as the Working Fluid

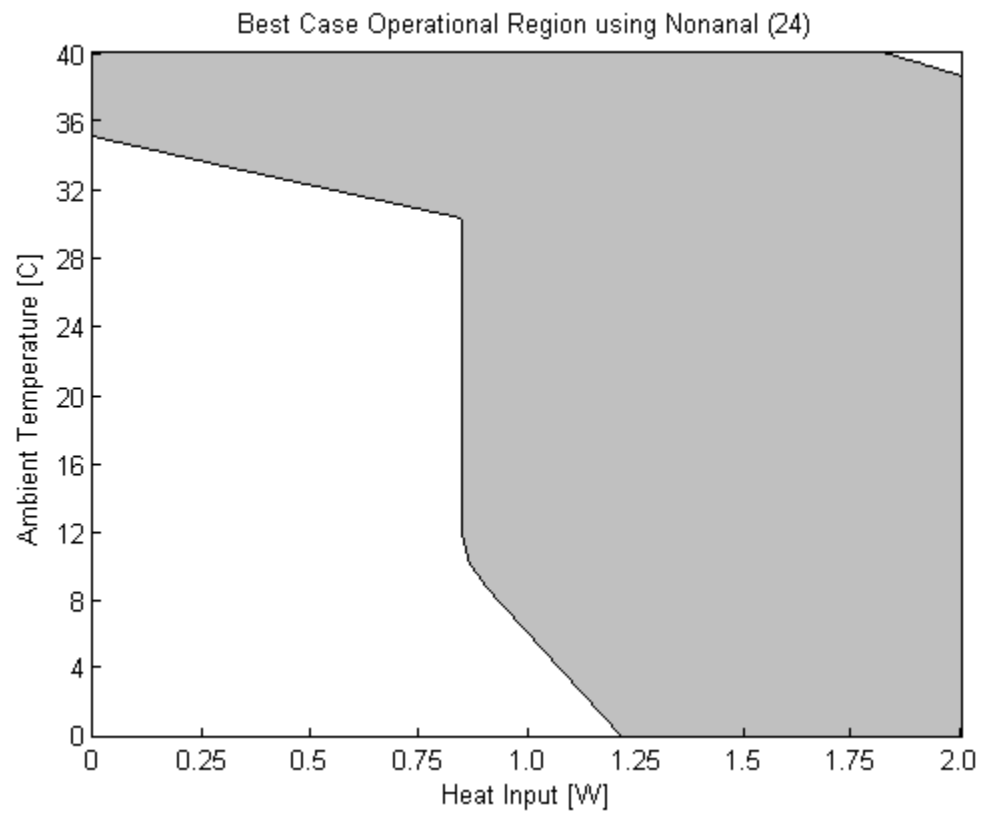


Fig. 29. Operational Region for Twenty Embedded Micro Heat Pipes Containing Hydrazine as the Working Fluid

Finally, the resulting information from the previous set of plots is summarized in Table V which lists the percentage of operational area that falls between the desired temperature control region for the best-case number of embedded micro heat pipes.

Table V. Resulting Operational Regions for Various Fluids

Working Fluid	Number of Pipes	Percent Region Operational
Water	9	41.0
Nonanal	24	62.9
Deuterium Oxide	12	39.6
Hydrazine	20	32.9
Thiacyclohexane	21	29.9
Hydrogen Peroxide	24	47.0

## B. Discussion

As can be seen by the table on page 84, this application of a series of micro heat pipes seems to provide for only a very marginal level of thermal control for the system as a whole in that much of the desired operational area remains unaccounted for, even for the most promising of fluids. Although the level of thermal control that is exhibited does not fully satisfy the initially stated design requirements, one truly should take into account the base operational region within the solution space using the original aluminum plate as well as the operational region that is actually feasible given the established level of thermal leakage to ambient before making that assessment. This comparison serves to put the actual level of improvement into perspective.

The first of these comparisons may be made by evaluating the operational region

that is satisfies for a system having no thermally isolating rubber barrier and no embedded micro heat pipes, that is a simple continuous aluminum plate. A plot representing the operation region resulting from this case if shown in Fig. 30.

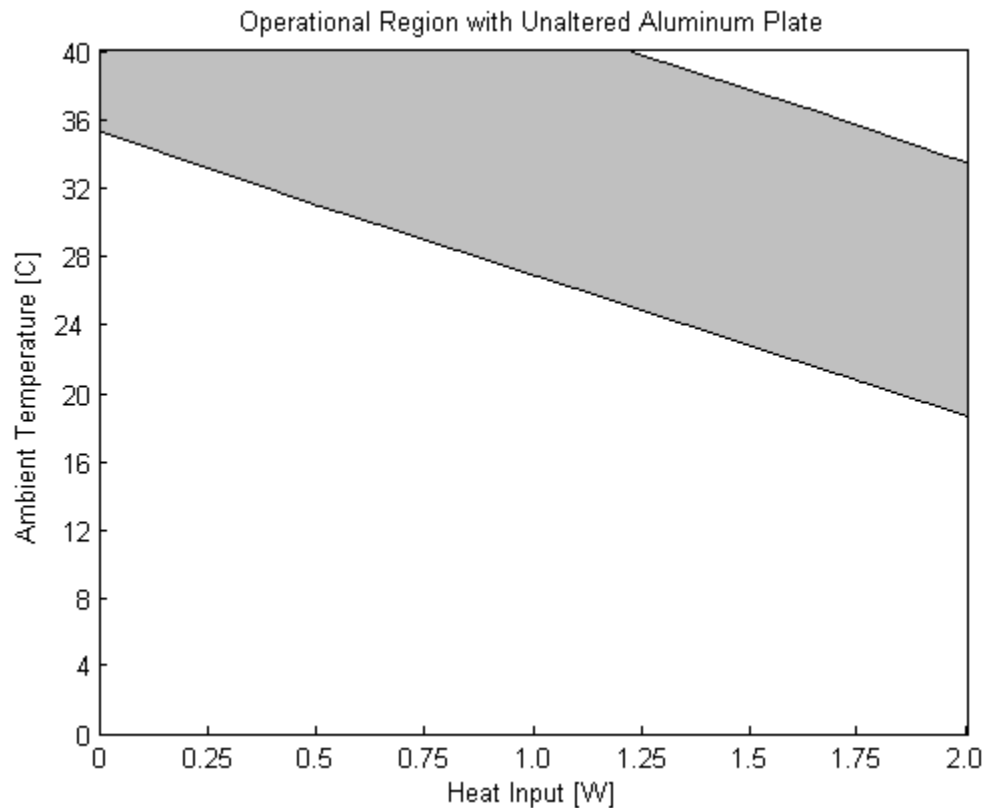


Fig. 30. Operational Region Resulting from the Use of a Continuous Aluminum Plate

It can be seen that this operational region comprises of only about 29.9 percent of the desired operation region and that at no point does the region exist at an ambient temperature below approximately 19°C. The next comparison may be made by evaluating a system having having a “perfect” insulating thermal barrier, that is, one that completely thermally isolates the heated section of the device from the section that is exposed to ambient and no embedded micro heat pipes. A plot representing

the operation region resulting from this case if shown in Fig. 31.

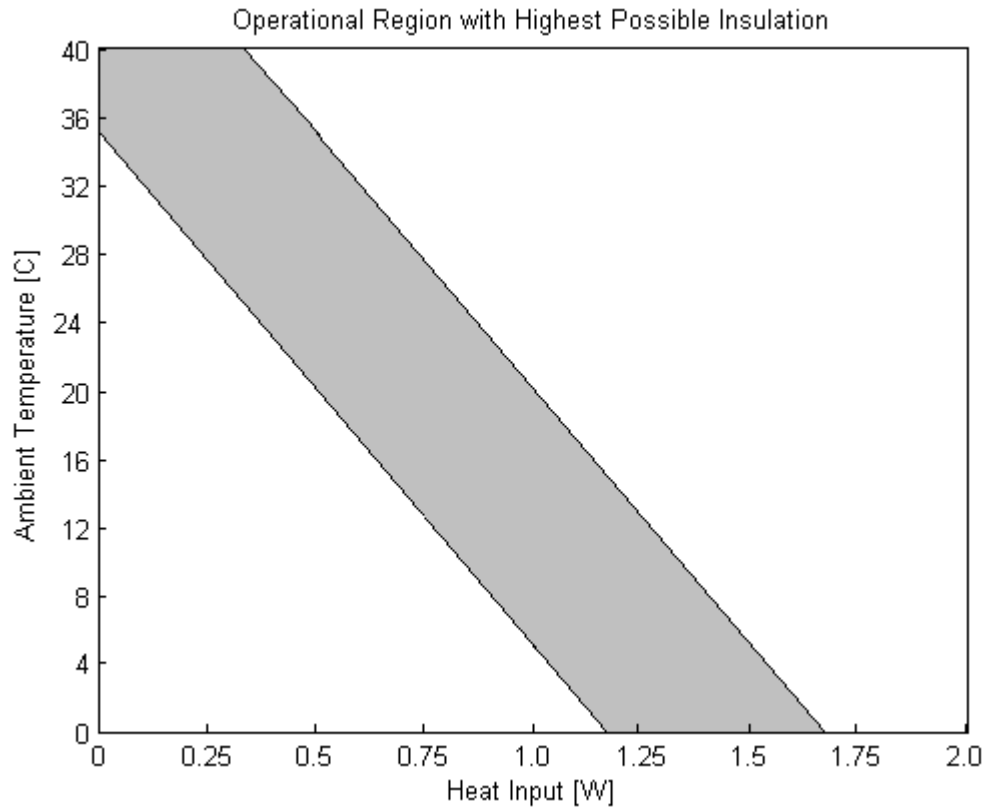


Fig. 31. Operational Region Resulting from the Use of “Perfect” Insulating Thermal Barrier Between the Two Sections of the Device

Since this region represents the most insulated case, it should be understood that the entire area lying below and to the left of the operational region in Fig. 31 is simply unattainable given the high level of thermal leakage to ambient that was assumed. In other words, there is no way any thermal control device could be expected to conduct less thermal energy than a “perfect” insulator. Given this revelation, Fig. 32 compares the, now much more impressive, best-case operational region of Nonanal with the

physically possible operational region, given the high level of assumed thermal leakage.

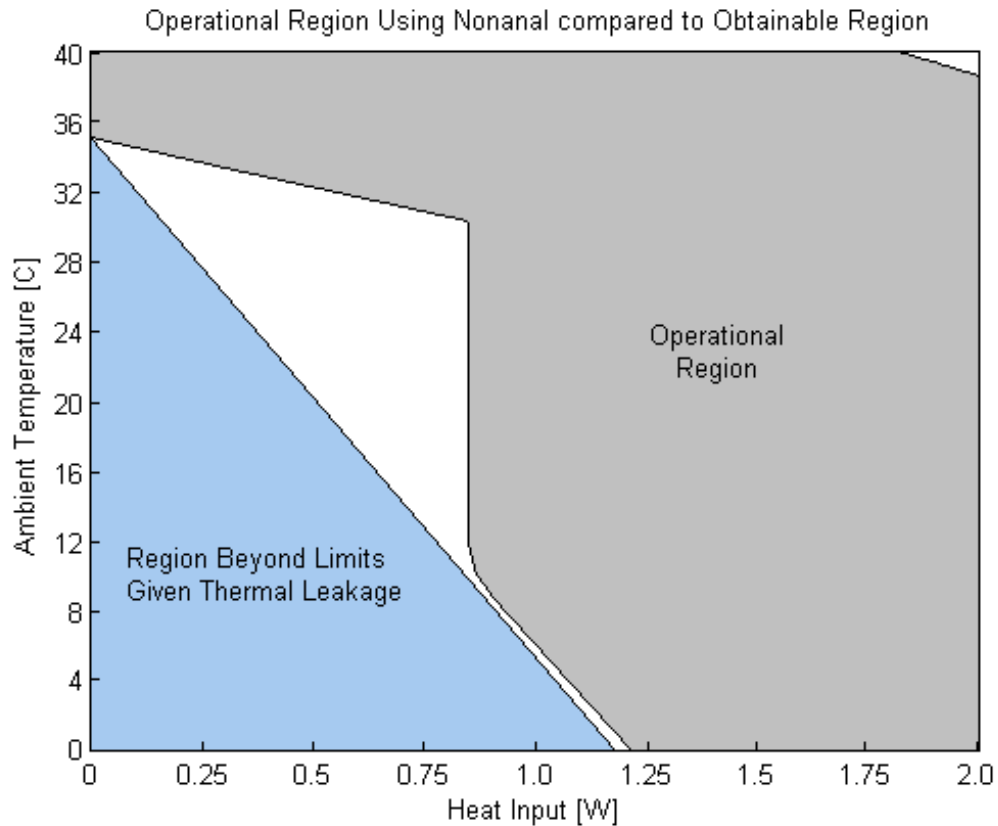


Fig. 32. Maximum Operational Region Using 24 Nonanal Heat Pipes Compared to Physically Possible Region

With these considerations in mind, there now exists two new parameters by which to evaluate the performance of the various working fluid/number of heat pipe combinations. The first of these is the relative improvement in the percentage of operation region over the base design, that of a continuous aluminum plate, and the second is the percentage of operational area based on what is physically possible due to the considerable thermal leakage. Table VI summarizes these two new factors for



each of the fluids of interest.

Table VI. Adjusted Performance of Various Fluids

Working Fluid	Percent Improvement	Percent of Possible Region
Water	37.4	55.1
Nonanal	110.6	84.5
Deuterium Oxide	32.5	53.2
Hydrazine	10.4	44.3
Thiacyclohexane	0.2	40.2
Hydrogen Peroxide	57.3	63.1

### 1. Further Considerations

This study does illustrate, quite dramatically, to what extent improvements to the level of thermal control can be made with the incorporation of micro heat pipes and a smart and deliberate choice of working fluid.

Water, which is by far, the most commonly used working fluid for heat pipe applications, allows for a 41.03 percent overall operational region, which is significant when compared to the operational region of a system having no micro heat pipes. Two other fluids, Nonanal and Hydrogen Peroxide, however, yielded operational regions that are higher than that offered with the use of water. Given the extremely wide range of prospective operating conditions and the fact that this improvement can be made simply by exchanging the working fluid within the system and number of heat pipes rather than physical design modification, this improvement is not trivial.

Upon further review of the resulting data, there are some considerations regard-

ing the thermal leakage that serve to put the performance of some of the better fluids into perspective. As was discussed in the opening chapters of this thesis, it was, for the purpose of attempting to modeling a more “real-world” scenario, assumed that there is a thermal leakage from the system, having a resistance of  $30\text{ W/K}$ . The placement of this leakage as a constraint on the system was an attempt to model a possible path for the travel of thermal energy through an electronic device to ambient. Such paths of thermal leakage are ever present in all electronics for a variety of reasons including poor insulations as well as interfaces with other components. The value that was assumed in this case was a conservative estimate of what would be a likely value for a device such as a PDA with a large viewable screen area having very little thermal insulation as a means of maintaining a level of compactness.

In recent years, however, there has been a great deal of research in the area of advanced materials for thermal insulation. Many devices currently being manufactured, however, are using technologies for thermal insulation that are somewhat older relative to this new research. It can be seen that as new devices are manufactured, better levels of thermal insulation may be incorporated by making use of these emerging technologies. To that end, it is of some interest to investigate whether the described thermal control system may be better able to control temperatures in the presence of greater levels of thermal insulation.

The following plot in Fig. 33 illustrates the extent to which the operational region of the device is affected when undergoing a change in the level of thermal insulation. Plotted are the operating regions for the optimal system design (that made up of 24 micro heat pipes with Nonanal as the working fluid) with the original level and double the level of thermal insulation. These values correspond to resistances of thermal leakage to ambient of 30, and  $60\text{ K/W}$ , respectively.

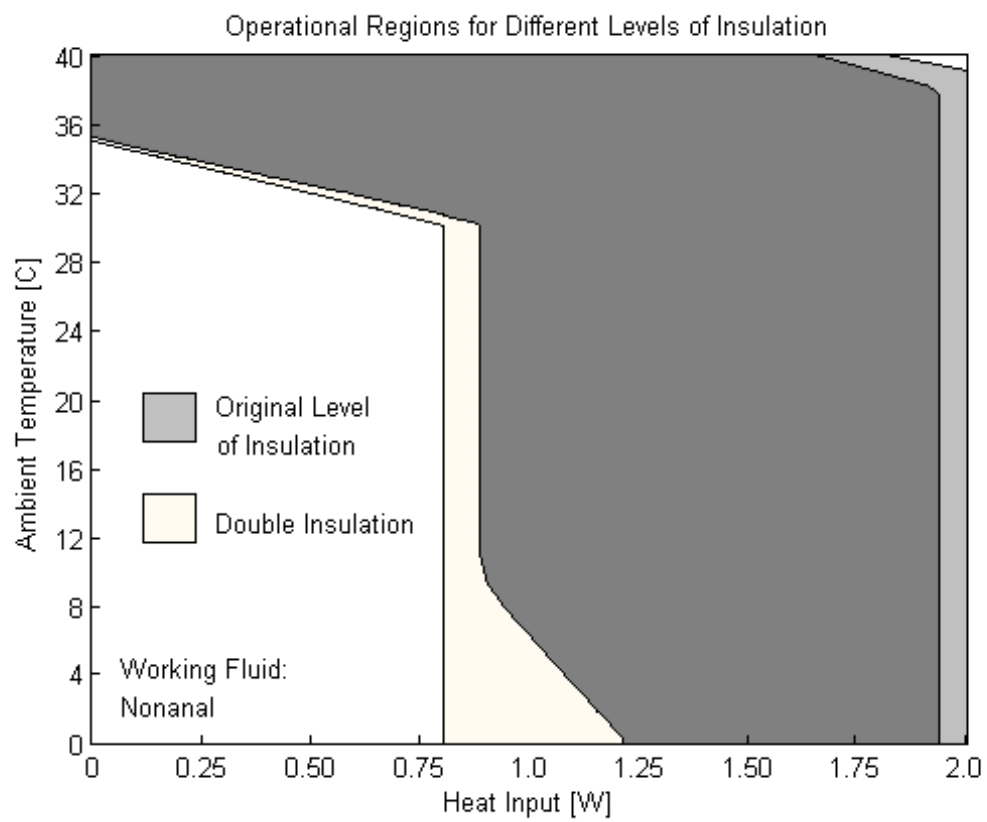


Fig. 33. Changes in Operating Region Given Changes in the Level of Thermal Insulation

It can be seen that as the level of thermal insulation is increased, there is clearly an improvement in the operational area at low levels of heat input. However, this added resistance does not significantly increase the total operational area in that, in areas of higher heat input, the temperature becomes too high, exceeding the 50°C upper limit. This indicates that the amount of operational region lying within the acceptable temperature limits depends to a much greater extent on the behavior of the working fluid rather than bulk thermal insulation.

Another important issue that should be taken further into consideration is that of material compatibility. As mentioned briefly in the previous chapter, compatibility issues were not taken into account during the initial stages of analysis when calculating heat transport capacity of individual heat pipes. Material compatibility, to the extent that is possible, was considered when narrowing down the potential list of fluids, however, due to the rare nature of several of the fluids, one may not be able to completely rule out the possibility of an interaction between the stainless steel case material that would result in the generation of noncondensable gas. One common example of an issue involving material compatibility is that of water as a working fluid with aluminum as a case [2]. In addition to issues of simple compatibility, there are also issues such as the environmental concerns of the working fluids as well as cost and comparability with the case materials.

### C. Summary of Findings

The following list of items summarizes the important findings that were presented and discussed in this chapter that were the result of this analysis:

- It was found that none of the prospective working fluid-configuration combinations were able to completely satisfy the initial design requirements of main-

taining the temperature of the heated end of the device to within 35 and 50 °C for the entire range of operating conditions.

- It was found, however, that the percentage of operational area for the device, that is the percentage of time the heated section temperature was held to within the specified temperature limits at differing ambient temperature/heat input combinations was increased significantly with the implementation of a micro heat pipe thermal control system. This operational area increased from 29.9 percent for a device made simply of aluminum to 62.9 percent for a device having a thermal barrier and embedded micro heat pipes using nonanal as the working fluid.
- Further, it was shown that this percentage of operation area is actually better than it seems at first glance if once is to consider the large level of thermal leakage exists in the device. The unmodified aluminum plate allows the device to be within the desired temperature limits for 40.1 percent of the **attainable** ambient temperature/heat input combinations while the use of the nonanal heat pipe system increased this area to 84.5 percent of the **attainable** operational region.
- It was found that there were two fluids that seemed to be better choices in this situation than what is the most common heat pipe working fluid, water. These two best performing fluids were nonanal and hydrogen peroxide, both of which had a larger change in heat transport capacity over the operating temperature range from 35 to 50 °C.
- Finally, it was shown that although operating at low ambient temperature/heat input combinations resulted in the temperature falling below the desired range,

simply increasing insulation, which in turn would reduce the level of thermal leakage does not significantly increase operational area. Although a simple increase in insulation may seem like a likely course of action to accommodate this region of operating conditions, the impact is not as significant as one may initially hope. In the case of nonanal, the operational region was not increased at all, but rather shifted to accommodate lower levels of heat input while exceeding the acceptable operational temperature high levels of heat input.

## CHAPTER VII

### CONCLUSIONS

This chapter serves to summarize in more general terms, what was learned from this work and offers some final conclusions that may be drawn. Listed below are these points with some remarks:

- It can be concluded that the more constrained a thermal management problem is, the more difficult it will be to find an appropriate working fluid and configuration that is able to satisfy those constraints.
- In terms of providing an adequate level of thermal control, micro heat pipes, with any working fluid, do not exhibit a significant change in heat transport capacity over narrow changes in operating temperature such that they are able to significantly control temperature.
- When a fluid is chosen correctly, however, there is a beneficial result, more so than would be possible with the use of a standard thermal insulator. Again, this beneficial result would become increasingly obvious with broader control temperatures ranges and narrower operating ranges.
- A final conclusion was that a very appropriate method for visualizing the compliance of a thermal device over a range of operating regions is by illustrating the solution space which is satisfied relative to the entire solution space. This representation could be easily used for a 3-parameter case, in which the volume compliance would be evaluated.

## CHAPTER VIII

### RECOMMENDATIONS FOR FUTURE WORK

It is felt that the work that was done in this thesis has shown some promising results for the use of a smart choice of working fluids in micro heat pipes in relation to effective temperature control. However, there are many more facets that may be of some interest to further explore. Some of these areas of interest may include the following:

- The first issue that could be addressed in the future is whether it is feasible to mechanically vary the contact resistance between the area of heat input and the heat pipe. There are several methods for accomplishing such a task, among them being a passively activated bimetallic switch or even an actively controlled switch. Such a method would allow for an even higher level of thermal control than possibly, the method involving that of the micro heat pipe system. This combination of approaches would make use of the extremely high level of thermal conductivity exhibited by a heat pipe with a high level of variability that could only be attained by making use of the significant contact resistance.
- The second area that is of future concern is that of material compatibility and fluid stability. This issue was not addressed in great detail, but is one that could present a large obstacle in future work when it comes time to actually build prototypes.
- Another area of future research could actually be applied through two different approaches. This is the area of using multiple fluids. In this investigation, all of the possible cases involved the use of a single component fluid which was also the consistent working fluid within all of the individual heat pipes. One may be



able to achieve a higher level of thermal control by introducing multiple pipe, containing different fluids or mixtures of fluids within the same pipes. The first of these approaches would likely be easier to investigate analytically and assume that some degree of accuracy would be obtained while the second would likely be better left to experimental data gathering. Each of these methods, however may be of some benefit if the various fluids were chosen in such a way that they complimented one another at the extremes of the temperature range.

- A final area of interest involved limiting the level of leakage from a heat source to the ambient environment. There is already a high level of work looking at increasing the thermal resistance for given materials in an effort to create better insulators. Further development in this field would only serve to increase the extent to which a given temperature can be maintained.

## REFERENCES

- [1] D.G. Gilmore, *Satellite Thermal Control Handbook*, El Segundo, CA: The Aerospace Corporation, 1994.
- [2] G.P. Peterson, *An Introduction to Heat Pipes: Modeling, Testing and Applications*, New York, New York: John Wiley and Sons, Inc., 1994.
- [3] A. Faghri, *Heat Pipe Science and Technology*, Washington, DC: Taylor & Francis, 1995.
- [4] T.P. Cotter, “Principals and Prospects of Micro Heat Pipes,” in *Proceedings of the 5th International Heat Pipe Conference*, Tsukuba, Japan, 1984, pp. 328–335.
- [5] G.P. Peterson, “Overview of Micro Heat Pipe Research and Development,” *Applied Mechanical Reviews*, vol. 45, no. 5, pp. 175–189, May 1992.
- [6] S.W. Chi, *Heat Pipe Theory and Practice: A Sourcebook*, Washington, DC: Hemisphere Publishing Corporation, 1976.
- [7] P.D. Dunn, and D.A. Reay, *Heat Pipes*, 3rd ed., New York, New York: Pergamon Press, 1976.
- [8] B.R. Babin, G.P. Peterson, and D. Wu, “Steady-State Modeling and Testing of a Micro Heat Pipe,” *AMSE Journal of Heat Transfer*, vol. 112, No. 3, pp. 595–601, 1990.
- [9] A.B. Duncan, and G.P. Peterson, “Charge Optimization for Triangular Shaped Micro Heat Pipe,” *ASME Fundamentals of Heat Pipes*, HTD-Vol. 278, pp. 1-10, 1994.

- [10] J.M. Ha, “Capillary Performance and Heat Transfer Characteristics of the Evaporating Thin Liquid Film in a Triangular Micro Groove,” Ph.D. dissertation, Texas A&M University, College Station, 1995.
- [11] K. Wantanabe, A. Kimura, K. Kawabata, T. Yanagida, and M. Yamauchi, “Development of a Variable-Conductance Heat-Pipe for a Sodium-Sulfur (NAS) Battery,” *Furukawa Review*, vol. 20, pp. 71–76, April 2001.
- [12] D. Liepmann, *Design and Fabrication of a Micro-CPL for Chip-Level Cooling*, ASME International Mechanical Engineering Congress and Exposition, New York: November 11-16, 1987.
- [13] M. Schneider, ‘*Investigation of Interconnected Mini Heat Pipe Arrays for Micro Electronics Cooling*, Institute for Nuclear Technology and Energy Systems, Stuttgart, Germany.
- [14] S. Kalahasti, and Y.K. Joshi, “Performance Characterization of a Novel Flat Plate Micro Heat Pipe Spreader,” *IEEE Transactions on Components and Packaging Technologies*, vol. 25, no. 4, pp. 554–560, December 2002.
- [15] M.L. Berre, S. Launay, V. Sartre and M. Lallemand, “Fabrication and Experimental Investigation of Silicon Micro Heat Pipes for Cooling Electronics,” *Journal of Micromechanics and Microengineering*, vol. 13, pp. 436–441, 2003.
- [16] D. A. Pruzan, K.E. Torrance and C.T. Avedisian, “Two-phase Flow and Dryout in a Screen Wick Saturated with a Fluid Mixture,” *International Journal of Heat and Mass Transfer*, vol. 33, no. 4 pp. 673–681, 1990.
- [17] T. Nagasaki and K. Hijikata, “A Numerical Study on a Variable Conductance

- Heat Pipe Using a Binary Mixture,” in *ASME/JSME Thermal Engineering Conference*, vol. 2, 1995.
- [18] T. Kiatsiriroat, A. Nuntaphan and J. Tiansuwan, “Thermal Performance Enhancement of Thermosyphon Heat Pipe with Binary Working Fluids,” *Experimental Heat Transfer*, vol. 13, pp. 137–152, 2000.
- [19] D.A. Johnson, J. Baumann and B. Cullimore, “CAD-based Methods for Thermal Modeling of Coolant Loops and Heat Pipes,” in *Proc. Eighth Intersociety Conference on Thermal and Thermomechanical Phenomena in Electronic Systems*, Piscataway, NJ, 2002, pp. 46–53.
- [20] F.P. Incropera, and D.P. DeWitt, *Introduction to Heat Transfer*, 4th ed., New York: John Wiley and Sons, Inc., 2002.
- [21] C.L. Yaws, *Chemical Properties Handbook*, New York, New York: McGraw-Hill, 1999.

## APPENDIX A

## SELECTED DERIVATIONS

The following derivations for available capillary pumping pressure, and liquid and vapor pressure drop are extracted from Chi [6]. It is there that the reader is encouraged to read the full unabridged derivation less the simplifications made with the assumptions for this investigation.

The liquid pressure drop can be obtained by integrating the liquid pressure gradient.

$$\Delta P_l(x_1 - x_2) = - \int_{x_1}^{x_2} \frac{dP_l}{dx} dx \quad (\text{A.1})$$

Since, in general, the liquid velocity is very low, the dynamic pressure can be neglected. Further, given the size scale in question, it is also a reasonable assumption to neglect the gravitational force acting on the liquid. Thus, the liquid pressure gradient in the direction of the flow can be expressed by the following:

$$\frac{dP_l}{dx} = - \frac{2\tau_l}{r_{h,l}} \quad (\text{A.2})$$

where  $\tau_l$  is the frictional stress at the liquid-solid interface and  $r_{h,l}$  is the hydraulic radius of the liquid flow channel. The dimensionless Reynolds number  $Re_l$  is given to be the following:

$$Re_l = \frac{2r_{h,l}\rho_l V_l}{\mu_l} \quad (\text{A.3})$$

and the drag coefficient  $f_l$  is defined to be

$$f_l = \frac{2\tau_l}{\rho_l V_l^2} \quad (\text{A.4})$$

where  $\mu$  is the viscosity of the liquid,  $V_l$  is the velocity and  $\rho_l$  is the liquid density. For heat pipe applications, it can be shown that the velocity of the liquid is related to the axial heat flux as follows:

$$V_l = \frac{Q}{\epsilon A_w \rho_l \lambda} \quad (\text{A.5})$$

where  $\lambda$  is the latent heat of vaporization of the fluid and  $A_w$  is the wick cross-sectional area and  $\epsilon$  is the wick porosity. By substitution, the following expression for liquid pressure gradient can be developed:

$$\frac{dP_l}{dx} = -\frac{(f_l Re_l) \mu_l Q}{2\epsilon A_w r_{h,l}^2 \lambda \rho_l} \quad (\text{A.6})$$

In the case of a micro heat pipe, the wick porosity,  $\epsilon$  can be considered to be unity and the cross sectional area of the wick is essentially the total liquid flow cross sectional area, which can be denoted at  $A_l$ . By these assumptions and by integrating along the length of the micro heat pipe, the liquid pressure drop across the effective length of the heat pipe can be expressed as the following:

$$\Delta P_l = -\frac{(f_l Re_l) \mu_l L_{eff} q}{2A_l r_{h,l}^2 \lambda \rho_l} \quad (\text{A.7})$$

where the effective length of the heat pipe can be expressed as [7]:

$$L_{eff} = L_a + \frac{L_e + L_c}{2} \quad (\text{A.8})$$

where  $L_a$ ,  $L_e$ , and  $L_c$  are the lengths of the adiabatic, evaporator, and condenser sections, respectively.

Like the derivation of the liquid pressure drop, the pressure loss associated with the vapor loss can also be found derived in great detail in Chi [6]. A brief derivation is summarized as follows:

The vapor pressure drop can be obtained by integrating the vapor pressure gradient.

$$\Delta P_v(x_1 - x_2) = - \int_{x_1}^{x_2} \frac{dP_v}{dx} dx \quad (\text{A.9})$$

where the pressure gradient on the vapor flow direction is  $(dP_v/dx)$ . Due to the difference in density when compared to the liquid flow rate, which must be equal, the pressure drop results from the frictional drag as well as the dynamic effect. This analysis is subject to further obfuscation due to the transition between laminar and turbulent flow regimes as well as compressibility considerations. For the purposes of this analysis, it is to be assumed that the flow will remain, steady state, laminar and having a fully developed velocity profile. The vapor pressure gradient can then be expressed as the following:

$$\frac{dP_v}{dx} = \frac{-(f_v Re_v) \mu \dot{m}_v}{2A_v r_{h,v}^2 \rho_v} \quad (\text{A.10})$$

Since the vapor mass flux,  $\dot{m}_v$ , is related to the axial heat flux at a given axial location, the following equation holds true.

$$\dot{m}_v = \frac{Q}{\lambda} \quad (\text{A.11})$$

By substituting this equation for mass flow into the previous equation for pressure gradient and then integrating over the effective length of the heat pipe,  $L_{eff}$ , the following expression for vapor pressure loss of obtained:

$$\Delta P_v = \frac{-(f_v Re_v)\mu_v L_{eff} q}{2r_{h,v}^2 A_v \rho_v \lambda} \quad (\text{A.12})$$



## APPENDIX B

## ANALYZED WORKING FLUIDS

**Organic Fluids**

abietic acid	p-aminodiphenylamine
acenaphthene	2-aminoethoxyethanol
acetal	N-aminoethylethanolamine
acetaldehyde	N-aminoethyl piperazine
acetamide	1-aminoheptane
acetanilide	6-aminohexanol
acetic acid	1-amino-2-propanol
acetic anhydride	3-amino-1-propanol
acetone	p-tert-amylphenol
acetonitrile	aniline
acetophenone	anisole
acetylacetone	anthracene
acetyl chloride	ascorbic acid
acrolein	azulene
acrylamide	benzaldehyde
acrylic acid	benzene
acrylonitrile	1,2-benzenediol
adipic acid	1,3-benzenediol
adiponitrile	1,2,3-benzenetriol
allyl alcohol	benzoic acid

Continued on next page

allylamine	benzophenone
p-aminodiphenyl	benzothiophene
benzotrichloride	1-bromopentane
benzotrifluoride	1-bromopropane
benzoyl chloride	2-bromopropane
benzyl acetate	3-bromo-1-propene
benzyl alcohol	p-bromotoluene
benzylamine	bromotrichloromethane
benzyl benzoate	bromotrifluoroethylene
benzyl chloride	bromotrifluoromethane
benzyl dichloride	1,2-butadiene
benzyl ethyl ether	1,3-butadiene
bicyclohexyl	butadiyne(biacetylene)
biphenyl	n-butane
bis(chloromethyl)ether	1,3-butanediol
bis(cyanoethyl) ether	1,4-butanediol
bisphenol a	2,3-butanediol
bromobenzene	n-butanol
1-bromobutane	sec-butanol
2-bromobutane	tert-butanol
bromochlorodifluoromethane	cis-2-butene
bromochloromethane	trans-2-butene
bromoethane	1-butene

Continued on next page

1-bromoheptane	cis-2-butene-1,4-diol
2-butoxyethanol	butyl ethyl sulfide
n-butyl acetate	tert-butylformamide
sec-butyl acetate	n-butyl formate
tert-butyl acetate	butyl hexadecyl sulfide
n-butyl acrylate	butyl hexyl sulfide
n-butylamine	n-butyl mercaptan
sec-butylamine	sec-butyl mercaptan
tert-butylamine	tert-butyl mercaptan
n-butylbenzene	n-butyl methacrylate
sec-butylbenzene	butyl methyl sulfide
tert-butylbenzene	1-n-butyl naphthalene
n-butyl benzoate	2-butyl naphthalene
n-butyl n-butyrate	n-butyl nonanoate
p-tert-butylcatechol	butyl nonyl sulfide
n-butyl chloride	butyl octyl sulfide
sec-butyl chloride	butyl pentadecyl sulfide
tert-butyl chloride	butyl pentyl sulfide
n-butylcyclohexane	p-tert-butylphenol
butylcyclopentane	n-butyl propionate
butyl decyl sulfide	butyl propyl sulfide
butyl dodecyl sulfide	n-butyl stearate
n-butyl ethyl ether	butyl tetradecyl sulfide

Continued on next page

butyl tridecyl sulfide	o-chloroaniline
butyl undecyl sulfide	p-chloroaniline
n-butyl valerate	p-chlorobenzotrifluoride
butyl vinyl ether	m-chlorobenzoyl chloride
n-butyraldehyde	1-chloro-1,1-difluoroethane
n-butyric acid	2-chloro-1,1-difluoroethylene
butyric anhydride	chlorodifluoromethane
n-butyronitrile	2-chloroethanol
camphene	chloroform
camphor	1-chloro-3-methylbutane
e-caprolactam	2-chloro-2-methylbutane
e-caprolactone	1-chloronaphthalene
carbon dioxide	m-chloronitrobenzene
carbon disulfide	o-chloronitrobenzene
carbon monoxide	p-chloronitrobenzene
carbon tetrachloride	chloropentafluoroethane
carbon tetrafluoride	1-chloropentane
carbonyl fluoride	m-chlorophenol
carbonyl sulfide	o-chlorophenol
chloroacetaldehyde	p-chlorophenol
chloroacetyl chloride	chloroprene
m-chloroaniline	2-chloropropene
3-chloropropene	1,3-cyclohexadiene

Continued on next page

o-chlorotoluene	cyclohexane
p-chlorotoluene	1,4-cyclohexanedicarboxylic acid
chlorotrifluoroethylene	cyclohexanol
chlorotrifluoromethane	cyclohexanone
chrysene	cyclohexene
citraconic acid	cyclohexylamine
m-cresol	cyclohexylbenzene
o-cresol	1-cyclohexyldodecane
p-cresol	1-cyclohexylheptane
trans-crotonaldehyde	1-cyclohexylhexadecane
cis-crotonic acid	1-cyclohexylhexane
trans-crotonic acid	1-cyclohexylnonane
trans-crotonitrile	1-cyclohexyloctane
cumene	1-cyclohexylpentadecane
p-cumylphenol	1-cyclohexyltetradecane
cyanogen	1-cyclohexyltridecane
cyanogen chloride	1-cyclohexylundecane
cyclobutane	1,5-cyclooctadiene
cyclobutene	cyclooctane
cycloheptane	1,3,5,7-cyclooctatetraene
1,3,5-cycloheptatriene	cyclopentane
cyclopentanethiol	1-decanal
cyclopentanone	n-decane

Continued on next page

cyclopentene	n-decanoic acid
1-cyclopentyldecane	1-decanol
1-cyclopentyldecane	1-decene
1-cyclopentylheptane	n-decylamine
1-cyclopentylhexadecane	n-decylbenzene
1-cyclopentylhexane	n-decylcyclohexane
1-cyclopentylnonane	decyl ethyl sulfide
1-cyclopentyldecane	n-decyl mercaptan
1-cyclopentylpentadecane	decyl methyl sulfide
1-cyclopentylpentane	1-n-decyl naphthalene
1-cyclopentyltetradecane	decyl propyl sulfide
1-cyclopentylundecane	1-decyne
cyclopropane	dehydroabietylamine
1-cyclopentyltridecane	diacetone alcohol
m-cymene	diallyl maleate
o-cymene	dibenzyl ether
p-cymene	m-dibromobenzene
decafluorobutane	dibromodifluoromethane
cis-decahydronaphthalene	1,1-dibromoethane
trans-decahydronaphthalene	1,2-dibromoethane
dibromomethane	1,3-dichloro-trans-2-butene
1,2-dibromopropane	1,4-dichloro-cis-2-butene
1,2-dibromotetrafluoroethane	1,4-dichloro-trans-2-butene

Continued on next page

di-n-butylamine	3,4-dichloro-1-butene
2,6-di-tert-butyl-p-cresol	dichlorodifluoromethane
dibutyl disulfide	1,1-dichloroethane
di-n-butyl ether	1,2-dichloroethane
di-sec-butyl ether	cis-1,2-dichloroethylene
di-tert-butyl ether	trans-1,2-dichloroethylene
dibutyl phthalate	1,1-dichloroethylene
dibutyl sebacate	dichlorofluoromethane
dibutyl sulfide	dichloromethane
di-n-butyl sulfone	1,5-dichloropentane
dichloroacetaldehyde	1,1-dichloropropane
dichloroacetic acid	1,2-dichloropropane
dichloroacetyl chloride	1,3-dichloropropane
3,4-dichloroaniline	2,2-dichloropropane
m-dichlorobenzene	1,2-dichlorotetrafluoroethane
o-dichlorobenzene	2,4-dichlorotoluene
p-dichlorobenzene	dicumyl peroxide
2,4-dichlorobenzotrifluoride	cis-dicyano-1-butene
1,4-dichlorobutane	trans-dicyano-1-butene
1,4-dicyano-2-butene	3,3-diethyl-2-methylpentane
dicyclohexylamine	diethyl oxalate
didecyl disulfide	3,3-diethylpentane
didecyl sulfide	diethyl phthalate

Continued on next page

diethylamine	diethyl succinate
2,6-diethylaniline	diethyl sulfide
m-diethylbenzene	m-difluorobenzene
o-diethylbenzene	p-difluorobenzene
p-diethylbenzene	1,1-difluoroethane
diethyl disulfide	1,2-difluoroethane
diethylene glycol	1,1-difluoroethylene
diethylene glycol di-n-butyl ether	difluoromethane
diethylene glycol diethyl ether	diglycolic acid
diethylene glycol ethyl ether acetate	diheptyl disulfide
diethylene glycol monobutyl ether	diheptyl sulfide
diethylene triamine	dihexyl adipate
diethyl ether	dihexyl disulfide
3,3-diethylhexane	di-n-hexyl ether
3,4-diethylhexane	dihexyl sulfide
diethyl ketone	2,5-dihydrofuran
diethyl maleate	diiodomethane
diethyl malonate	diisobutylamine
diisobutyl ketone	cis-1,4-dimethylcyclohexane
diisodecyl phthalate	trans-1,2-dimethylcyclohexane
diisooctyl phthalate	trans-1,3-dimethylcyclohexane
diisopropanolamine	trans-1,4-dimethylcyclohexane
diisopropylamine	1,1-dimethylcyclohexane

Continued on next page



m-diisopropylbenzene	cis-1,2-dimethylcyclopentane
p-diisopropylbenzene	cis-1,3-dimethylcyclopentane
diisopropyl ether	trans-1,2-dimethylcyclopentane
diisopropyl ketone	trans-1,3-dimethylcyclopentane
1,2-dimethoxyethane	1,1-dimethylcyclopentane
N,N-dimethylacetamide	2,3-dimethyl-2,3-diphenylbutane
dimethylamine	dimethyl disulfide
p-dimethylaminobenzaldehyde	dimethyl ether
N,N-dimethylaniline	2,2-dimethyl-3-ethylpentane
2,3-dimethyl-1,3-butadiene	2,4-dimethyl-3-ethylpentane
2,2-dimethylbutane	N,N-dimethylformamide
2,3-dimethylbutane	2,2-dimethylheptane
2,3-dimethyl-1-butene	2,3-dimethylheptane
2,3-dimethyl-2-butene	2,4-dimethylheptane
3,3-dimethyl-1-butene	2,5-dimethylheptane
cis-1,2-dimethylcyclohexane	2,6-dimethylheptane
cis-1,3-dimethylcyclohexane	3,4-dimethylheptane
3,5-dimethylheptane	2,4-dimethyloctane
4,4-dimethylheptane	2,5-dimethyloctane
2,6-dimethyl-4-heptanol	2,6-dimethyloctane
2,2-dimethylhexane	2,7-dimethyloctane
2,3-dimethylhexane	3,3-dimethyloctane
2,4-dimethylhexane	3,4-dimethyloctane

Continued on next page

2,5-dimethylhexane	3,5-dimethyloctane
3,3-dimethylhexane	3,6-dimethyloctane
3,4-dimethylhexane	4,4-dimethyloctane
2,4-dimethyl-3-isopropylpentane	4,5-dimethyloctane
dimethyl maleate	2,2-dimethylpentane
1,2-dimethylnaphthalene	2,3-dimethylpentane
1,3-dimethylnaphthalene	2,4-dimethylpentane
1,4-dimethylnaphthalene	3,3-dimethylpentane
1,5-dimethylnaphthalene	dimethyl phthalate
1,6-dimethylnaphthalene	2,2-dimethyl-1-propanol
1,7-dimethylnaphthalene	2,6-dimethylpyridine
2,3-dimethylnaphthalene	dimethyl silane
2,6-dimethylnaphthalene	dimethyl sulfoxide
2,7-dimethylnaphthalene	dimethyl terephthalate
2,2-dimethyloctane	m-dinitrobenzene
2,3-dimethyloctane	o-dinitrobenzene
p-dinitrobenzene	di-n-propyl sulfone
dinonylphenol	m-divinylbenzene
dinonyl sulfide	divinyl ether
dioctyl disulfide	1-dodecanal
di-n-octyl ether	n-dodecane
dioctyl phthalate	n-dodecanoic acid
dioctyl sulfide	1-dodecanol

Continued on next page

1,4-dioxane	1-dodecene
dipentyl disulfide	dodecylamine
di-n-pentyl ether	n-dodecylbenzene
dipentyl sulfide	dodecyl ethyl sulfide
diphenylacetylene	n-dodecyl mercaptan
diphenylamine	dodecyl methyl sulfide
1,1-diphenylethane	dodecyl propyl sulfide
1,2-diphenylethane	1-dodecyne
diphenyl ether	n-eicosane
N,N'-diphenyl-p-phenylenediamine	1-eicosanethiol
di-n-propylamine	1-eicosanol
dipropyl disulfide	1-eicosene
dipropylene glycol	a-epichlorohydrin
di-n-propyl ether	1,2-epoxybutane
dipropyl sulfide	ethane
ethanol	3-ethyl-2,3-dimethylhexane
2-ethoxyethanol	3-ethyl-2,4-dimethylhexane
2-(2-ethoxyethoxy)ethanol	3-ethyl-2,5-dimethylhexane
2-ethoxyethyl acetate	3-ethyl-3,4-dimethylhexane
ethyl acetate	4-ethyl-2,2-dimethylhexane
ethylacetoacetate	4-ethyl-2,3-dimethylhexane
ethylacetylene	4-ethyl-2,4-dimethylhexane
ethyl acrylate	4-ethyl-3,3-dimethylhexane

Continued on next page

ethylamine	3-ethyl-2,3-dimethylpentane
o-ethylaniline	ethylene
ethylbenzene	ethylenediamine
ethyl benzoate	ethylene glycol
2-ethyl-1-butanol	ethylene glycol diacetate
2-ethyl-1-butene	ethylene glycol monopropyl ether
ethyl n-butyrate	ethyleneimine
2-ethylbutyric acid	ethylene oxide
ethyl chloride	ethyl-3-ethoxypropionate
ethyl chloroformate	ethyl fluoride
ethyl cyanoacetate	ethyl formate
ethylcyclohexane	ethyl heptadecyl sulfide
ethylcyclopentane	3-ethylheptane
3-ethyl-2,2-dimethylhexane	4-ethylheptane
ethyl heptyl sulfide	4-ethyl-4-methylheptane
ethyl hexadecyl sulfide	5-ethyl-2-methylheptane
2-ethylhexanal	3-ethyl-2-methylhexane
3-ethylhexane	3-ethyl-3-methylhexane
2-ethyl-1-hexanol	3-ethyl-4-methylhexane
2-ethyl-1-hexene	4-ethyl-2-methylhexane
2-ethylhexyl acetate	2-ethyl-3-methylnaphthalene
2-ethylhexyl acrylate	2-ethyl-6-methylnaphthalene
ethyl hexyl sulfide	2-ethyl-7-methylnaphthalene

Continued on next page

ethylidene diacetate	3-ethyl-2-methylpentane
ethyl iodide	ethyl methyl sulfide
ethyl isobutyrate	1-ethylnaphthalene
ethyl isopropyl ketone	2-ethylnaphthalene
ethyl isovalerate	ethyl nonyl sulfide
ethyl lactate	ethyl octadecyl sulfide
ethyl methacrylate	3-ethyloctane
3-ethyl-2-methylheptane	4-ethyloctane
3-ethyl-3-methylheptane	ethyl octyl sulfide
3-ethyl-4-methylheptane	ethyl pentadecyl sulfide
3-ethyl-5-methylheptane	3-ethylpentane
4-ethyl-2-methylheptane	2-ethyl-1-pentene
4-ethyl-3-methylheptane	3-ethyl-1-pentene
ethyl pentyl sulfide	ethynylbenzene
p-ethylphenol	fluoranthene
ethyl propionate	fluorene
ethyl propyl ether	fluorobenzene
ethyl propyl sulfide	p-fluorotoluene
ethyl tetradecyl sulfide	formanilide
m-ethyltoluene	formic acid
o-ethyltoluene	fumaric acid
p-ethyltoluene	furan
ethyl tridecyl sulfide	furfural

Continued on next page

3-ethyl-2,2,3-trimethylpentane	furfuryl alcohol
3-ethyl-2,2,4-trimethylpentane	glutaric acid
3-ethyl-2,3,4-trimethylpentane	glutaric anhydride
ethyl undecyl sulfide	glutaronitrile
ethyl vanillin	glycerol
ethyl vinyl ether	glyceryl triacetate
2-ethyl-m-xylene	halothane
2-ethyl-p-xylene	n-heptadecane
3-ethyl-o-xylene	1-heptadecanol
4-ethyl-m-xylene	1-heptadecene
4-ethyl-o-xylene	heptadecyl methyl sulfide
5-ethyl-m-xylene	heptadecyl propyl sulfide
1-heptadecyne	1-hexadecanol
1-heptanal	1-hexadecene
n-heptane	hexadecyl methyl sulfide
n-heptanoic acid	hexadecyl propyl sulfide
1-heptanol	1-hexadecyne
2-heptanol	cis,trans-2,4-hexadiene
2-heptanone	trans,trans-2,4-hexadiene
cis-2-heptene	1,5-hexadiene
cis-3-heptene	hexaethylbenzene
trans-2-heptene	hexafluoroacetone
trans-3-heptene	hexafluorobenzene

Continued on next page

1-heptene	hexafluoroethane
n-heptylbenzene	hexafluoropropylene
n-heptyl mercaptan	hexamethylbenzene
heptyl methyl sulfide	hexamethyldisilazane
heptyl propyl sulfide	hexamethyldisiloxane
1-heptyne	hexamethylenediamine
hexachlorobenzene	hexamethyleneimine
hexachloro-1,3-butadiene	1-hexanal
hexachlorocyclopentadiene	n-hexane
1-hexadecanethiol	1,6-hexanediol
n-hexadecanoic acid	hexanenitrile
n-hexanoic acid	p-hydroxybenzaldehyde
1-hexanol	2-hydroxyethyl acrylate
2-hexanol	indane
2-hexanone	indene
3-hexanone	indole
cis-2-hexene	iodobenzene
cis-3-hexene	3-iodo-1-propene
trans-2-hexene	isobutane
trans-3-hexene	isobutanol
1-hexene	isobutene
n-hexyl acetate	isobutyl acetate
n-hexylamine	isobutyl acrylate

Continued on next page

n-hexylbenzene	isobutylamine
hexylene glycol	isobutylbenzene
hexyl methyl sulfide	isobutyl formate
1-n-hexylnaphthalene	isobutyl isobutyrate
hexyl propyl sulfide	isobutyl mercaptan
1-hexyne	isobutyraldehyde
2-hexyne	isobutyric acid
3-hexyne	isobutyronitrile
hydrogen cyanide	isodecanol
p-hydroquinone	isopentane
isopentyl acetate	maleic anhydride
isopentyl isovalerate	malic acid
isophorone	malononitrile
isoprene	3-mercaptopropionic acid
isopropanol	mesitylene
isopropyl acetate	mesityl oxide
isopropylamine	methacrolein
isopropyl-tert-butyl ether	2-methacrylamide
isopropylcyclohexane	methacrylic acid
4-isopropylheptane	methacrylonitrile
isopropyl iodide	methane
isopropyl mercaptan	methanol
3-isopropyl-2-methylhexane	methoxyacetic acid

Continued on next page



isopropyl methyl sulfide	2-methoxyethanol
isoquinoline	2-(2-methoxyethoxy)ethanol
isovaleric acid	p-methoxyphenol
itaconic acid	3-methoxypropionitrile
ketene	N-methylacetamide
lactonitrile	methyl acetate
D-limonene	methyl acetoacetate
linoleic acid	methylacetylene
maleic acid	methyl acrylate
methylal	methyl chloroformate
methylamine	methyl chlorosilane
N-methylaniline	methyl cyanoacetate
methyl benzoate	methylcyclohexane
methyl bromide	cis-2-methylcyclohexanol
3-methyl-1,2-butadiene	cis-3-methylcyclohexanol
2-methyl-2-butanethiol	cis-4-methylcyclohexanol
2-methyl-1-butanol	trans-2-methylcyclohexanol
2-methyl-2-butanol	trans-3-methylcyclohexanol
3-methyl-1-butanol	trans-4-methylcyclohexanol
3-methyl-2-butanol	1-methylcyclohexanol
2-methyl-1-butene	N-methylcyclohexylamine
2-methyl-2-butene	methylcyclopentadiene
3-methyl-1-butene	methylcyclopentane

Continued on next page

2-methyl-1-butene-3-yne	1-methylcyclopentene
methyl sec-butyl ether	3-methylcyclopentene
methyl tert-butyl ether	4-methylcyclopentene
3-methyl-1-butyne	methyl dichlorosilane
methyl n-butyrate	methyl diethanolamine
2-methylbutyric acid	methyl dodecanoate
methyl chloride	methylethanolamine
methyl chloroacetate	1-methyl-1-ethylcyclopentane
methyl ethyl ether	methyl isopropyl ether
methyl ethyl ketone	methyl isopropyl ketone
3-methyl-3-ethylpentane	methyl methacrylate
methyl fluoride	1-methylnaphthalene
N-methylformamide	2-methylnaphthalene
methyl formate	methyl nonadecyl sulfide
methylglutaronitrile	2-methylnonane
2-methylheptane	3-methylnonane
3-methylheptane	4-methylnonane
4-methylheptane	5-methylnonane
2-methylhexane	methyl nonyl sulfide
3-methylhexane	methyl octadecyl sulfide
5-methyl-1-hexanol	2-methyloctane
5-methyl-2-hexanone	3-methyloctane
2-methyl-1-hexene	4-methyloctane

Continued on next page

3-methyl-1-hexene	methyl octyl sulfide
4-methyl-1-hexene	methyl oleate
methyl iodide	methyl pentadecyl sulfide
methyl isobutyl ether	2-methylpentane
methyl isobutyl ketone	3-methylpentane
methyl isocyanate	2-methyl-1-pentanol
methyl isopropenyl ketone	4-methyl-2-pentanol
trans-3-methyl-2-pentene	3-methylsulfolane
2-methyl-1-pentene	methyl tetradecyl sulfide
2-methyl-2-pentene	2-methylthiophene
3-methyl-cis-2-pentene	3-methylthiophene
3-methyl-1-pentene	methyl trichlorosilane
4-methyl-cis-2-pentene	methyl tridecyl sulfide
4-methyl-trans-2-pentene	methyl undecyl sulfide
4-methyl-1-pentene	methyl vinyl ether
methyl tert-pentyl ether	monochlorobenzene
methyl pentyl sulfide	monoethanolamine
methyl propionate	morpholine
methyl propyl sulfide	naphthalene
2-methylpyridine	neopentane
3-methylpyridine	neopentyl glycol
4-methylpyridine	m-nitroaniline
N-methylpyrrole	o-nitroaniline

Continued on next page

N-methyl-2-pyrrolidone	1-nitrobutane
methyl salicylate	2-nitrobutane
m-methylstyrene	nitroethane
o-methylstyrene	nitromethane
p-methylstyrene	1-nitropropane
a-methylstyrene	2-nitropropane
m-nitrotoluene	1-octadecyne
o-nitrotoluene	octafluoro-2-butene
p-nitrotoluene	octafluorocyclobutane
n-nonadecane	octafluoropropane
nonadecanoic acid	octamethylcyclotetrasiloxane
1-nonadecanol	1-octanal
1-nonanal	n-octane
n-nonane	n-octanoic acid
n-nonanoic acid	1-octanol
1-nonanol	2-octanol
2-nonanol	2-octanone
1-nonene	trans-2-octene
n-nonylamine	trans-3-octene
n-nonylbenzene	trans-4-octene
1-n-nonylnaphthalene	1-octene
nonylphenol	n-octylamine
nonyl propyl sulfide	n-octylbenzene

Continued on next page

1-nonyne	n-octyl formate
2-norbornene	n-octyl mercaptan
n-octadecane	p-tert-octylphenol
1-octadecanol	octyl propyl sulfide
1-octadecene	oleic acid
paraldehyde	3-pentanol
pentachloroethane	2-pentanone
n-pentadecane	cis-2-pentene
1-pentadecanethiol	trans-2-pentene
pentadecanoic acid	1-pentene
1-pentadecene	1-pentene-3-yne
pentadecyl propyl sulfide	1-pentene-4-yne
1-pentadecyne	n-pentyl acetate
cis-1,3-pentadiene	n-pentylamine
trans-1,3-pentadiene	n-pentylbenzene
1,2-pentadiene	pentylcyclohexane
1,4-pentadiene	n-pentyl formate
2,3-pentadiene	n-pentyl mercaptan
pentaerythritol	1-pentyl naphthalene
pentaethylbenzene	2-pentyl naphthalene
pentafluoroethane	pentyl propyl sulfide
2,2,3,3,4-pentamethylpentane	1-pentyne
2,2,3,4,4-pentamethylpentane	2-pentyne

Continued on next page

n-pentane	a-phellandrene
1,5-pentanediol	b-phellandrene
1-pentanol	phenanthrene
2-pentanol	p-phenetidine
phenetole	propargyl alcohol
phenol	propargyl chloride
m-phenylenediamine	cis-propenylbenzene
o-phenylenediamine	trans-propenylbenzene
p-phenylenediamine	b-propiolactone
2-phenylethanol	n-propionaldehyde
1-phenylhexadecane	propionic acid
phenyl mercaptan	propionic anhydride
1-phenylnaphthalene	propionitrile
1-phenylpentadecane	n-propyl acetate
2-phenyl-2-propanol	n-propyl acrylate
1-phenyltetradecane	n-propylamine
phosgene	n-propylbenzene
phthalic anhydride	n-propyl n-butyrate
a-pinene	n-propyl chloride
b-pinene	n-propylcyclohexane
piperazine	n-propylcyclopentane
piperidine	propylene
propadiene	1,2-propylene glycol

Continued on next page

propane	1,3-propylene glycol
1,2-propanediamine	propyleneimine
n-propanol	1,2-propylene oxide
1,3-propylene oxide	sebacic acid
n-propyl formate	sorbitol
4-propylheptane	spiropentane
n-propyl iodide	stearic acid
n-propyl mercaptan	styrene
n-propyl methacrylate	succinic acid
1-propylnaphthalene	succinic anhydride
2-propylnaphthalene	succinonitrile
n-propyl propionate	sulfolane
propyl tetradecyl sulfide	m-terphenyl
propyl tridecyl sulfide	o-terphenyl
propyl undecyl sulfide	p-terphenyl
pyrene	a-terpinene
pyridine	g-terpinene
pyromellitic acid	terpinolene
pyrrole	1,1,2,2-tetrabromoethane
pyrrolidine	1,1,2,2-tetrachlorodifluoroethane
2-pyrrolidone	1,1,1,2-tetrachloroethane
pyruvic acid	1,1,2,2-tetrachloroethane
quinaldine	tetrachloroethylene

Continued on next page

quinoline	n-tetradecane
salicylaldehyde	1-tetradecanethiol
n-tetradecanoic acid	2,2,4,4-tetramethylhexane
1-tetradecanol	2,2,4,5-tetramethylhexane
1-tetradecene	2,2,5,5-tetramethylhexane
tetradecylamine	2,3,3,4-tetramethylhexane
1,2,3,4-tetraethylbenzene	2,3,3,5-tetramethylhexane
1,2,3,5-tetraethylbenzene	2,3,4,4-tetramethylhexane
1,2,4,5-tetraethylbenzene	2,3,4,5-tetramethylhexane
tetraethylene glycol	3,3,4,4-tetramethylhexane
tetraethylene glycol dimethyl ether	2,2,3,3-tetramethylpentane
tetraethylenepentamine	2,2,3,4-tetramethylpentane
1,1,1,2-tetrafluoroethane	2,2,4,4-tetramethylpentane
tetrahydrofuran	2,3,3,4-tetramethylpentane
tetrahydrofurfuryl alcohol	tetramethylsilane
1,2,3,4-tetrahydronaphthalene	tetraphenylethylene
tetrahydrothiophene	thiacyclobutane
1,2,3,4-tetramethylbenzene	thiacycloheptane
1,2,3,5-tetramethylbenzene	thiacyclohexane
1,2,4,5-tetramethylbenzene	thiacyclopropane
2,2,3,3-tetramethylbutane	thiophene
2,2,3,3-tetramethylhexane	p-tolualdehyde
2,2,3,4-tetramethylhexane	toluene

Continued on next page



2,2,3,5-tetramethylhexane	toluenediamine
o-toluic acid	n-tridecylbenzene
p-toluic acid	1-tridecyne
m-toluidine	triethanolamine
o-toluidine	triethylamine
p-toluidine	1,2,3-triethylbenzene
tribromomethane	1,2,4-triethylbenzene
tri-n-butylamine	1,3,5-triethylbenzene
trichloroacetaldehyde	triethylene glycol
trichloroacetyl chloride	triethylene glycol dimethyl ether
1,2,4-trichlorobenzene	triethylene tetramine
1,1,1-trichloroethane	1,1,1-trifluoroethane
1,1,2-trichloroethane	trifluoroethene
trichloroethylene	trimellitic anhydride
1,1,1-trichlorofluoroethane	trimethylamine
trichlorofluoromethane	1,2,3-trimethylbenzene
1,2,3-trichloropropane	1,2,4-trimethylbenzene
1,1,2-trichlorotrifluoroethane	2,2,3-trimethylbutane
1-tridecanal	2,3,3-trimethyl-1-butene
n-tridecane	cis,cis-1,3,5-trimethylcyclohexane
1-tridecanethiol	cis,trans-1,3,5-trimethylcyclohexane
1-tridecanol	2,2,3-trimethylheptane
1-tridecene	2,2,4-trimethylheptane

Continued on next page

2,2,5-trimethylheptane	1,2,3-trimethylindene
2,2,6-trimethylheptane	2,2,3-trimethylpentane
2,3,3-trimethylheptane	2,2,4-trimethylpentane
2,3,4-trimethylheptane	2,3,3-trimethylpentane
2,3,5-trimethylheptane	2,3,4-trimethylpentane
2,3,6-trimethylheptane	2,4,4-trimethyl-1-pentene
2,4,4-trimethylheptane	2,4,4-trimethyl-2-pentene
2,4,5-trimethylheptane	2,4,6-trinitrotoluene
2,4,6-trimethylheptane	triphenylethylene
2,5,5-trimethylheptane	tripropylamine
3,3,4-trimethylheptane	1-undecanal
3,3,5-trimethylheptane	n-undecane
3,4,4-trimethylheptane	1-undecanol
3,4,5-trimethylheptane	1-undecene
2,2,3-trimethylhexane	n-undecylbenzene
2,2,4-trimethylhexane	undecyl mercaptan
2,2,5-trimethylhexane	1-undecyne
2,3,3-trimethylhexane	valeraldehyde
2,3,4-trimethylhexane	valeric acid
2,3,5-trimethylhexane	valeronitrile
2,4,4-trimethylhexane	vanillin
3,3,4-trimethylhexane	vinyl acetate
vinylacetonitrile	o-xylene

Continued on next page

vinyl bromide	p-xylene
vinyl chloride	2,3-xylenol
vinylcyclohexene	2,4-xylenol
vinyl fluoride	2,5-xylenol
vinyl formate	2,6-xylenol
vinyl propionate	3,4-xylenol
m-xylene	3,5-xylenol

### **Inorganic Fluids**

ammonia	iron pentacarbonyl
antimony pentachloride	mercury
arsenic pentafluoride	molybdenum fluoride
arsenic tribromide	monobromosilane
arsenic trichloride	monochlorosilane
arsenic trifluoride	nickel carbonyl
arsine	nitric acid
borine triamine	nitrogen dioxide
boron tribromide	nitrogen tetraoxide
boron trichloride	nitrogen trichloride
bromine	nitrogen trioxide
bromine pentafluoride	nitrosyl chloride
bromodichlorofluorosilane	nitrosyl fluoride

Continued on next page

carbon disulfide	osmium tetroxide - white
carbon oxyselenide	osmium tetroxide - yellow
carbon selenosulfide	pentaborane
carbonyl sulfide	perchloric acid
cesium	perchloryl fluoride
chlorine	phosgene
chlorine dioxide	phosphonium iodide
chlorine heptoxide	phosphorus oxychloride
chlorine monoxide	phosphorus thiobromide
chlorine pentafluoride	phosphorus thiochloride
chlorine trifluoride	phosphorus tribromide
chlorosulfonic acid	phosphorus trichloride
chromium oxychloride	phosphorus trioxide
cyanogen	potassium
cyanogen bromide	radon
cyanogen chloride	rubidium
deuterium oxide	selenium oxychloride
diborane hydrobromide	silicon tetrachloride
dichlorodifluorosilane	stannic bromide
dichlorosilane	stannic chloride
digermane	stibine
diiodosilane	sulfur dioxide
disilane	sulfur monochloride

Continued on next page

disilanyl chloride	sulfur tetrafluoride
disiloxane	sulfur trioxide
gallium	sulfuryl chloride
gallium trichloride	tetraborane
germanium bromide	tetrahydropentaborane
germanium chloride	tetrasilane
hexachlorodisilane	thionyl bromide
hexachlorodisiloxane	thionyl chloride
hydrazine	titanium tetrachloride
hydrogen bromide	tribromosilane
hydrogen cyanide	trichlorofluorosilane
hydrogen disulfide	trichlorogermane
hydrogen fluoride	trichlorosilane
hydrogen iodide	trichlorotrifluorodisiloxane
hydrogen peroxide	trifluorobromosilane
hydrogen selenide	trigermane
hydrogen sulfide	trisilane
hydrogen telluride	trisilazane
iodine	tungsten fluoride
iodine heptafluoride	uranium fluoride
iodosilane	vanadium tetrachloride
water	

## VITA

Scott Joseph Coughlin was born in August of 1981 in Phoenix, Arizona. He resided in Scottsdale, Arizona for most of his life before moving to Tucson, Arizona to attend The University of Arizona. It is from here that he received the degree of Bachelor of Science in Mechanical Engineering in May 2003.

He received his Master of Science in Mechanical Engineering at Texas A&M in December of 2005. While in College Station, he worked as a Research Assistant with the Center for Space Power.

The permanent address at which Scott Coughlin can be contacted is 22419 North Los Caballos Drive, Scottsdale, Arizona, 85255.

The typist for this thesis was Scott Coughlin.